

# **IAP antagonization promotes inflammatory destruction of vasculature endothelium and inhibits tumor growth**

Inaugural-Dissertation

zur

Erlangung des Doktorgrades

der Mathematisch-Naturwissenschaftlichen Fakultät

der Universität zu Köln

vorgelegt von

**Axel Witt**

aus Herne

Berichtersteller:

Dr. Thomas Wunderlich

Prof. Dr. Manolis Pasparakis

Tag der mündlichen Prüfung:

2015-01-19

---

## Table of contents

<b>Abbreviations</b>	III
<b>Abstract</b>	1
<b>Zusammenfassung</b>	2
<b>1. Introduction</b>	4
1.1 The inhibitor of apoptosis protein gene family	4
1.2 Inhibitor of apoptosis proteins and programmed cell death	6
1.3 Apoptosis	6
1.3.1 The intrinsic apoptotic pathway	7
1.3.2 The extrinsic apoptotic pathway	9
1.4 Necroptosis	10
1.5 Inhibitor of apoptosis proteins as key regulators of apoptosis and necroptosis	11
1.6 Inhibitor of apoptosis proteins as regulators of nuclear factor $\kappa$ B signaling pathways	12
1.7 Inhibitor of apoptosis proteins and human cancer	15
1.8 Targeting inhibitor of apoptosis proteins for cancer therapy	16
1.9 Development of SM as antagonists of inhibitor of apoptosis proteins	17
1.10 Mechanisms of the antitumoral activities of SM	21
1.11 Aim of the work	24
<b>2. Materials and Methods</b>	25
2.1 Chemicals and reagents	25
2.2 Cell lines	26
2.3 Animal tumor models	26
2.4 Tumor and matrigel plug preparation	27
2.5 Cell viability and cell death measurements	27
2.6 FITC-dextran application	27
2.5 Cell viability and cell death measurements	27
2.7 Cell growth assay	28
2.8 NF- $\kappa$ B activity	28
2.9 TNF-ELISA	28
2.10 RNA isolation	28

---

2.11 DNaseI	29
2.12 Agarose gel electrophoresis	29
2.13 Reverse transcription (RT)	29
2.14 Quantitative Real-Time PCR (qRT-PCR)	29
2.15 Sample preparation for immunoblotting (IB)	30
2.16 Clonogenicity Assays	31
2.17 Tube formation assay	32
2.18 Tissue Immunostaining	32
2.19 Microscopy	32
2.20 Statistical analyses	33
<b>3. Results</b>	<b>35</b>
3.1 IAP antagonization inhibits tumor growth <i>in vivo</i>	35
3.2 IAP antagonization inhibits tumor vasculature <i>in vivo</i>	41
3.3 IAP antagonization promotes TNF-induced endothelial cell death	48
3.4 IAP antagonization potentiates TNF-induced vascular disruption <i>in vivo</i>	54
<b>4. Discussion</b>	<b>60</b>
4.1 IAP antagonization inhibits tumor growth without inducing direct cytotoxicity against tumor cells	60
4.2 IAP antagonization results in the destruction of the vasculature in the tumor Microenvironment	62
4.3 IAP antagonization promotes TNF-induced cell death of endothelial cells	64
4.4 IAP antagonization leads to TNF induced vascular disruption <i>in vivo</i>	66
4.5 Therapeutic implications	67
4.6 Conclusion	69
<b>5. References</b>	<b>71</b>
<b>6. Appendix</b>	<b>85</b>
6.1 Danksagung	85
6.2 Erklärung	86
6.3 Lebenslauf	87

## Abbreviations

<b>BSA</b>	Bovine serum albumin	<b>MOMP</b>	Mitochondrial outer membrane permeabilization
<b>Ca<sup>2+</sup></b>	Calcium	<b>NF-κB</b>	Nuclear factor kappa B
<b>cIAP</b>	Cellular IAP	<b>Nec-1</b>	Necrostatin-1
<b>Cpd A</b>	Compound A	<b>PAGE</b>	Polyacrylamid gel electrophoresis
<b>Cpd B</b>	Compound B	<b>PBS</b>	Phosphate buffered saline
<b>Da, kDa</b>	Dalton, Kilodalton	<b>PCR</b>	Polymerase chain reaction
<b>DIABLO</b>	Direct IAP binding protein with low pI	<b>pmol</b>	Picomol
<b>DMSO</b>	Dimethylsulfoxid	<b>PMSF</b>	Phenylmethanesulfonyl fluoride
<b>dNTP</b>	deoxynucleotide	<b>RIPK</b>	Receptor-interacting serine/threonine-protein kinase
<b>DTT</b>	Dithiothreitol	<b>rpm</b>	Revolutions per minute
<b>EC</b>	Endothelial cell	<b>RT</b>	Room temperature
<b>EDTA</b>	Ethylenediamine-tetraacetic acid	<b>SDS</b>	Sodium dodecylsulfate
<i>et al.</i>	et alteri /-a /-um (and others)	<b>SM</b>	SMAC mimetics
<b>ent-SM</b>	inactive SMAC mimetic enantiomer	<b>SMAC</b>	Second mitochondrial derived activator of caspases
<b>FITC-Dextran</b>	Fluorescein isothiocyanate-dextran	<b>TNF</b>	Tumor necrosis factor
<b>HUVEC</b>	Human umbilical vein Endothelial cells	<b>VEGF</b>	vascular endothelial growth factor
<b>HDMEC</b>	human dermal microvascular endothelial cells	<b>VCAM</b>	vascular cell adhesion molecule
<b>IAP</b>	Inhibitor of apoptosis	<b>XIAP</b>	X-linked inhibitor of apoptosis
<b>IBM</b>	IAP-binding motif		
<b>M</b>	molar, mol/l		
<b>MTS</b>	mitochondrial targeting sequence		
<b>NF-κB</b>	Nuclear Factor κB		
<b>MAPK</b>	Mitogen activated protein Kinase		

## Abstract

The inhibitor of apoptosis (IAP) protein family encodes a group of structurally related proteins that were initially identified based on their ability to inhibit cell death. Due to their cytoprotective properties and their elevated expression levels in many types of human cancer, small molecular pharmacological inhibitors of IAPs (SMAC mimetics, SM) were developed in the last years (Kashkar, 2010; Fulda & Vucic, 2012; Bai *et al*, 2014). Numerous studies have focused on the role of SM-induced cell death in cancer cells. Accordingly, many SM compounds are currently in clinical trials to evaluate their potential in cancer therapy and so far, SM-mediated cell death is believed to directly target malignant cells (Fulda & Vucic, 2012; Fulda, 2014; Bai *et al*, 2014).

In order to study the underlying mechanisms in more detail *in vivo*, we used a B16 melanoma mouse model with immune competent mice. The obtained results demonstrated that IAP antagonization by a pan-IAP antagonist inhibits tumor growth *in vivo* not by inducing direct cytotoxicity towards tumor cells. In fact, our work showed that SM triggers a TNF-dependent disruption of the vasculature in the tumor microenvironment.

Specifically, SM treatment facilitated the production of TNF by B16 melanoma tumor cells, which is consistent with previous observations concerning the cellular responses to SM exposure (Wu *et al*, 2007). Two key components of tumor stroma, infiltrating immune cells and endothelial vasculature, were scrutinized in our study. While no significant differences in the immune cell infiltration of B16 mouse tumors were observed, we found a striking reduction of the vascularization in B16 tumors treated with SM. The lack of vascularization in B16 melanoma tumors or implanted matrigel plugs in wild type but not in TNF-R1/2<sup>-/-</sup> mice and the potentiated susceptibility of two independent EC cultures towards TNF in the presence of SM, identified the endothelial cells of the tumor vasculature as the major target of SM-induced cell death within the tumor microenvironment.

Taken together, our work identified a novel anti-angiogenic activity of a pan-IAP antagonist in the presence of elevated TNF levels under inflammatory conditions within the tumor microenvironment. This could constitute an additional and perhaps complementary potential of SM, which could improve current cancer therapies.

## Zusammenfassung

Die Mitglieder der Familie der *inhibitor of apoptosis* Proteine (IAPs) wurden ursprünglich aufgrund ihrer Fähigkeit beschrieben den Zelltod zu blockieren. IAPs haben nicht nur zytoprotektive Eigenschaften, sondern werden zudem in malignen Zellen häufig überexprimiert und stellen daher ein attraktives therapeutisches Ziel in der Krebstherapie dar. In den letzten Jahren wurde eine große Anzahl von kleinen, pharmakologischen IAP-Inhibitoren, sogenannte SMAC mimetics (SM), mit dem Ziel der Einleitung der Apoptose in Krebszellen entwickelt. Eine Vielzahl an SM werden derzeit in klinischen Studien getestet um ihr Potential in der Behandlung von malignen Erkrankungen zu untersuchen (Kashkar, 2010; Fulda & Vucic, 2012; Bai *et al*, 2014). Zur Zeit wird angenommen, dass die anti-karzinogene Wirkung von SM auf einen direkten zytotoxischen Effekt von SM auf maligne Zellen zurückzuführen ist (Fulda & Vucic, 2012; Fulda, 2014; Bai *et al*, 2014).

Zur genaueren Untersuchung des zugrundeliegenden Wirkmechanismus von SM *in vivo*, wurde in der vorliegenden Arbeit ein B16 Melanom Modell in immun-kompetenten Mäusen verwendet. In diesen Untersuchungen wurde eine Reduktion des Tumorwachstums bei der Verabreichung eines pan-IAP Antagonisten, allerdings ohne dabei eine direkte Zytotoxizität in Tumorzellen auszulösen, beobachtet. Es konnte vielmehr veranschaulicht werden, dass SM zu einer TNF-abhängigen Zerstörung der Tumor-Blutgefäße führte.

In Übereinstimmung mit veröffentlichten Studien in anderen Tumorzellen (Wu *et al*, 2007) haben unsere weiteren detaillierten Untersuchungen gezeigt, dass B16 Zellen durch die Behandlung mit SM TNF sezernieren. Zur genaueren Identifikation des Wirkmechanismus wurden zwei Hauptkomponenten des Tumor-Stromas untersucht, Tumor-infiltrierende Immunzellen und die endotheliale Vaskulatur. Hierbei wurden keine Veränderungen der Infiltration von Immunzellen festgestellt. Es konnte jedoch eine deutliche Reduktion an Tumor-Blutgefäßen beobachtet werden. Diese Reduktion konnte in implantierten Matrigel-Plugs bestätigt werden. Bemerkenswerterweise war dieser Effekt bei implantierten Matrigel-Plugs und bei der Analyse des Tumorwachstums in TNF-R1/2<sup>-/-</sup>-Mäusen nicht zu beobachten, wodurch die Rolle von TNF-induzierten zytotoxischen Signalkaskaden in der anti-karzinogenen Wirkung von SM bestätigt wurde. Im Gegensatz zu malignen Zellen wurde eine hohe Anfälligkeit gegenüber SM/TNF induzierten Zelltod in zwei Endothelzelllinien gezeigt. Diese Ergebnisse veranschaulichen, dass vor allem

Endothelzellen der Blutgefäße im Tumorstroma durch die Behandlung mit SM zerstört werden, wobei die zytotoxische Wirkung auf maligne Zellen marginal ist

Zusammenfassend wurde in dieser Arbeit erstmalig gezeigt, dass pan-IAP Antagonisten aufgrund von erhöhtem TNF im Tumorstroma zu einer Reduktion der Blutgefäße führen. Diese bisher unbekannte Charakteristik könnte zu einer Verbesserung des therapeutischen Nutzens von SM in der Krebstherapie führen.



# 1. Introduction

## 1.1 The inhibitor of apoptosis protein gene family

The IAP (inhibitor of apoptosis protein) gene family encodes a group of structurally related proteins that were initially identified based on their ability to inhibit cell death. The baculovirus inhibitors of apoptosis Cp-IAP and Op-IAP were the first members of the IAP family that were discovered as functional homologs of the cell death inhibitor p35 in 1993. They were able to complement the cell death function of p35 in mutant virus (lacking p35) (Crook *et al*, 1993). Subsequent work by Clem and co-workers demonstrated that IAPs were capable of blocking apoptosis induced by the RNA synthesis inhibitors actinomycin D or *Autographa californica* nuclear polyhedrosis virus (AcMNPV) infection (Clem & Miller, 1994). A common structural feature of IAP family proteins is the presence of up to three copies of a BIR (baculoviral IAP repeat) domain (Birnbaum *et al*, 1994) frequently in conjunction with a carboxy-terminal zinc-finger like motifs. In the following years, IAPs were identified in a variety of eukaryotic species like yeast, nematode, fruit fly and in the mammalian species mice, rats, pigs, and humans (Deveraux, & Reed, 1999).

The first human IAP, NAIP (neuronal apoptosis inhibitory protein) also called BIRC1 (BIR containing protein 1) was found to be involved in the neuronal disease SMA (spinal muscular atrophy) in which it blocks cell death in response to treatment such as menadione and TNF (tumor necrosis factor) (Roy *et al*, 1995; Liston *et al*, 1996). Further IAPs including cIAP1 (cellular IAP1; BIRC2), cIAP2 (cellular IAP2; BIRC3), XIAP (X-chromosome-linked IAP; BIRC4), survivin (BIRC6), apollon (BIR-containing ubiquitin-conjugating BIR domain enzyme; BIRC6), ML-IAP (melanoma IAP; Livin; BIRC7) and ILP-2 (IAP-like protein; BIRC8) (Fig. 1.1) were subsequently identified based on their conserved BIR-domains and examined for their anti-apoptotic capacity. Despite their nomenclature, several IAPs have functions other than regulating apoptosis and are involved in a plethora of different cellular actions including cell cycle regulation, protein degradation, immune signaling and inflammation (Salvesen & Duckett, 2002; Estornes & Bertrand, 2014).

Several IAPs regulate apoptosis and a direct caspase (Cysteine Aspartic Acid Specific Protease) inhibition was assumed as an important conserved function among most family members. However, detailed biochemical and structural studies have mapped the elements of IAPs required for caspase inhibition, showing that these elements are not

conserved among IAPs, suggesting that XIAP is probably the only *bona fide* cellular caspase inhibitor. Especially the BIR2 and BIR3 domains of XIAP were biochemically identified as the elements with inhibitory capacity towards caspases (Uren *et al*, 1996; Deveraux *et al*, 1997; Eckelman *et al*, 2006). Within these binding-sites a conserved surface groove was found, defined as the IBM (IAP-binding motif)-interacting groove. Beside their BIR domains, some IAP proteins such as XIAP, cIAP1, cIAP2 or ML-IAP have a carboxy-terminal domain termed RING (Really Interesting New Gene), which has been demonstrated to act as a E3 ubiquitin ligase hence conducting important functions of IAPs in survival and signaling pathways (Vaux & Silke, 2005; Varfolomeev *et al*, 2008). Furthermore, cIAPs, ILP2 and XIAP can bind to mono- or polyubiquitin chains of various linkages because of a UBA (conserved ubiquitin-binding) domain (Gyrd-Hansen *et al*, 2008). Some IAPs, such as cIAPs, have an additional CARD domain (caspase recruitment domain) that suppresses the activation of the RING domain E3 ligase activity (Lopez *et al*, 2011).

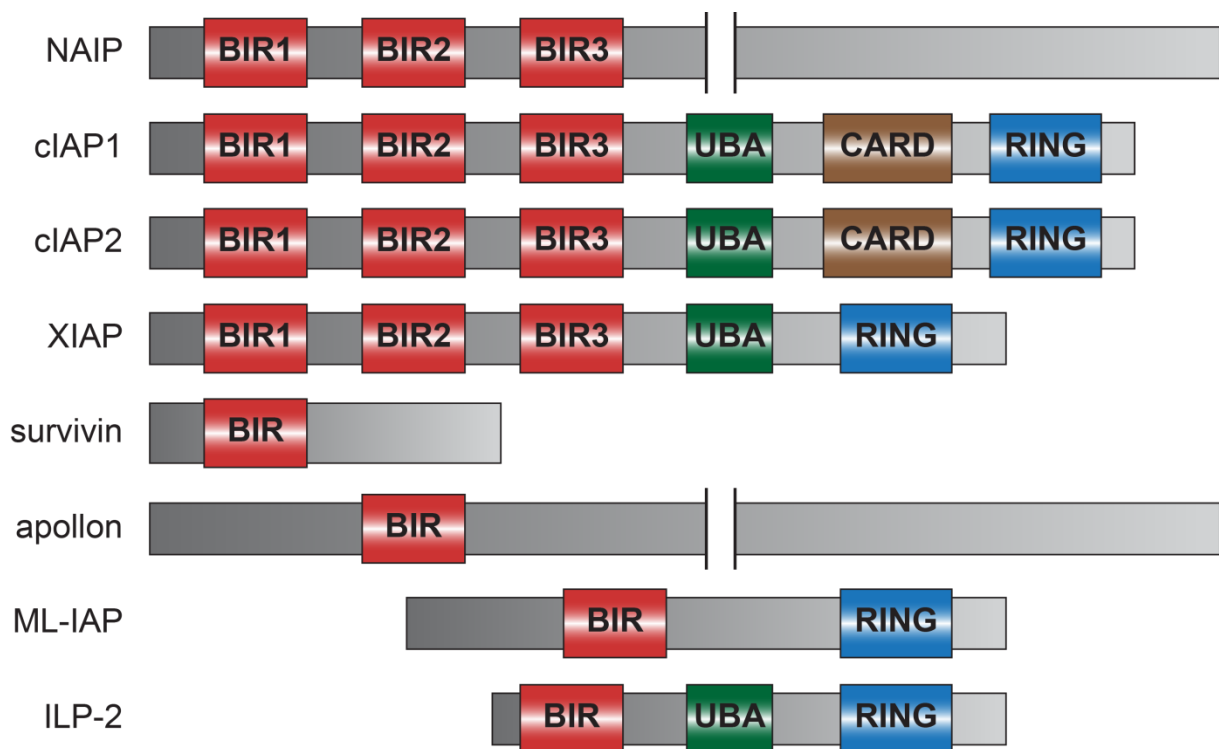


**Fig 1.1 Functional domains of mammalian inhibitors of apoptosis proteins (IAPs).**

The mammalian family of IAPs including NAIP (neuronal apoptosis inhibitory protein, BIRC1, BIR-containing 1), cIAP1 (cellular IAP1; BIRC2), cIAP2 (cellular IAP2; BIRC3), XIAP (X-chromosome-linked IAP; BIRC4), survivin (BIRC6), apollon (BIR-containing ubiquitin-conjugating BIR domain enzyme; BIRC6), ML-IAP (melanoma IAP; Livin; BIRC7) and ILP-2 (IAP-like protein; BIRC8). All IAPs feature the conserved BIR domain (baculoviral IAP repeat domain) up to three copies. Beside

BIR domains, IAPs can harbor different functional domains: UBA: ubiquitin-associated domain; CARD: caspase recruitment domain; RING: really interesting new gene finger domain.

## 1.2 Inhibitor of apoptosis proteins and programmed cell death

Inhibitor of apoptosis proteins are best characterized in the regulation of apoptosis that plays an important role in organismal and embryonic development and adult tissue homeostasis.

In general, the execution of programmed cell death can involve different pathways like apoptosis and necroptosis. In addition to the well-studied apoptosis, necroptosis has recently been identified as a new type of caspase-independent cell death leading to necrosis. Contrary to necroptosis, apoptosis involves the activation of caspases leading to a tightly controlled removal of dying cells.

## 1.3 Apoptosis

Apoptosis is a well described and the most common form of programmed cell death and was first described based on the distinct morphological features of an apoptotic cell (Kerr *et al*, 1972). It is essential for, amongst others, embryonic development, tissue homeostasis and immune system functions. The greek word “apoptosis” describing the “dropping off” petals from flowers was introduced by Kerr and co-workers, based on their observation that programmed cell death could be morphologically distinguished from necrotic (traumatic) cell death (termed necrosis), which is caused by external factors like infections, toxins or trauma (Kerr *et al*, 1972). Apoptosis leads to characteristic morphological cell changes including cell shrinkage, nuclear fragmentation, chromatin condensation and chromosomal DNA fragmentation (Wyllie *et al*, 1980), resulting in the fragmentation of dying cells and the appearance of apoptotic bodies. Subsequent clearance of apoptotic bodies by phagocytosis prevents from damage to the surrounding tissue and assures the recovery of precious cellular constituents. By contrast, necrosis results in cellular swelling, disorganized hydrolysis of chromatin and perturbations of the cell membrane. The loss of membrane integrity leads to the uncontrolled burst and spilling of intracellular contents characteristic for necrosis, subsequently increasing tissue damage.

Apoptosis can be induced either by cell autonomous mechanisms, e.g. overwhelming intracellular stress caused by e.g. DNA damage, viral infections or growth factor

withdrawal (intrinsic pathway) or by extracellular signals involving the TNF-receptor family (extrinsic pathway). The cellular decomposition during apoptosis is mainly mediated by a family of cysteine proteases known as caspases (Fuentes-Prior & Salvesen, 2004). This family of proteases cleave their substrates after specific aspartate residues (the “asp” in the word caspases) and the hydrolysis of the peptide bond is catalyzed by a cysteine in the active site (the “c” in the word caspases) (Nicholson & Thornberry, 1997). Caspases are highly conserved and can be divided in three subgroups according to their function: cytokine activators (caspase-1, -4, -5, -11, -12, -13 and -14), initiator caspases (caspase-2, -8, -9 and 10) and effector caspases (caspase-3, -6 and -7) (Denault JB, 2002). Of these, initiator together with effector caspases trigger apoptosis and they occur in two major pathways named “intrinsic or mitochondrial” and “extrinsic” apoptotic pathways (Kumar & Lavin, 1996; Nicholson & Thornberry, 1997) (Fig. 1.2).

### 1.3.1 The intrinsic apoptotic pathway

The intrinsic pathway of apoptosis is often described as the mitochondrial pathway of apoptosis, highlighting that MOMP (mitochondrial outer membrane permeabilization) and the release of mitochondrial IMS (intermembrane space) proteins into the cytoplasm is a key event, initiated by a cell autonomously upon overwhelming intracellular damage. Upon cellular stress such as DNA damage, viral infection or growth factor withdrawal, the pro-apoptotic Bcl2 proteins BAX and BAK undergo conformational changes and form homodimers in the mitochondrial outer membrane (Hsu *et al*, 1997) thereby provoking the release of mitochondrial IMS proteins such as cyt c (cytochrome c), SMAC/DIABLO (second mitochondria-derived activator of caspases/direct IAP binding protein with low pI) and OMI (also called HtrA2) (Youle & Strasser, 2008; Chipuk *et al*, 2010; Czabotar *et al*, 2014). Cytosolic cyt c, together with APAF1 (apoptotic protease activating factor 1) forms the multi-protein complex termed apoptosome at which the initiator caspase-9 is cleaved and activated (Li *et al*, 1997). Activated caspase-9 then cleaves and activates executioner caspases (caspase-3 and caspase-7), leading to the cleavage of downstream substrates and ultimately resulting in apoptosis (Fig. 1.2).

The mitochondrial apoptotic pathway is tightly controlled by Bcl2 protein family members. The Bcl2 protein family consists of anti-apoptotic (e.g. Bcl2, Bcl<sub>XL</sub> and A1) and two groups of pro-apoptotic members: the multi-domain proteins BAX and BAK and the divergent class of BH3-only proteins (e.g. Bid, Bad, Bik, Noxa and Puma).

BAX and BAK, responsible for MOMP, are regulated by pro- and anti-apoptotic Bcl2 proteins. Anti-apoptotic Bcl2 proteins such as Bcl2, BclxL and Mcl-1 can directly bind and inhibit BAX- or BAK-mediated MOMP. The divergent class of BH3-only proteins including Bad, Bid, Bik, Bim, Bmf, Noxa and Puma, feature a conserved BH3-domain. BH3-only proteins are sentinels for cellular damage and promote apoptosis either by neutralizing anti-apoptotic Bcl2 proteins (sensitizer) (Westphal *et al*, 2014) or by activating BAX and BAK directly (direct activators) (Tait & Green, 2010).

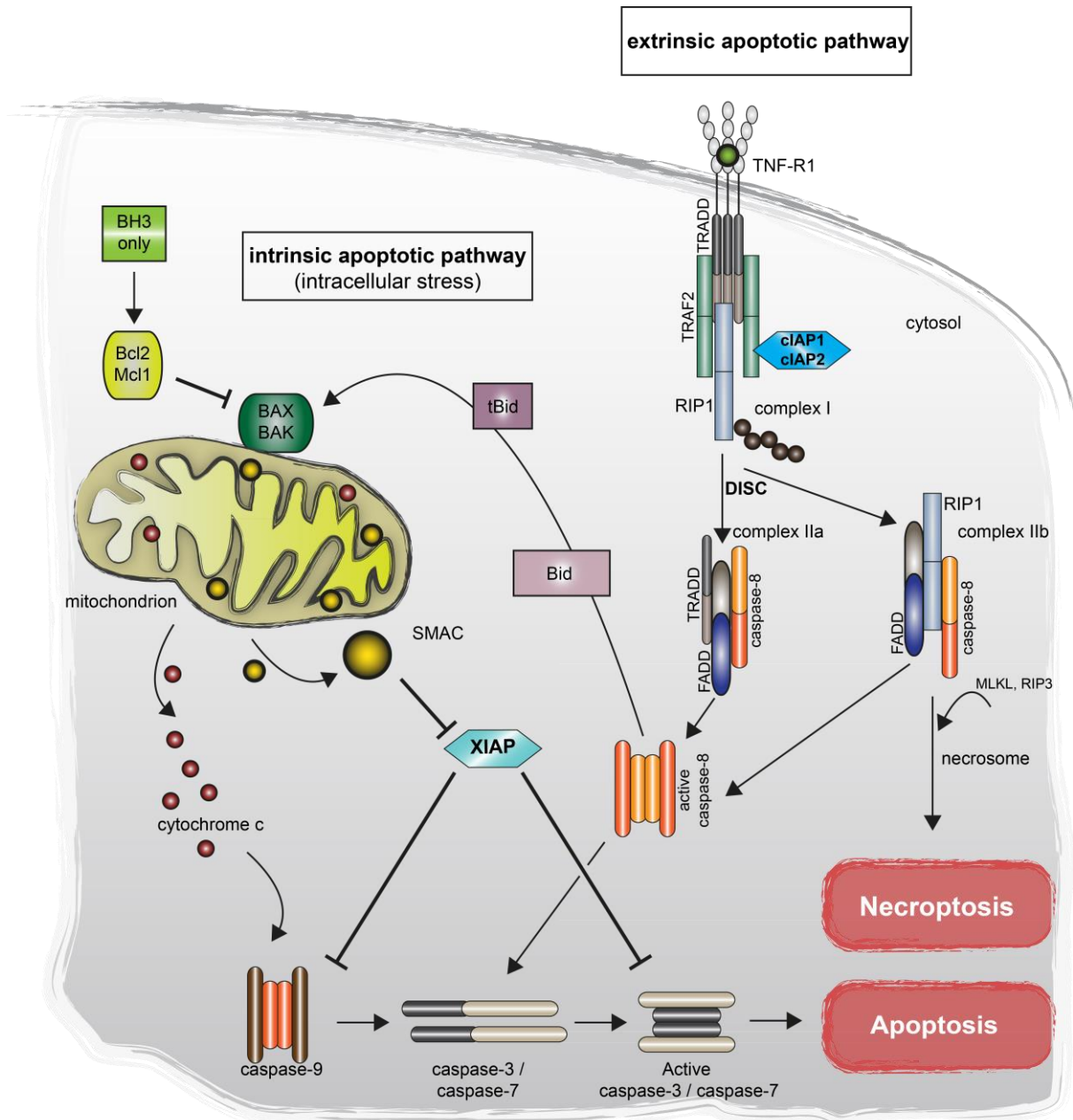


**Fig. 1.2 Programmed cell death pathways**

Upon binding of a death ligand like TNF to its receptor on the surface of the plasma membrane, the DISC (death inducing signaling complex) complex assembles. This can either lead to necroptosis involving the formation of the necrosome or to apoptosis by activation of caspase-8. Caspase-8 can directly activate executioner caspase-3/-7 or indirectly by cleaving the BH3-only protein Bid to

tBid which subsequently translocates to mitochondria. On the outer mitochondrial membrane tBid can activate the pro-apoptotic BAX/BAK. Activation of BAX/BAK is regulated by anti-apoptotic Bcl-2 proteins. Induction of MOMP by Bax/Bak results in the release of SMAC and cytochrome c from the mitochondria into the cytosol. SMAC potentiates apoptosis by binding to and antagonizing IAPs like XIAP. Cytochrome c release results in the activation of caspase-9, followed by activation of caspase-3/-7. Activated caspase-3/-7 lead to apoptotic cell death.

### 1.3.2 The extrinsic apoptotic pathway

The extrinsic apoptotic pathway is mediated by DRs (death receptors) of the TNF-receptor (TNF-R, tumor necrosis factor receptor) family, including TNF-R1 (DR1), Fas/Apo-1 (DR2) and DR4/5 on the cell surface (Bhardwaj & Aggarwal, 2003). Characteristic for these DRs is a cytosolic DD (death domain) and a DED (death effector domain) which initiate the receptor-oligomerization and interaction with adapter proteins upon activation by binding of specific death ligands such as TNF- $\alpha$ , FAS (TNF receptor superfamily member 6) or TRAIL (TNF-related apoptosis inducing ligand). For instance, upon activation, TNFR1 recruits the signaling adaptor TRADD (TNF receptor 1 associated death domain) which serves as a signaling scaffold for the assembly of the receptor bound complex (Ermolaeva *et al*, 2008). Additionally, this complex contains TRAF2 (TNF-R1 associated factor 2), TRAF5, RIPK1 (receptor interacting protein kinase 1), cIAP1 and cIAP2 and is frequently referred to as complex I. In the presence of cIAPs this complex mainly mediates cell survival signals such as NF- $\kappa$ B (nuclear factor kappa B) signaling through the IKK (I $\kappa$ B kinase) complex, MAPK signaling (p38 mitogen-activated protein kinases) and JNK activation (c-Jun N-terminal kinase). In contrast, activation of the TNF receptor signaling can also lead to the formation of a cytoplasmic complex after internalization of TNFR-1, resulting in a switch from pro-survival signaling to cell death. In detail, the dissociation of TRAF2 and RIPK1 from TRADD that in turn associates with FADD (FAS-associated via death domain protein) leads to the recruitment of caspase-8 to the cytosolic complex termed complex IIa (Fig. 1.2). In complex IIa, procaspase-8 forms homotypic procaspase-8 dimers leading to subsequent activation of caspase-8 by reciprocal cleavage of the procaspase-8 isoforms. The activated caspase-8 initiates cleavage activation of the executioner caspases-3, -6 and -7 leading to apoptosis (Ashkenazi, 2008).

Both pathways of apoptosis are interconnected by the cleavage of the BH3-only protein Bid to tBid (truncated Bid) by caspase-8. tBid translocates to the mitochondrial membrane, binds to BAX and BAK, subsequently leading to the initiation of MOMP (Luo *et al*, 1998; Wright *et al*, 2007; Kaufmann *et al*, 2012).

Alternatively to complex IIa, RIPK1 instead of TRADD can bind FADD and thereby recruit procaspases-8 to a complex referred to as complex IIb. This RIPK1-dependent complex can only be formed in the absence of cIAPs (Vince *et al*, 2007; Varfolomeev *et al*, 2007; Petersen *et al*, 2007) or in presence of the deubiquitinase CYLD (Wright *et al*, 2007; Wang *et al*, 2008) either resulting in apoptosis or necroptosis (Fig. 1.2).

## 1.4 Necroptosis

Although initial studies concerned apoptosis as the only form of programmed cell death governing tissue homeostasis, recent evidence indicates that apoptosis may not solely represent the controlled demolition of a cell. Accumulating evidence indicated that the execution of programmed cell death involves more than just the apoptotic program. Necroptosis has recently been identified as a new type of programmed cell death which does not involve caspase activity and lead to necrotic cell death. First reports on programmed necrotic cell death in the 1980s and 1990s showed that TNF is able to induce both apoptotic and necrotic cell death (Laster *et al*, 1988; Fady *et al*, 1995). Further findings challenged the notion that necrosis is only an unregulated form of cell death showing that TNF stimuli (or FAS and TRAIL) can induce a RIPK1 dependent cell death (Holler *et al*, 2000). After the discovery of necrostatin-1, the inhibitor of RIPK1 kinase, that was able to block necrosis after death receptor signaling, programmed necrosis was termed necroptosis (Degterev *et al*, 2005).

Upon TNF stimulation the death-promoting complex IIb can be formed which leads to apoptotic signaling when functional caspase-8 is present. In contrast to that, cells lacking functional caspase-8 (or FADD) undergo necroptosis (Holler *et al*, 2000). Here, RIPK1 interacts with RIPK3 resulting in a cross-phosphorylation step that stabilizes their association and leads to the activation of their pro-necroptotic kinase activity. Activated RIPK3 binds to and phosphorylates MLKL (mixed lineage kinase domain-like) leading to the formation of a so called necrosome, a pro-necroptotic complex initiating necroptosis (Declercq *et al*, 2009; Vandenabeele *et al*, 2010; Sun *et al*, 2012). To date, not all details are known about the signaling events downstream of the necrosome, but it is suggested that RIPK3 activation regulates key metabolic enzymes leading to increased production of ROS (reactive oxygen species) in turn facilitating necrosis (Zhang *et al*, 2009). Recent findings also imply that MLKL can be located at the membrane to mediate Ca<sup>2+</sup> influx and TNF-induced apoptosis (Cai *et al*, 2014).

## 1.5 Inhibitor of apoptosis proteins as key regulators of apoptosis and necroptosis

IAPs were initially identified as the key regulators of apoptotic signaling by inhibiting the activities or activation of caspases. Although the precise mechanism is still debated, initial evidence demonstrated that IAP proteins, in particular XIAP, can act as direct inhibitors of pro-apoptotic caspases (Deveraux & Reed, 1999). However, subsequent biochemical analyses identified XIAP as the only *bona fide* caspase inhibitor within this protein family (Eckelman *et al*, 2006). Further biochemical analysis unraveled that the BIR2 and BIR3 domains of XIAP are responsible for the inhibition of caspases by a two-site binding mechanism (Uren *et al*, 1996; Deveraux *et al*, 1997; Eckelman *et al*, 2006). On the one hand, XIAP can bind to the dimerization surface of initiator caspase-9, thereby preventing its homodimerization and subsequent activation. Furthermore, structural studies showed that the inhibition of caspase-9 is mediated by the peptide-binding groove of the BIR3 domain of XIAP, interacting with a N-terminal region of the small subunit p12 of processed caspase-9 containing a four-amino-acid IBM (IAP binding motif) (Srinivasula *et al*, 2001; Shiozaki *et al*, 2003). On the other hand, XIAP has also been shown to inhibit effector caspases-3 and -7 by interaction of the linker region of its BIR1 and 2 domains with the substrate-binding site in the small subunits of the activated caspases (Chai *et al*, 2001; Riedl *et al*, 2001). The IBM is not only present in the small subunits of caspases but also in several mitochondrial IBM-containing proteins which regulate the inhibitory action of XIAP. The most important IBM-containing members involved in apoptosis are SMAC and OMI that reside in the mitochondrial IMS and are released into the cytosol after MOMP (Vaux & Silke, 2003). SMAC harbors an N-terminal MTS (mitochondrial-targeting sequence) that is proteolytically removed upon its release, whereby the IBM, a AVPI (Ala-Val-Pro-Ile) tetrapeptide motif for binding of XIAP, cIAP1 and cIAP2 (Chai *et al*, 2000a; Verhagen *et al*, 2000; Du *et al*, 2000) becomes exposed. Even though cIAP1 and cIAP2 are described only as weak inhibitors of caspases, they can bind to SMAC with high affinity and thereby may prevent it from blocking XIAP-mediated caspase inhibition (Eckelman *et al*, 2006).

Furthermore, cIAPs are also key regulators of the extrinsic apoptotic pathway by stabilizing complex I and thereby inhibiting the formation of complex II. Unlike the BIR1 domain of XIAP, the BIR1 domain of both cIAPs mediate the interaction with TRAF2 in complex I of the TNFR1 signaling pathway (Samuel *et al*, 2006; Varfolomeev *et al*, 2007). cIAP-mediated ubiquitination (K63-linked chains) of RIPK1 is essential for the activation of NF- $\kappa$ B signaling beside ubiquitination by LUBAC (Mahoney *et al*, 2008; Varfolomeev *et al*,



2006; Bertrand *et al*, 2008). Non-ubiquitinated RIPK1 (instead of TRADD) recruits FADD and caspase-8 to complex IIb and induce a switch to cell death signaling. This complex can only be formed in the absence of cIAPs and results in the activation of caspase-8 and induction of apoptosis (Petersen *et al*, 2007; Varfolomeev *et al*, 2007; Vince *et al*, 2007) or in the activation of RIPK1-RIPK3 mediated necrosis (Zheng *et al*, 2006; He *et al*, 2009).

## 1.6 Inhibitor of apoptosis proteins as regulators of nuclear factor $\kappa$ B signaling pathways

Beside the role in apoptotic signaling, IAPs are also key regulators of pro-survival NF- $\kappa$ B signaling pathways, regulating a range of target genes that are involved in several pathways such as inflammation, survival, cell death, migration and angiogenesis (Perkins, 2012; DiDonato *et al*, 2012). In mammals, the NF- $\kappa$ B family of transcription factors consists of the five proteins p65 (RelA), RelB, c-Rel, NF- $\kappa$ B1 (p105/p50) and NF- $\kappa$ B2 (p100/52) that form distinct homo- and heterodimeric complexes which bind to  $\kappa$ B sites in promoter- and enhancer-regions of target genes. Under unstimulated conditions NF- $\kappa$ B proteins are bound to inhibitor of  $\kappa$ B (I $\kappa$ B) proteins to retain inactive NF- $\kappa$ B dimers in the cytosol. Different stimuli like bacterial and viral infection, oxidative stress and inflammatory cytokines induce the degradation of I $\kappa$ B proteins through phosphorylation by the I $\kappa$ B kinase (IKK) complex. This complex consists of IKK $\alpha$  and IKK $\beta$ , two catalytically active kinases and the regulatory subunit IKK $\gamma$  (also known as NEMO, NF- $\kappa$ B essential modulator). The expression of NF- $\kappa$ B genes can be either regulated by the canonical or the non-canonical signaling pathway, but both involve the cIAPs as crucial regulators (Fig. 1.3).

The canonical signaling pathway is activated by cIAPs through their ubiquitin ligase activity upstream of the activation of NF- $\kappa$ B in a number of TNF superfamily receptors such as TNFR1. For instance, in the TNF-R signaling complex I, cIAPs promote a K63-linked poly-ubiquitination of RIPK1 (Bertrand *et al*, 2008; Varfolomeev *et al*, 2008) serving as a binding platform to recruit the IKK complex, TAK complex (TAK1 and TAB1/2) and LUBAC (linear ubiquitin chain assembly complex) (see Fig. 1.3). This results in the activation of IKK $\beta$  that in turn phosphorylates the inhibitor of NF- $\kappa$ B, I $\kappa$ B and leads to its poly-ubiquitylation and subsequent degradation. This yields in the activation and nuclear translocation of NF- $\kappa$ B (RelA-p50) and hence the expression of canonical NF- $\kappa$ B target genes.

Noteworthy, beside the regulation by cIAPs, XIAP can also induce the NF- $\kappa$ B activation during TGF- $\beta$  and BMP signaling in response to genotoxic stress. TAB1 is activated by the BIR1 domain of XIAP and couples the activated TAK1 to the IKK complex, promoting canonical NF- $\kappa$ B signaling (Lu *et al*, 2007; Jin *et al*, 2009). Furthermore, in addition to the well-recognized function as an inhibitor of apoptosis, XIAP has also been shown to play an important role in NOD signaling, regulating the activation of NF- $\kappa$ B during inflammatory signaling (Andree *et al*, 2014; Gyrd-Hansen & Meier, 2010).

In contrast to their positively regulating role in canonical NF- $\kappa$ B signaling, cIAP proteins are also main negative regulators of non-canonical signaling (Fig. 1.3). In unstimulated cells cIAPs reside in a cytoplasmic complex composed of NIK, TRAF2 and TRAF3 proteins, maintaining low levels of NIK (NF- $\kappa$ B inducing kinase) by its constitutive ubiquitin-dependent proteasomal degradation (Varfolomeev *et al*, 2007; Vince *et al*, 2007). Upon stimulation of a member of the TNFR family such as the TWEAK receptor FN14 (TNF-related weak inducer of apoptosis, fibroblast growth factor-inducible 14), CD40 ligand receptor and LT- $\beta$ R (lymphotoxin- $\beta$  receptor), TRAF2, TRAF3 and cIAPs are recruited to the receptor-signaling complex. This leads to the self-ubiquitination and subsequent degradation of cIAPs accompanied by the degradation of TRAF2 and TRAF3. As a consequence, NIK is stabilized and accumulates followed by phosphorylation and activation of IKK $\alpha$  which in turn triggers the nuclear translocation of NF- $\kappa$ B (RelB-p52) (Senftleben *et al*, 2001; Xiao *et al*, 2001).

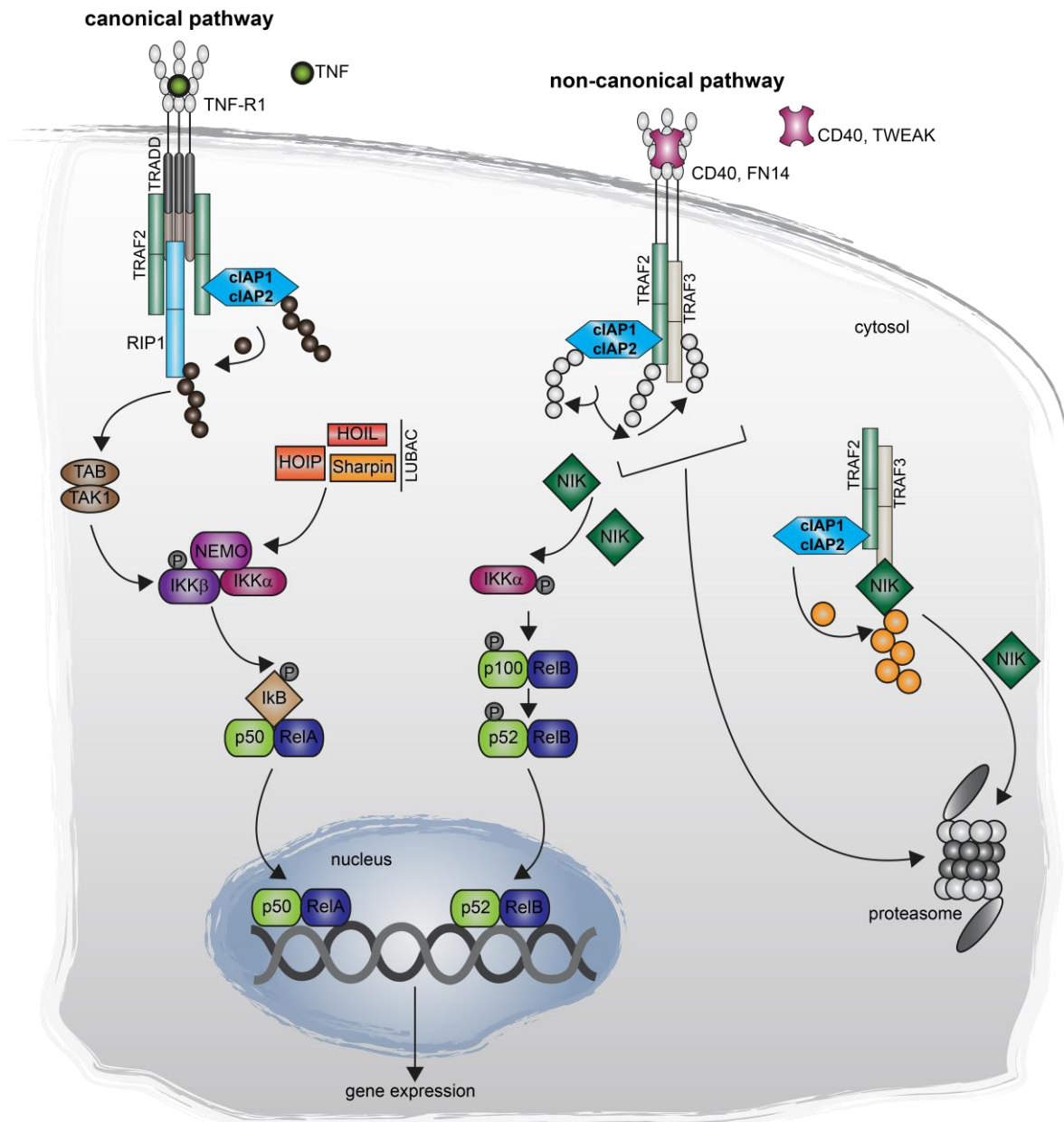


**Fig. 1.3 Canonical and non-canonical NF- $\kappa$ B signaling pathways**

cIAPs are positive key regulators of canonical NF- $\kappa$ B signaling and negative key regulators of non-canonical NF- $\kappa$ B signaling. In the canonical NF- $\kappa$ B signaling pathway, ubiquitinated cIAPs and RIPK1 (ubiquitinated by cIAPs) serve as a binding platform for the recruitment of TAB/TAK, the IKK complex (NEMO, IKK $\beta$ , IKK $\alpha$ ) and the LUBAC complex (HOIL, HOIP, Sharpin) to activate IKK $\beta$ . This leads to the degradation of I $\kappa$ B and the translocation of p50 and RelA to the nucleus. In the non-canonical NF- $\kappa$ B pathway, cIAPs together with the adapter proteins TRAF2/3 constitutively ubiquitinate NIK, leading to its proteasomal degradation. Upon activation of TNF family receptors (e.g. CD40, FN14) cIAPs get recruited to a receptor-signaling complex, followed by self-ubiquitination and subsequent degradation of cIAPs. This liberates NIK leading to the activation of IKK $\alpha$ , partial degradation of p100 to p52. Translocation of p52 and RelB to the nucleus results in the activation of non-canonical NF- $\kappa$ B signaling.

## 1.7 Inhibitor of apoptosis proteins and human cancer

Apoptosis is substantial for maintaining tissue homeostasis by counteracting mitosis or by eliminating the so called un-wanted cells such as transformed or infected cells (Hanahan & Weinberg, 2011). Dysregulation of apoptosis has been implicated in numerous pathological conditions, including autoimmune diseases, degenerative disorders and cancer. The expression and function of IAPs are reported to be dysregulated in a variety of human cancers. This can be due to genetic aberrations, an increase in their mRNA or protein expression or the loss of endogenous regulatory circuits e.g. mitochondrial IBM proteins. The elevated expression of IAPs in cancer frequently correlated with the resistance to anti-cancer therapy and poor prognosis in several types of cancer entities (Fulda & Vucic, 2012; Bai *et al*, 2014). In the following, the role of XIAP, cIAP1 and cIAP2 in human cancer will be discussed in more detail.

The genomic amplification of 11q21-22 which contains the genes encoding for cIAP1 and cIAP2 have been identified in several types of cancers indicating that alteration of cIAPs may contribute to oncogenic transformation. The 11q21-22 amplification is found in human cancers including esophageal carcinoma (Imoto *et al*, 2001), glioblastoma (Weber *et al*, 1996), hepatocellular carcinoma (Zender *et al*, 2006), non-small-cell lung cancer (NSCLC), small cell lung cancer (Dai *et al*, 2003) and pancreatic cancer (Bashyam *et al*, 2005). Furthermore, in cervical squamous cell carcinoma an elevated cIAP1-expression is associated with resistance to radiotherapy (Imoto *et al*, 2002) and a correlation of elevated cIAP protein level with advanced stages of tumors and poor survival is seen in colorectal and bladder cancer (Che *et al*, 2012; Krajewska *et al*, 2005). A constitutive activation of the NF- $\kappa$ B signaling pathway is frequently observed in mucosa-associated lymphoid tissue lymphoma (Morgan *et al*, 1999; Zhou *et al*, 2005; Varfolomeev *et al*, 2006). Here, a t(11;18)(q21;q21) translocation results in a fusion protein composed of the BIR domains of cIAP2 with MALT1 (paracaspase mucosa-associated lymphoid tissue lymphoma translocation protein 1) (Akagi *et al*, 1999; Dierlamm *et al*, 1999). Elevated levels of XIAP are associated with poor prognosis in many types of human cancer such as breast cancer (Zhang *et al*, 2011), colorectal cancer (Moussata *et al*, 2012), prostate cancer (Seligson *et al*, 2007) and chronic lymphocytic leukemia (Grzybowska-Izydorczyk *et al*, 2010). In 55% of patients with diffuse large B cell lymphoma, elevated levels of XIAP were observed, correlating with poor clinical outcome (Hussain *et al*, 2010). High expression of XIAP, cIAP1 and cIAP2 correlate with poor outcome of multiple myeloma patients after chemotherapy (Nakagawa *et al*, 2006). Furthermore, the natural IAP antagonist SMAC is also associated with different tumor stages. For instance, low levels of SMAC correlate with advanced tumor stage, high grade and poor prognosis in renal cell carcinoma

(Kempkensteffen *et al*, 2008) and in breast carcinoma SMAC expression inversely correlates with the tumor stage (Pluta *et al*, 2011).

Taken together, these observations indicated a possible role of IAPs in human cancer and identified a promising therapeutic target in cancer patients.

## **1.8 Targeting inhibitor of apoptosis proteins for cancer therapy**

From the discovery of XIAP in the second half of the 1990s, research on this unique IAP has been exponential, giving us a detailed structural and mechanistic view of its function. As a result, XIAP was considered as a promising therapeutic target in mammalian cancer, and research efforts have been focusing on the development of drugs targeting XIAP (IAP inhibitors), as a new way to counteract cancer and overcome drug resistance (Kashkar, 2010). Two broad approaches have been taken to develop clinical inhibitors of XIAP, including antisense oligonucleotides diminishing XIAP expression and small molecule inhibitors antagonizing XIAP function (caspase binding and/or inhibition). In particular, the generation of small-molecule IAP antagonists is considered to be one of the most promising amongst them (Vucic & Fairbrother, 2007; Ndubaku *et al*, 2009; Fulda & Vucic, 2012).

Within a cell IAPs can be antagonized by their natural antagonist SMAC which has been used to design and to develop small-molecule IAP antagonists (Du *et al*, 2000; Verhagen *et al*, 2000). After proteolytic cleavage of the N-terminal MTS and the release upon MOMP, the cytosolic SMAC with an N-terminal AVPI motif can directly bind and inhibit the interaction of IAP with their target proteins e.g. caspases. Eventually, SMAC dimerizes and binds to the BIR2 and BIR3 domain of XIAP and disrupt its interaction with caspase-9, 3 and 7 (Liu *et al*, 2000; Wu *et al*, 2000). SMAC may additionally bind to the BIR3 domain of cIAPs, promoting the auto-ubiquitination of cIAPs which in turn results in their degradation (Yang & Du, 2004). These observations indicated that SMAC can antagonize different IAPs and the therapeutic targeting of XIAP based on the biochemical features of cellular SMAC may result in the antagonization of XIAP but also cIAPs. The feasibility of disrupting IAP function by SMAC-derived peptidomimetic compounds frequently referred to as SMAC mimetics (SM) has been broadly accepted and an increasing number of patent applications and reports on the use of SM compound in pre-clinical and clinical studies aims at evaluation of these compound in cancer therapy.

The design of SM was greatly facilitated by the determination of the structural and biochemical basis of apoptotic activation by SMAC. Especially, co-crystal structure of the SMAC protein with the XIAP-BIR3 domain (Chai *et al*, 2000) and the solution structure of a SMAC peptide complexed with XIAP-BIR3 domain (Liu *et al*, 2000) form the basis for the design of SM. Biochemical data indicate that the four-residue peptide AVPI can bind to the XIAP-BIR3 domain with similar affinity as SMAC protein and coupled with understanding of the topology of SMAC peptide binding in a well-defined surface groove on XIAP-BIR3, resulted in the design of various SM and several of them are currently in clinical development for cancer treatment (Fulda & Vucic, 2012).

### **1.9 Development of SM as antagonists of inhibitor of apoptosis proteins**

Initial studies developed SMAC-derived peptides using the IAP-binding motif to mimic the activity of SMAC proteins (Vucic *et al*, 2002; LaCasse *et al*, 2008). These and other studies could show that SMAC-derived peptides have the capacity to induce an anti-tumoral effect *in vitro* and in xenograft models but unfortunately these peptides do not possess good pharmacological properties. However, these studies provided scientific and technical insights which led to the development of small-molecule IAP antagonists (Vucic *et al*, 2002; Arnt *et al*, 2002; Fulda *et al*, 2002).

In the following years, SMAC mimicking IAP antagonists (SMAC based peptidomimetics) with improved IAP-binding capacities and better pharmacological properties were developed. Here, an important step in the development was the increased rigidity into the scaffold. Altogether, small-molecule IAP antagonists can be divided into monovalent versus bivalent compounds and IAP-selective versus pan-selective compounds. While monovalent compounds harbor one IAP binding motif, bivalent compounds consist of two SM connected with a chemical linker (Ndubaku *et al*, 2009). Though bivalent SM are shown to generally display higher binding affinities to IAPs than monovalent compounds, featuring a high potency in cell death assays and inhibition of tumor growth they may also be associated with more toxic side effects (Varfolomeev *et al*, 2007; Vince *et al*, 2007; Bertrand *et al*, 2008). However, both types of SM were (so far) well tolerated in clinical trials, suggesting that both may be useful and tolerated in the clinic.

The majority of developed SM are pan-selective inhibitors, having a broad specificity to simultaneously antagonize XIAP, cIAP1 and cIAP2. During the last years SM were also designed to be specific for one IAP or a group of IAPs to target individual IAP proteins that have a defined biological role. Comparison of pan-IAP and IAP-selective antagonists

suggest that pan-IAP antagonists are in general more potent in promoting cell death in tumor cells (Ndubaku *et al*, 2009).

The first monovalent SMAC mimetic that showed a therapeutic potential for the treatment in a subset of cancer was compound 1 which was developed by Oost and colleagues (Oost *et al*, 2004) (Fig.1.4). Compound 1, is a potent and cell-permeable peptidomimetic, designed through extensive chemical modifications of residues in the AVPI motif. Compound 1 inhibits cell growth in several cancer cell lines and was active in a MDA-MB-231 breast cancer mouse xenograft model, representing the first study of a small-molecule SMAC mimetic with therapeutic potential. Another potent and orally active monovalent pan-IAP antagonist, primarily binding to cIAP1/2 (SM-406, AT-406, Fig.1.4) has been advanced into clinical development (Cai *et al*, 2011). Genentech developed a pan-IAP antagonist which inhibits tumor growth in the MDA-MB-231 xenograft model and has advanced into clinical development showing low oral clearance in mouse, rat and dog (GDC-0917, Fig.1.4) (Wong *et al*, 2013).

Bivalent SM were designed due to the fact that the natural SMAC forms a homodimer that is able to block the BIR2 and BIR3 domain of XIAP thereby blocking the interaction of XIAP with caspase-9/-3/-7. Therefore, it was hypothesized that bivalent SM may have a much higher binding affinity to XIAP. The first bivalent SMAC mimetic that linked two identical AVPI motifs (compound 2, Fig. 1.4) was reported 2004 by the Harran group (Li *et al*, 2004). Compound 2 revealed a high potency against a subset of human cancer cell lines and inhibited tumor growth in xenograft models of non-small cell lung cancer. In the following, recognizing the huge potential of this new class of SM, great efforts were made to develop new bivalent IAP antagonists. SM-164 was developed in 2007, showing very high affinity for targeting BIR2 and BIR3 of XIAP, being 100-times more potent than its monovalent counterpart and the natural SMAC AVPI peptide (Fig. 1.4) (Sun *et al*, 2007).

TetraLogic Pharmaceuticals developed a bivalent SM for clinical applications named Compound A (Cpd A, Fig.1.4) (Vince *et al*, 2007). Cpd A, is a pan-IAP antagonist which is shown to efficiently antagonize XIAP, cIAP1 and cIAP2 leading to killing of several cancer cell lines. Here, compound A is able to induce cell death as a single agent by sensitizing cells for a TNF-induced apoptotic death. The degradation of cIAP enhances RIPK1 binding to TNF-R1, stabilizes NIK, activates the non-canonical NF- $\kappa$ B signaling and induced TNF secretion (Vince *et al*, 2007). Moulin and co-workers highlighted the role of cIAPs in signaling and cell death during development and could also show that Cpd A, together with TNF can lead to a necroptotic cell death of MEFs (Moulin *et al*, 2012a). Recent findings imply that cIAPs and XIAP regulate myelopoiesis through cytokine production (Wong *et al*, 2014). The combined loss of XIAP, cIAP1 and cIAP2 can lead to death of macrophages and treatment with a pan-IAP antagonist induces the production of

several inflammatory cytokines in a TNF-R1 signaling dependent manner including TNF. These data indicate that a systemic treatment with pan-IAP SM could influence tumor immune cell infiltration. Despite its beneficial effects, recently it was shown that Cpd A is poorly tolerated *in vivo*, leading to body weight loss and treatment-related deaths of mice (Condon *et al*, 2014b).

In the last years, TetraLogic Pharmaceuticals generated a second-generation SMAC mimetic called Birinapant (TL32711, Fig.1.4) (Krepler *et al*, 2013; Benetatos *et al*, 2014). It is shown to primarily bind to cIAP1 and potentiated the activity of a variety of chemotherapeutic cancer drugs leading to inhibition of tumor growth in multiple primary patient-derived xenotransplant models. Furthermore, it can be used in well-tolerated doses and is currently in clinical trials. Future studies will illustrate the potential of Birinapant in human cancer therapy, and quite recently it got available for scientific and commercial use.



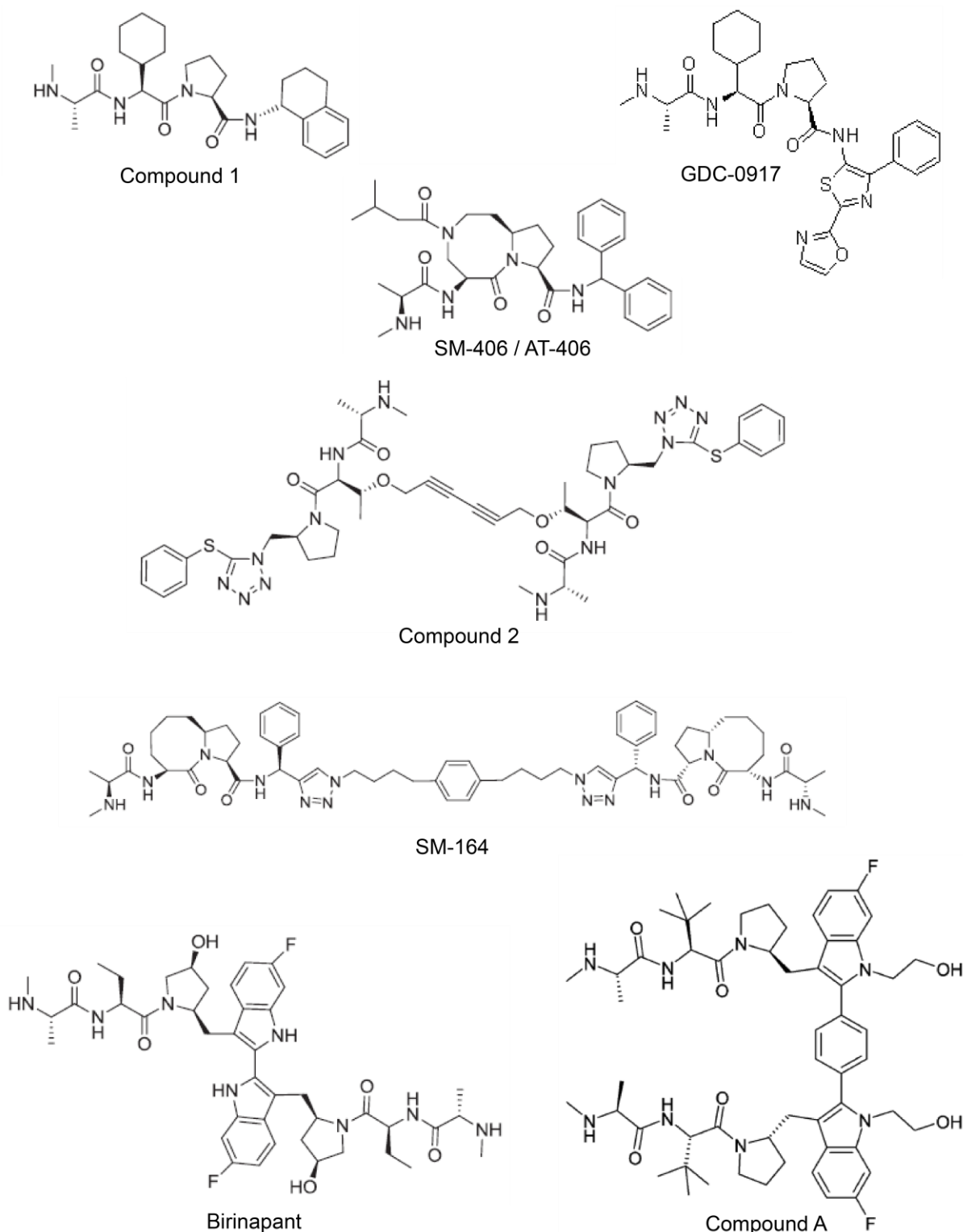


**Fig. 1.5 Chemical structures of representative SMAC mimetics**

Monovalent SMAC mimetics: Compound 1 ((Oost *et al*, 2004), SM-406 /AT-406 (Cai *et al*, 2011)) and GDC-0917 (Genentech) (Wong *et al*, 2013). Bivalent SMAC mimetics: Compound 2 (Li *et al*, 2004), Compound A (TetraLogic Pharmaceuticals) (Vince *et al*, 2007) and Birinapant (TetraLogic Pharmaceuticals) (Krepler *et al*, 2013).

## 1.10 Mechanisms of the antitumoral activities of SM

The majority of IAP antagonists was designed to harbor an antitumoral effect due to the binding to XIAP and to relieve caspase activity. However, studies on SM application in different cancer models demonstrated, that IAP antagonists induce apoptosis by specifically triggering cIAP degradation, NF- $\kappa$ B activation and autocrine TNF production (Varfolomeev *et al*, 2007; Vince *et al*, 2007).

Biochemical studies of unstimulated cIAP1 proteins show that the unliganded, multidomain cIAP sequester the RING domain within a compact, monomeric structure that prevents RING dimerization and thereby its E3-ligase activity (Dueber *et al*, 2011). Upon binding of SM to the BIR3 domain, crucial BIR3-RING interactions are blocked. This causes a conformational re-arrangement enabling RING dimerization and formation of the active E3 ligase which leads to the auto-ubiquitination of cIAP1 (Fig. 1.6).

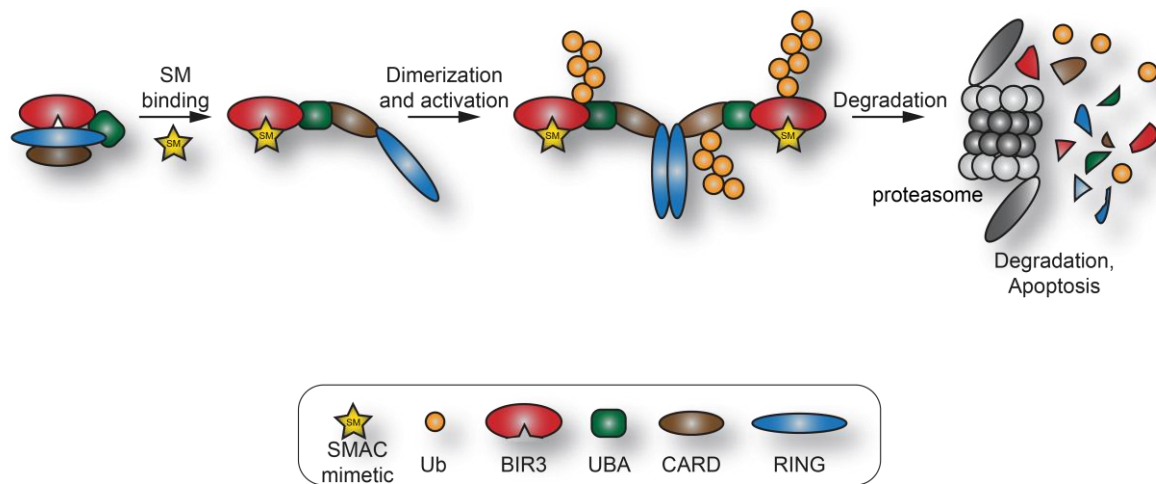


**Fig. 1.6 Model for the induction of cIAP protein ligase activity by IAP antagonists**

Unstimulated cIAP proteins form a closed, inactive and monomeric form. Upon SM binding to the BIR3 domain, crucial BIR3 interactions with the RING domain are disrupted, leading to a conformational change. The RING domains dimerize and form an active ubiquitin ligase. Subsequent auto-ubiquitination (K48) leads to proteasomal degradation of cIAP proteins and initiation of apoptosis.

Following the subsequent degradation of cIAP proteins NIK can accumulate, resulting in the activation of the non-canonical NF- $\kappa$ B signaling (Varfolomeev *et al*, 2007; Vince *et al*, 2007). One of the responsive genes is TNF that can in turn activate TNF-R1 in a paracrine/autocrine manner (Gaither *et al*, 2007; Petersen *et al*, 2007) (Fig. 1.7). Due to the loss of cIAPs in the transmembrane TNF-R1 complex, RIPK1 is non-ubiquitinated which allows the binding of FADD and caspase-8 to form the so called complex IIb leading to apoptosis (Fig.1.7). Therefore, IAP antagonization by SM leads to elimination of cIAPs

by activating its E3 ligase activity, resulting in a switch from pro-survival TNF signaling to pro-apoptotic signaling especially in cancer cells.

In contrast to the well established induction of apoptosis by SM compounds in tumor cells via degradation of cIAPs, the role of XIAP is less defined. On the one hand, activation of caspase-3 and -8 play a major role in SM induced apoptosis, whereas caspase-9 plays no or only minimal role. This suggests that the binding to the XIAP BIR3 domain is less important. On the other hand, absence of XIAP by siRNA or genetic deletion enhances the potency of SM to induce cell death in cancer cells. In addition, antagonization of cIAP and XIAP by pan-IAP antagonists is more potent in apoptosis induction than cIAP selective antagonists (Lu *et al*, 2007; Ndubaku *et al*, 2009b). Altogether, these observations suggest that an effective antagonization of XIAP can facilitate the TNF-dependent cell death upon SM treatment in cancer cells.

Aside from activating apoptosis, SM is reported to activate necroptosis in some cancer cells by involving the formation of necrosome (Fig. 1.7). While inhibiting caspase activity, a strong necroptotic response is seen in SMAC-resistant cancer cells which is determined by RIPK3 (He *et al*, 2009). Likewise, apoptosis resistant FADD- or caspase-8 deficient leukemia cells are primed for TNF-induced necroptotic death by treatment with SM (Laukens *et al*, 2011).

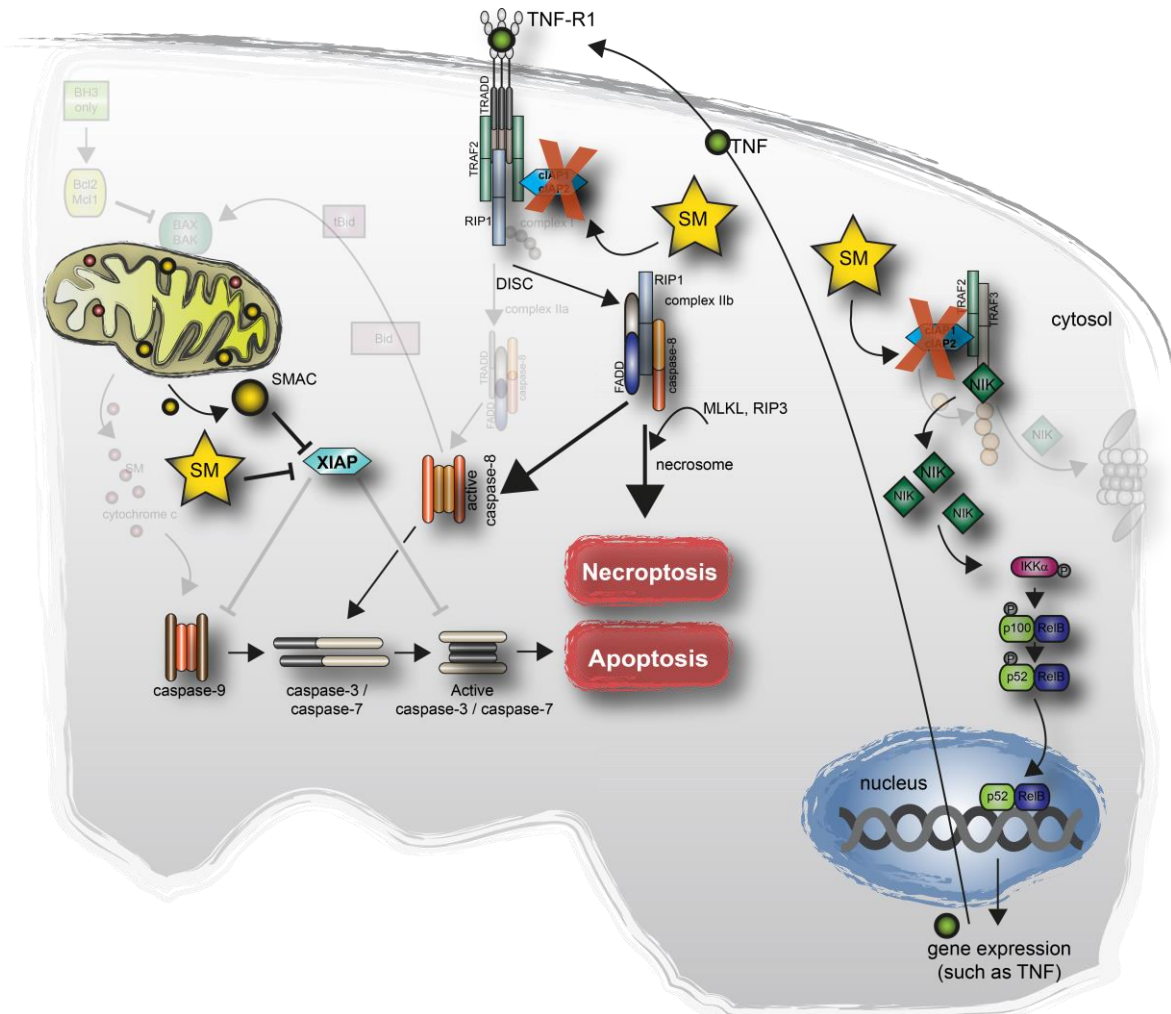


**Fig.1.7 IAP antagonization by SM results in NF- $\kappa$ B activation and induction of apoptosis or necroptosis**

Antagonization of cIAP1/2 results in the activation of the non-canonical NF- $\kappa$ B signaling due to a stabilization of NIK which can lead to the expression and secretion of TNF. TNF can activate the TNF-R1 signaling in a paracrine/autocrine manner resulting in a switch from pro-survival signaling towards cell death. Here, non-ubiquitinated RIPK1 together with caspase-8, FADD form the so called complex IIb that can either result in the activation of caspase-8 and apoptosis or in the formation of a necrosome (involving MLKL and RIPK3) leading to necroptosis. Additional antagonization of XIAP can effectively support the SM induced cell death.

Collectively, SM compounds so far were able to act directly on tumor cell survival primarily by promoting a TNF-dependent cell death which was enabled upon degradation of cIAPs.

### **1.11 Aim of the work**

IAP proteins are promising targets for drug development, given their potent anti-apoptotic activity and their overexpression which frequently occurs in various human tumor entities. Therefore, great effort has been made to design small pharmacological inhibitors of IAPs, called SMAC mimetics for the treatment of cancer.

One of the major focuses of our laboratory is to understand the role of IAPs in cancer. Based on our own previous results and accumulating evidence obtained by a number of *in vitro* analyses, the current work aims to explore the efficacy of SM as an anti-cancer drug *in vivo*. So far, SM treatment of cancer models like melanoma, are mainly performed in immune deficient NUDE mice (Lecis *et al*, 2010; Krepler *et al*, 2013; Condon *et al*, 2014; Benetatos *et al*, 2014). Here we study the impact of the SMAC mimetic compound A (Tetralogic) on tumor growth, using a B16 melanoma model in immune competent C57/BL-6 mice.

## 2. Materials and Methods

### 2.1 Chemicals and reagents

Unless indicated otherwise, all chemicals were from Sigma (Deisenhofen, Germany) or Roth (Karlsruhe, Germany). Compound A (Cpd A, SM) and Compound B (Cpd B, *ent*-SM) were provided by TetraLogic Pharmaceuticals (Malvern, USA) and m-TNF by Roche Applied Sciences (Mannheim, Germany). Necrostatin-1 and zVAD-fmk were obtained from Enzo Life Science. Matrigel (Phenol-red free, high conc.) was purchased from BD Biosciences (Heidelberg, Germany).

**Table 1: Primary and secondary antibodies**

Antibody	Isotype	Supplier
$\beta$ -Actin	mouse, monoclonal	Sigma-Aldrich (Deisenhofen, Germany)
CD31	rat, monoclonal	BD Biosciences (Frankfurt a.M., Germany)
CD45	rat, monoclonal	AbD Serotec (Puchheim, Germany)
CD68	rat, monoclonal	AbD Serotec (Puchheim, Germany)
cIAP1	goat, polyclonal	R&D Systems (Wiesbaden, Germany)
cIAP2	mouse, monoclonal	R&D Systems (Wiesbaden, Germany)
cleaved caspase-3	rabbit, monoclonal	Cell Signalling, (Frankfurt a.M., Germany)
Ki67	rabbit, polyclonal	Abcam (Cambridge, UK)
PARP	mouse, monoclonal	BD Biosciences (Heidelberg, Germany)
LYVE	rabbit, polyclonal	Abcam (Cambridge, UK)

Tubulin	mouse, monoclonal	Sigma-Aldrich (Deisenhofen, Germany)
XIAP	mouse, monoclonal	BD Biosciences (Heidelberg, Germany)
<b>Antibody</b>	<b>Isotype</b>	<b>Supplier</b>
Anti-mouse IgG HRP-linked	goat	Sigma (Deisenhofen, Germany)
Anti-rabbit IgG HRP-linked	goat	Sigma (Deisenhofen, Germany)
Anti-goat IgG HRP-linked	donkey	Santa Cruz (Heidelberg, Germany)
Anti-rat IgG HRP linked	goat	Life Technologies (Karlsruhe, Germany)

## 2.2 Cell lines

The murine melanoma cell line B16-F1 was purchased from ATCC (Bethesda, Maryland, USA) and was maintained in DMEM supplemented with 10% FCS, 2 mM L-glutamine, 100 µg/mL streptomycin, and 100 U/mL penicillin (Biochrom, Berlin, Germany). Human Umbilical Vein Endothelial Cells (HUVEC) and Human Dermal Microvascular Endothelial Cells (HDMEC) were purchased from Promocell (Heidelberg, Germany) and cultivated in endothelial cell growth medium (Endothelial Cell Growth Medium 2, Endothelial Cell Growth Medium MV, respectively) between passage 2-6. Plastic material was obtained from TPP (Trasadingen, Switzerland), BD Biosciences (Falcon™, Franklin Lakes USA) or Nunc (Roskilde, Denmark).

In brief, cells were expanded to an adequate amount and aliquots were frozen by -150°C in FCS containing 10% DMSO. For experiments, cells were thawed and expanded for 2 passages while culturing at 37°C.

Cells were transfected using Lipofectamine™LTX (Life Technologies, Karlsruhe, Germany) according to manufacturer's instructions.

## 2.3 Animal tumor models

C57BL6/J mice were purchased from Charles River (Sulzfeld, Germany) and TNF-R1/2<sup>-/-</sup> mice were obtained from P. Knolle (Munich, Germany) (Wohlleber *et al*, 2012). For the tumor experiments, 400 µl of chilled matrigel (BD Bioscience, Heidelberg, Germany) were mixed with 1 × 10<sup>6</sup> B16-F1 tumor cells and the SMAC-mimetic Cpd A (at a final

concentration of 2 $\mu$ M) or vehicle (PBS) at 4°C, for subcutaneous injection into recipient mice. Tumor size was measured every other day using precision calipers. Tumor volume was calculated as length x width<sup>2</sup> x  $\pi/6$  and expressed as fold induction relative to day 1  $\pm$ SEM.

For the *in vivo* vascularization assay, 500  $\mu$ L matrigel was mixed (4 °C) with vehicle, SM (2  $\mu$ M), TNF (50 ng/mL) or SM combined with TNF and subcutaneously-injected into the flank region of recipient mice for 12 days (Coutelle *et al*, 2014).

Animals were housed in the animal care facility of the University of Cologne under standard pathogen-free conditions with a 12 hours light/dark schedule and provided with food and water ad libitum. All animal experiments were performed in accordance with the German animal protection law.

#### **2.4 Tumor and matrigel plug preparation**

Tumors or matrigel-plugs were removed after sacrificing the mice. Samples were cut into appropriate pieces for further processing: (i) H&E staining, (ii) immunostaining and (iii) multiphoton-microscopy.

(i) appropriate pieces of tumors or matrigel-plugs were fixed in paraformaldehyde (PFA, 3% in PBS) at 4°C overnight and paraffinized for storage. Paraffin sections were first deparaffinized by xylol and ethanol incubations, H&E (Shandon, Thermo Scientific) stained and recorded using a DM4000B microscope (Leica Microsystems, Wetzlar, Germany).

(ii) appropriate pieces of tumors or matrigel-plugs were directly snap-frozen in Tissue-Tek® OCT™ Compound for storage and further processing.

(iii) appropriate pieces of tumors or matrigel-plugs were fixed in PFA (3%) overnight and stored in 0,1% PFA for further analyses.

#### **2.6 FITC-dextran application**

For visualization of vessel perfusion, 200 $\mu$ l FITC-Dextran (15mg/ml in PBS, MW 2,000,000, Sigma-Aldrich) was injected into the tail vein of mice 30 minutes before animals were sacrificed.

#### **2.5 Cell viability and cell death measurements**

Cell death was measured after treatment and viability was quantified by trypan-blue exclusion using an automated cell counter (Countess, Invitrogen, Karlsruhe, Germany) according to the manufacturer's instructions. In brief, before counting cells were detached



with trypsin and diluted to appropriate working concentrations. Cell suspension was then diluted with trypan blue in a ratio of 1:1 (v/v) and dead cells were measured.

### **2.7 Cell growth assay**

Cells were seeded (30% confluence) on 3 cm dishes, treated as indicated. Cell growth was analyzed by relative change in confluence using JuLi Br Live Cell Analyzer.

JuLi Br Live Cell Analyzer, Peqlab (brightfield microscope in a cell incubator, 4xplus digital zoom, High resolution digital camera) was used for the longterm acquisition of growth curves. B16-F1 cells ( $3,5 \times 10^5$ , 4 hours prior to experiment) were treated for 48 hours. Images were taken every 10 min.

### **2.8 NF- $\kappa$ B activity**

ELISAs were performed after nuclear extraction using the TransAM®Nuclear Extract Kit and the TransAM Nf $\kappa$ B p65 or p52 Kit (Active motif, Roxensart, Belgium) according to the instructions of the manufacturer. Read out was performed on a ELISA reader (Anthos HT2) at a wavelength of 450/620 nm.

### **2.9 TNF-ELISA**

The amount of m-TNF was measured after treatment with SM (2 $\mu$ M) compared to control. After treatment of cells, supernatant was removed and used for the subsequent analyses of secreted m-TNF, using the Mouse TNF-alpha High Sensitivity ELISA (eBIOSCIENCE, Frankfurt a.M., Germany) according to the manufacturer's instructions.

### **2.10 RNA isolation**

To obtain pure RNA from indicated cells for the quantitative real-time analysis, the standard phenol-chloroform-method was used (Chomczynski & Sacchi, 1987). After resuspending the cells in TRIzol, samples were further homogenized using QIAshredder columns. Chloroform was added and the homogenate was incubated to allow separation into a red lower organic layer (DNA and Proteins), interphase and a clear upper aqueous layer (RNA). Precipitations of RNA were performed with isopropanol and washed with 70% EtOH prepared with nuclease free H<sub>2</sub>O. For quantification of RNA in solution, a spectral photometer (NanoDrop® instrument) was used at a wavelength of 260nm. RNA was dissolved in DNase/RNase free water and stored at -80°C.

### 2.11 DNaseI

Isolated RNA from cells was purified with DNaseI (Thermo Scientific, Rockford, USA) to digest contaminating single- and double-stranded DNA according to the manufacturer's instructions.

### 2.12 Agarose gel electrophoresis

The quality of purified RNA was confirmed by agarose gel electrophoresis (1% agarose). Intact total RNA running on a denaturing gel, will separate into two distinct bands, representing the 28S and 18S rRNA (eukaryotic samples like HUVECs).

### 2.13 Reverse transcription (RT)

RT-PCR was performed using the Maxima H Minus First Strand cDNA Synthesis Kit (Thermo Scientific, Rockford, USA) with oligo dt-primers to generate cDNA for subsequent real-time analysis. Template RNA, primers and dNTPs (+ additional nuclease free water) were pre-incubated at 65°C for 5 minutes. The samples were chilled on ice for 3 minutes. RT-buffer and enzyme were added and subsequently incubated first at 25°C for 10 minutes, followed by incubation at 60°C for 30 minutes. Afterwards the reaction was terminated by heating to 85°C for 5 minutes. cDNA was stored at -80°C for long term storage or at -20°C up to 1 week.

### 2.14 Quantitative Real-Time PCR (qRT-PCR)

Quantitative real time PCR was used to measure expression levels of genes listed in table 2. qPCR was performed using LightCycler®SYBR-Green I Mix in triplicates (Roche Applied Sciences, Mannheim, Germany) using a 96well-plate Multicolor Real-Time PCR Detection System (iQ™5, BIO-Rad, Herkules, USA). Specific primers were used for each gene (table 2) and GAPDH was used as housekeeping control for normalization. Data were further evaluated using the Pfaffl-method ((Pfaffl, 2001)).

Table 2: Primer for qRT-PCR

Primer notation	Sequence
h-Cyr61 fwd	5'-CCC GTT TTG GTA GAT TCT GG-3'
h-Cyr61 rev	5'-GCT GGA ATG CAA CTT CGG-3'
h-GAPDH fwd	5'-GGT ATC GTG GAA GGA CT-3'
h-GAPDH rev	5'-GGG TGT CGC TGT TGA A-3'
h-PDGF-A fwd	5'-GCA AGA CCA GGA CGG TCA TTT-3'

h-PDGF-A rev	5'-GGC ACT TGA CAC TGC TCG T-3'
h-VEGF-A fwd	5'-AGG GCA GAAT CAT CAC GAA GT-3'
h-VEGF-A rev	5'-AGG GTC TCG ATT GGA TGG CA-3'
h-VEGF-C fwd	5'-GAG GAG CAG TTA CGG TC TG TG-3'
h-VEGF-C rev	5'-TCC TTT CCT TAG CTG ACA CTT GT-3'
h-VCAM-1 fwd	5'-GTC TCC AAT CTG AGC AGC AA-3'
h-VCAM-1 rev	5'-TGA GGA TGG AAG ATT CTG GA-3'
m-GAPDH fwd	5'- TCA CCA CCA TGG AGA AGG C-3'
m-GAPDH rev	5'- GCT AAG CAG TTG GTG GTG CA-3'
m-TNF fwd	5'- AGA ACT CCA GGC GGT GC-3'
m-TNF rev	5'- AGG GTC TGG GCC ATA GAA CT-3'

Table 3: qPCR-program

qRT-PCR	Program
qPCR	1. 95°C 1min
	2. 95°C 15 sec
	3. 60°C 30 sec
	4. 72°C 30 sec
	40-45 cycles (step 2.-4.)
	5. 72°C 5 min
	6. 4°C endless

### 2.15 Sample preparation for immunoblotting (IB)

Whole cell lysates were prepared by incubating cell pellets upon washing in CHAPS lysis buffer on ice for 25 minutes. After centrifugation, either pellets were prepared for Poly (ADP-ribose) polymerase (PARP) cleavage or supernatants were recovered for further applications. For PARP cleavage pellets were incubated in urea extraction buffer following denaturation at 100°C for 10 minutes. Protein concentration of supernatants was determined using BCA assay (BCA Assay Protein Quantification; Pierce, Bonn, Germany) according to the instructions of the manufacturer.

For Western blotting, equal amounts of protein were adjusted in 1x Laemmli buffer containing 4% beta-mercaptoethanol, followed by incubation at 100°C for 5 minutes.

Proteins were separated by sodium dodecyl sulfate-polyacrylamide gel electrophoresis (SDS-PAGE) using 10-14% polyacrylamide gels and Western Blotting Apparatus (BIO-RAD laboratories, Herkules, USA). Gels were started at 100mV and continued at 140-160mV in SDS running buffer prior to transfer onto nitrocellulose membranes (Protran, Schleicher & Schuell, Dassel, Germany) for 90 minutes in blot transfer buffer. After blocking and appropriate incubation in primary and secondary antibodies, protein signals were visualized by enhanced chemiluminescence (ECL; Thermo Scientific, Rockford, USA)

**Table 4: Buffers for sample preparation and Western blotting**

CHAPS lysis buffer	10 mM HEPES, pH 7.4, 150 mM NaCl, 1% CHAPS, protease complete cocktail
Urea extraction buffer	50 mM Tris (pH 6.8), 6 M urea, 3% SDS, 10% glycerol, 0.00125% bromphenol blue, 5% 2-mercaptoethanol
HEP buffer	20 mM Hepes, pH 7.5, 10 mM KCl, 1.5 mM MgCl <sub>2</sub> , 1 mM EDTA, 10 μM cytochalasin B, 1 mM DTT, protease inhibitor
SDS running buffer	14.4 % (w/v) Glycin, 3 % (w/v) Tris Base, 0.1% (w/v) SDS
Laemmli sample buffer (5 x)	0,6 M Tris-HCL pH 6.8, 144 mM SDS, 25 % (v/v) Glycerol, 0.1% (w/v) bromphenol blue, 5% (v/v) β-Mercaptoethanol
Blot transfer buffer	25 mM Tris base pH 8.3, 192 mM Glycin, 20 % (v/v) Methanol
Blocking buffer	10 mM Tris-HCl pH 7.4 – 7.6, 150 mM NaCl, 5 % (w/v) skim milk powder, 2 % (w/v) BSA, 0.1 % (v/v) Tween-20
Antibody dilution buffer	50 mM Tris, pH 7.6, 150 mM NaCl, 0.1% Tween-20, 5% BSA
S-PBS	1.2 M NaCl, 0.1 M NaH <sub>2</sub> PO <sub>4</sub> , 0.3 M K <sub>2</sub> HPO <sub>4</sub> , pH 7.6

### 2.16 Clonogenicity Assays

1x10<sup>4</sup> cells per well were seeded in 6-well plates and allowed to settle. Cells were then transiently exposed to Cpd A, Cpd B or TNF at indicated concentrations for 48 hours. After recovering for 10 days in fresh medium without treatment, colony formation was assessed by crystal violet staining. Cells were washed in PBS, stained with crystal-violet (0.2% in 2% EtOH) and dissolved in 0.2 M sodium citrate and 100% EtOH (1:1).

### 2.17 Tube formation assay

Matrigel (500  $\mu$ l/12well) (5 mg/ml, BD Biosciences, Heidelberg, Germany) in 12 well plates was allowed to reach the solid phase after one hour at 37°C. HUVEC cells in endothelial cell growth medium containing Cpd A (2 $\mu$ M), Cpd B (2 $\mu$ M) or TNF (20ng/ml) at the indicated concentrations were seeded on top of the Matrigel at a density of 5x10<sup>4</sup> cells per well (developing network). After incubation at 37°C for 36 hours the wells were photographed using an inverted phase contrast microscope (Cell-R, Olympus, Hamburg, Germany). Established network: Tube formation assay; therefore HUVEC cells were incubated for 36 hours in endothelial cell growth medium before Cpd A and TNF was added to the media. The wells were photographed after additional 48 hours. Four images were used per well for quantification. For quantification of tubes, each branch point with 3 or more branches was counted. Branch point counts per image constituted the raw data for statistical analysis.

### 2.18 Tissue Immunostaining

H&E: Tumors or matrigel plugs were fixed in 4% paraformaldehyde overnight. Samples were processed using an ASP300 S Tissue Processor (Leica, Wetzlar, Germany). Embedded samples were cut using a sliding microtome HM 400 (Thermo Scientific, Fisher Scientific GmbH, Schwerte, Germany) to produce 7 - 15  $\mu$ m thick sections. Staining was performed with haematoxylin/eosin (Thermo Scientific, Fisher Scientific GmbH).

Immunostaining: Samples were cut to produce 20 – 30  $\mu$ m thick sections. These sections were fixed in acetone (-20°C) for 2 minutes. Blocking was performed with normal goat serum (10%) in PBS for 30 minutes (room temperature). Subsequently sections were incubated with primary antibodies at 4°C overnight. Followed by washing for two times with PBS for 5 minutes. Sections were incubated with secondary antibodies for 1 hour at room temperature and embedded with Immu-Mount (Thermo Scientific) subsequent to two washes with PBS for 5 minutes.

### 2.19 Microscopy

For immunofluorescence analyses, a motorized inverted microscope (Olympus IX81 or IX71 equipped with Cell<sup>^</sup>R Imaging Software; Tokyo, Japan) was used. For staining of HUVEC cells (Tubulin, DAPI, cleaved caspase-3), 3x10<sup>5</sup> were fixed with 3% Paraformaldehyde, permeabilized with 0.1% saponin for 30 minutes and blocked with

blocking buffer for 30 minutes. Subsequently cells were incubated with the appropriate primary antibody in blocking buffer containing 0.1% saponin over night at 4°C. Afterwards

cells were washed twice for 5 minutes with blocking buffer and incubated with secondary antibody for 1 h at room temperature. Cells were washed twice with blocking buffer and once with PBS for 5 minutes. DAPI (Molecular Probes, Life technologies, Karlsruhe, Germany) was added into the first washing step (1:5000) for nuclei staining. Cover slides were mounted using Mowiol mounting medium

Two-photon fluorescence microscopy for deep tissue imaging was performed with an upright laser scanning microscope (TCS SP8 MP, Leica). For excitation of FITC dextran staining, the infrared laser (Chameleon Vision II, Coherent) was tuned to 960 nm. Images were acquired using a 25x water objective (HCX IRAPO L25x/0.95 W) and the resulting signal was collected using an internal non-descanned detector. 3D presentation and volume rendering of the acquired images were performed using the software Imaris 7.0.0 (Bitplane).

Z-stacks of matrigel plugs were taken using a motorized Leica M165 FC fluorescent stereomicroscope equipped with a DFC490 CCD camera and GFP2 (ex.480/40nm) filter set. Images were processed using a Multifocus module of the LAS 3.7.0 software (Leica).

**Table 5: Buffers and sample preparation for microscopic analysis**

Permeabilization buffer	0.1% Saponin, PBS
Blocking buffer	3% BSA, 0.1% Saponin, PBS
Mowiol	10% Mowiol, 25% Glycerol, 0.1 M Tris, 2.5% DABCO, H <sub>2</sub> O
Phosphate buffer	0.12 M phosphate in H <sub>2</sub> O
Fixation buffer	2% glutaraldehyde, 0.12 M phosphate buffer

**2.20 Statistical analyses**

Significance of differences between the means of two groups were analyzed by two-sided unpaired Student's t-test. Differences were considered statistically significant at \* $p < 0.05$ , \*\* $p < 0.01$ , \*\*\* $p < 0.001$ . Statistical analyses were performed using GraphPad Prism5 (GraphPad Software, Inc., San Diego, CA, USA).

### 3. Results

#### 3.1 IAP antagonization inhibits tumor growth *in vivo*

Previous studies showed that SMAC mimetics (compound A, SM) efficiently promote cytotoxicity towards malignant tumor cells *in vitro* and the initial *in vivo* analyses employing the xenograft tumor models in immune incompetent mice confirmed the anti-tumor activity of these compounds (Lecis *et al*, 2010; Krepler *et al*, 2013; Condon *et al*, 2014a; Benetatos *et al*, 2014). To further investigate the anti-tumor activity of SM we established a melanoma mouse model by using immune competent mice bearing B16 melanoma tumors. Previous studies concerning the anti-tumor activity of SM demonstrated that the systemic application of compound A resulted in body weight loss (10-18%) and treatment-related deaths (4/7) (Condon *et al*, 2014a). Therefore, to overcome the poor systemic tolerability of this SM, B16 melanoma cells were mixed with matrigel containing SM at a final concentration of 2  $\mu\text{M}$  or vehicle (control) and injected into the flank region of C57/Bl6 mice (Fig. 3.1).

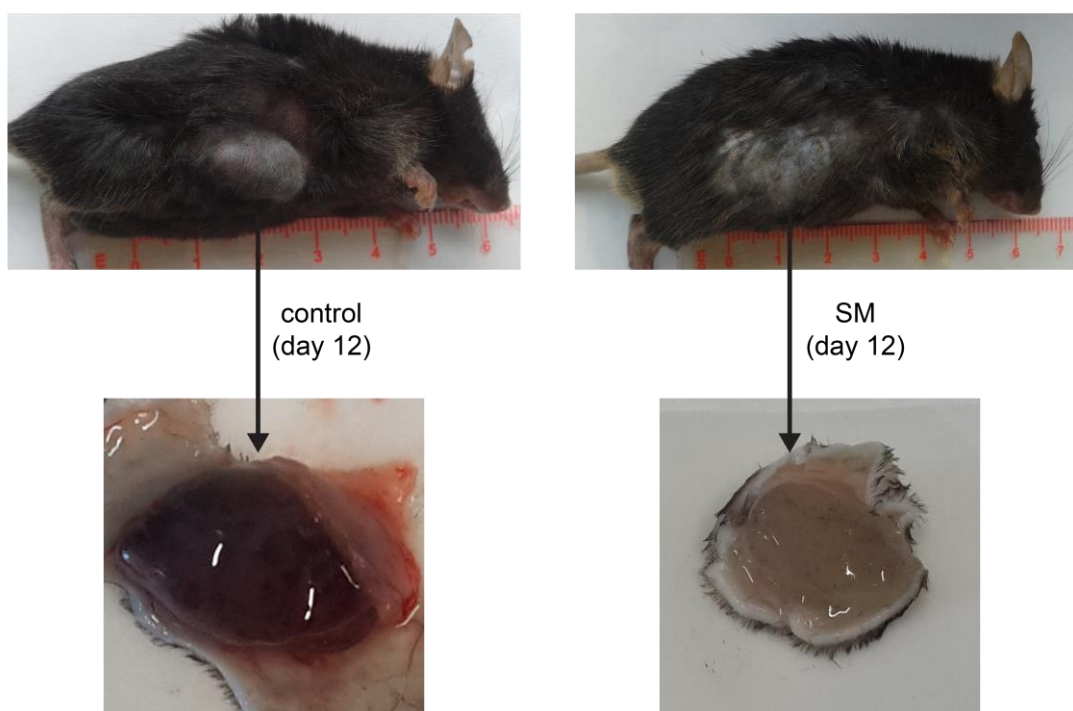


**Fig. 3.1 Subcutaneous application of (matrigel-) tumor cells into wt-mice**

B16 melanoma cells were mixed with matrigel ( $4 \times 10^5/400\mu\text{l}$ ) containing SM (compound A) at a final concentration of 2  $\mu\text{M}$  or vehicle. After injection into the flank region of C57/Bl6-mice, tumor growth was recorded for 12 days. After sacrificing the mice, (matrigel-) tumors were dissected for further analysis.



Tumors were recorded and measured daily for up to 12 days until the tumor volume reached a critical size (diameter, 2cm). These analyses showed that tumor growth was significantly attenuated in the presence of SM compared with vehicle-treated controls (Fig. 3.2A). Especially at day 6-7, tumor growth started to accelerate in vehicle treated mice. Histological analysis further confirmed the lack of tumor growth when matrigel plugs were supplemented with SM. H&E staining visualized tumor cells (blue) within control matrigel plugs, whereas the SM-containing matrigel plugs lack any tumor cells (pink) (Fig. 3.1B).

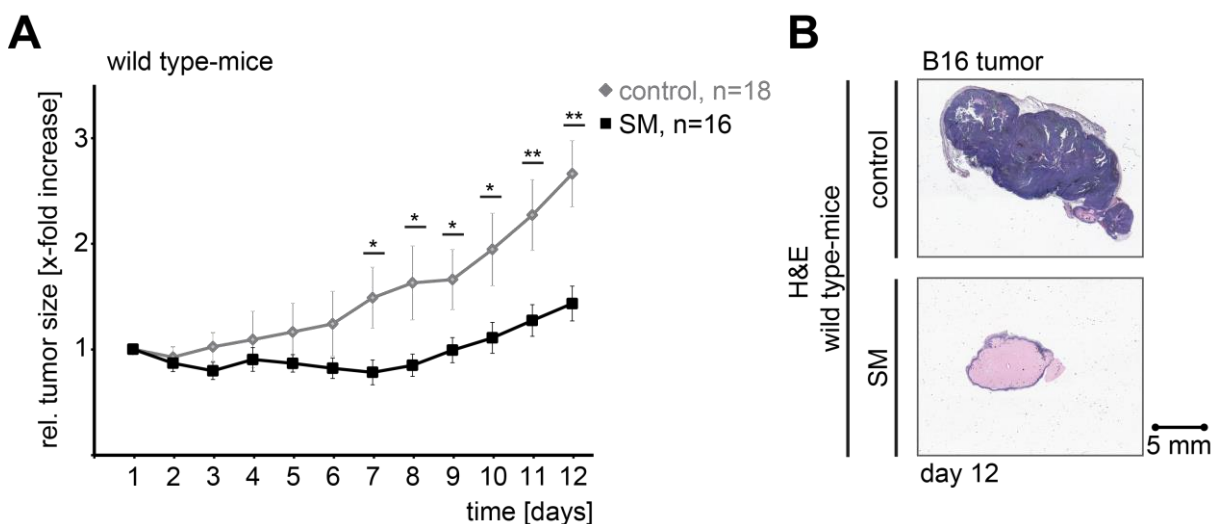


**Fig. 3.2 IAP antagonization inhibits tumor growth *in vivo***

**A.** The murine melanoma cell line B16 was mixed with matrigel and vehicle or SM (2  $\mu$ M) and subcutaneously injected into the flank region of recipient C57/Bl6 mice. Tumor size was measured in 2 dimensions and the calculated volume was recorded daily. Data points represent the mean  $\pm$  SEM.

**B.** Histological analysis of B16 tumors was performed on day 12 by H&E staining and representative pictures are illustrated.

In line with previous studies, our data showed that the IAP antagonist SM is also capable to inhibit tumor growth in immune competent mice (Fig. 3.2). Previous studies indicated that SM provokes direct cytotoxicity towards tumor cells. In order to prove this notion, tumor sections on day 5 and 12 were analyzed and tumor cell proliferation was assessed by specific staining of Ki67 (marker for proliferation), using a specific anti-Ki67 antibody (Fig. 3.3). The number of proliferating tumor cells however revealed no significant difference between control and SM-treated tumor cohorts (Fig. 3.3).

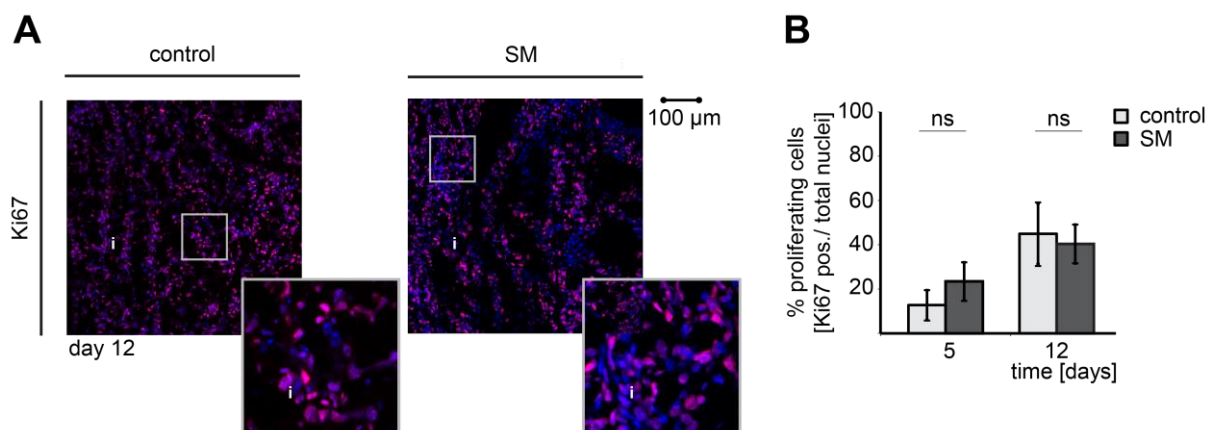


**Fig. 3.3 IAP antagonization inhibits tumor growth *in vivo* without an attenuated proliferation in tumor cells**

**A** Histological analysis of implanted tumors (Fig. 3.2) stained for proliferation using a Ki-67 antibody (red) and nuclei were counterstained with DAPI (blue). Sections on day 12 of intratumoral regions (i) are illustrated.

**B** The quantification of proliferating cells was made by automated counting of Ki67 positive and the total DAPI stained nuclei. The number of Ki67-positive cells was then expressed as a percentage of the total. The quantification was performed in 2 fields of 200x magnified tumor regions (intratumoral). Data represents the mean  $\pm$  SEM.

To investigate if the attenuated tumor growth in SM-treated mice is a result of an increased apoptotic death of tumor cells (as previously shown), the activation of the executioner caspase-3 was investigated using an anti-active-caspase-3 antibody in tumor sections on day 5 and 12 (Fig. 3.4). At day 5 (nearly) no cells underwent cell death. Tumors at later stages (day 12) showed only a weak immunoreactivity to the anti-active-caspase-3 antibody in SM-treated and untreated cohorts (Fig. 3.4B), indicating the lack of apoptotic death of tumor cells upon SM exposure.

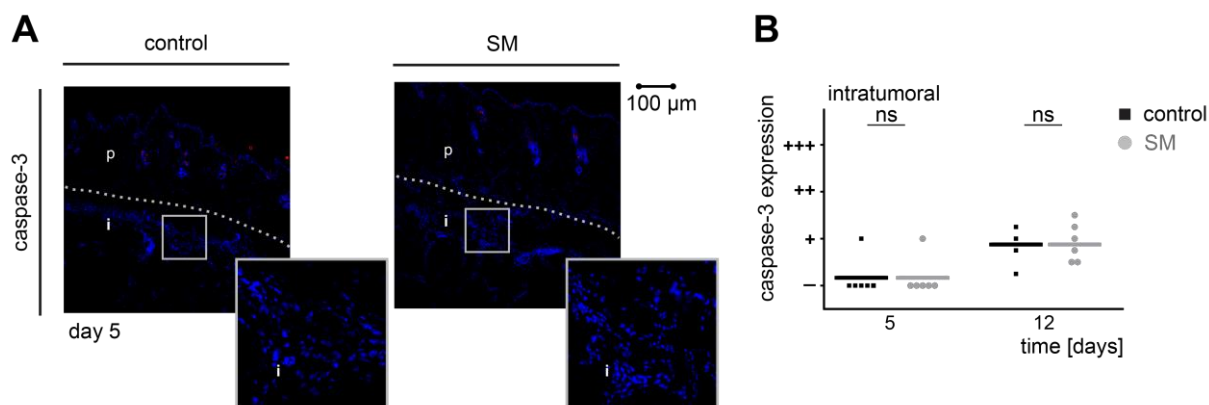


### Fig.3.4 IAP antagonization inhibits tumor growth *in vivo* without any direct cell death of tumor cells

**A** Histological analysis of implanted tumors (Fig. 3.2) stained for cell death using an antibody for active caspase-3 (red) and nuclei were counterstained with DAPI (blue). Sections on day 5 of intratumoral (i) and peritumoral (p) regions are illustrated.

**B** Amount of caspase-3 positive tumor cells was qualitatively estimated according to the intensity of specific staining and were arbitrarily set as the following: -, not expressed; +, low expression; ++, moderate expression; +++, strong expression.

To further substantiate our *in vivo* observations, cultured B16 cells were exposed to increasing amounts of SM or an inactive control SMAC mimetic enantiomer (compound B, *ent*-SM) and cell death was examined (Fig. 3.5). Notably, the majority of previous reports indicated that SM induces anti-tumor activity by promoting TNF-induced cell death. Therefore, cell death was also examined when tumor cells were exposed to SM or *ent*-SM in conjunction with TNF (20 ng/ml). Neither alone nor in combination with TNF, SM was able to induce any cytotoxicity in tumor cells up to 48 hours (Fig. 3.5A). Similar results were observed using *ent*-SM (Fig. 3.5B).

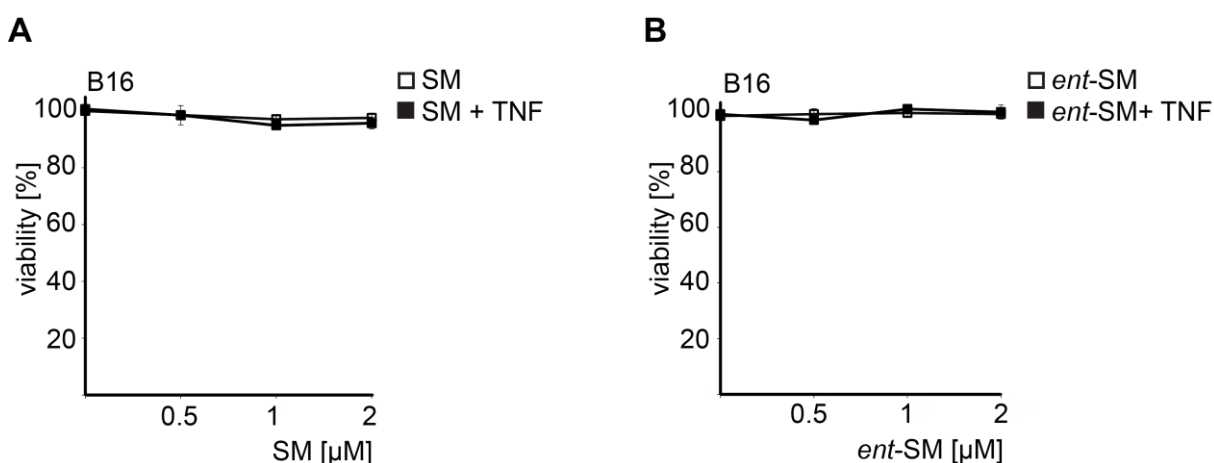
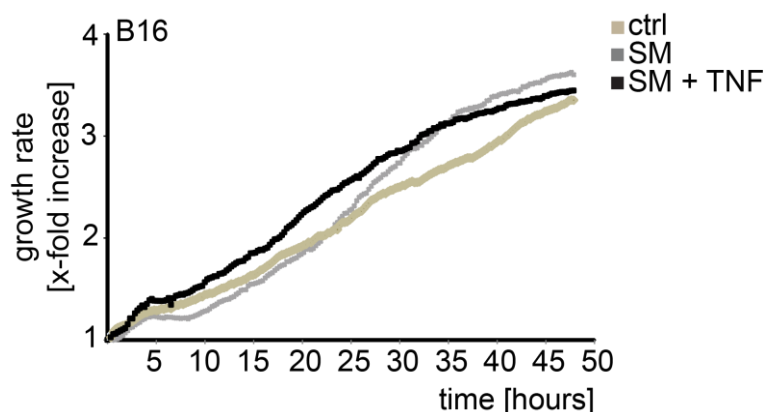


### Fig 3.5 B16 cells are resistant to SM and TNF treatment *in vitro*

B16 cells were treated with increasing amounts of SM (A) or *ent*-SM (B) alone or combined with TNF (20 ng/ml). Cell viability was measured by trypan blue exclusion after treatment for 48 hours. Data represent the mean  $\pm$  SEM.

To investigate the proliferation of cultured B16 cells upon treatment with SM or SM combined with TNF, growth rate of B16 cells was documented by videography every ten minutes for 48 hours. The confluency of cells was automatically calculated using a JuLi Br

Live Cell Analyzer (Peqlab). Analysis of growth rate of tumor cells revealed no significant difference in proliferation upon stimulation (Fig 3.6).

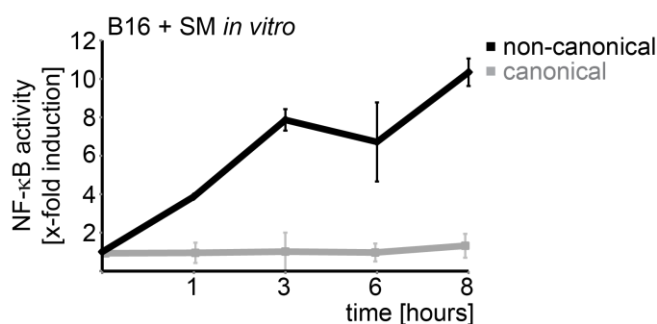
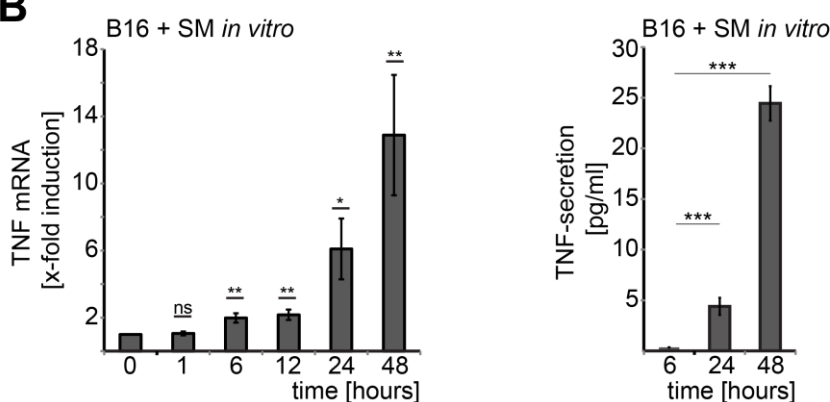


**Fig. 3.6 Cell growth of B16 cells is not altered upon SM and TNF treatment *in vitro***

The relative cell growth of B16 cells, treated with SM (2  $\mu$ M) alone or combined with TNF (20 ng/ml) was analyzed with JuLi Br Live Cell Analyzer (Peqlab) for 48 hours (interval of 10 minutes).

Taken together, our *in vitro* and *in vivo* analyses showed that SM did not induce any direct cytotoxicity towards tumor cells or attenuate their proliferation rate, either alone or in conjunction with TNF (Fig. 3.1–3.6)

In addition to its cytotoxic effects, the initial studies concerning the cellular response to SM compounds showed that SM treatment induced canonical and non-canonical p52 NF- $\kappa$ B activity (Vince *et al*, 2007; Varfolomeev *et al*, 2007; Petersen *et al*, 2007). In line with these observations, analysis of NF- $\kappa$ B activity using ELISAs showed that SM treatment potently induced the non-canonical NF- $\kappa$ B activation. In contrast to previous data, no induction of canonical NF- $\kappa$ B activity was observed when B16 cells were treated with SM (Fig. 3.7A). Non-canonical NF- $\kappa$ B signaling upon SM stimulation was reported to induce TNF secretion, which was shown to be responsible for the SM-mediated cytotoxicity in a subset of tumor cell lines. Consistent with the increased non-canonical NF- $\kappa$ B activation transcriptional up-regulation of TNF was detected in B16 melanoma cells upon SM treatment (Fig. 3.7B, left panel). TNF was also detectable in the supernatant of B16 cells after SM treatment as analyzed by TNF-ELISA (Fig. 3.7B, right panel).

**A****B**

**Fig. 3.7 IAP antagonization induces non-canonical NF-κB signaling and TNF secretion in B16 cells**

**A.** Measurement of canonical and non-canonical NF-κB activation in B16-F1 cells by ELISA (TransAM) after stimulation with SM (2 μM) at indicated time points. Data represent the mean ± SEM.

**B.** qRT-PCR analysis of B16 cells after stimulation with SM (2 μM) at indicated time points using specific primers for TNF (left panel). TNF secretion was measured by TNF-ELISA (right panel). Data represent the mean ± SEM.

Importantly, additional exposure to TNF did not impact on SM-induced non-canonical NF-κB activity, *vice versa* SM did not interfere with TNF-induced canonical NF-κB activation, together demonstrating the specific mode of SM in interacting with the non-canonical NF-κB signaling in B16 melanoma cells (Fig. 3.8).

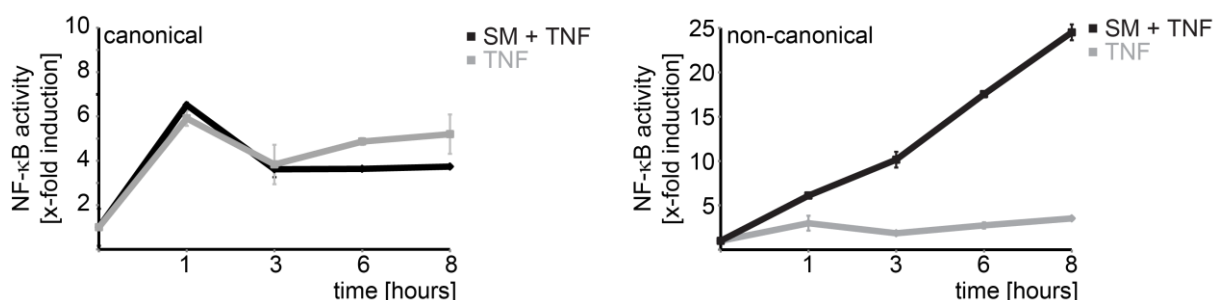


**Fig. 3.8 SM do not alter TNF induced canonical NF-κB signaling in B16 cells**

Measurement of canonical and non-canonical NF-κB activation in B16 cells by ELISA (TransAM) after stimulation with TNF (20 ng/ml) or TNF combined with SM (2 μM). Data represent the mean ± SEM

Due to the discrepancy between attenuated tumor growth *in vivo* and tumor cell resistance *in vitro* we hypothesized that rather the tumor microenvironment than the tumor cells themselves, represents the primary target of SM.

### 3.2 IAP antagonization inhibits tumor vasculature *in vivo*

The tumor microenvironment is made up of different components including blood vessels, tumor infiltrating immune cells, and cytokines that affect tumor growth and progression (Mantovani *et al*, 2008; Carmeliet & Jain, 2000). Therefore, we first investigated the vasculature structures and immune cell infiltration of B16 tumors after treatment with SM. Immunofluorescence microscopy of B16 melanoma tumor sections revealed CD31 (marker for endothelial cells) positive endothelial cells (ECs) 12 days after tumor cell implantation (control), whereas no CD31 signal was seen on day 5 (Fig. 3.9A, upper panel and 3.9B). This indicates that an angiogenic switch had occurred between day 5 and 12 coinciding with exponential tumor growth (Fig. 3.2). In contrast to control tumors, those treated with SM were significantly less vascularized intratumorally at day 12 (Fig. 3.9A, lower panel and 3.9B) as demonstrated by the lack of CD31 positive cells. These data suggest that SM may act as an anti-angiogenic drug.

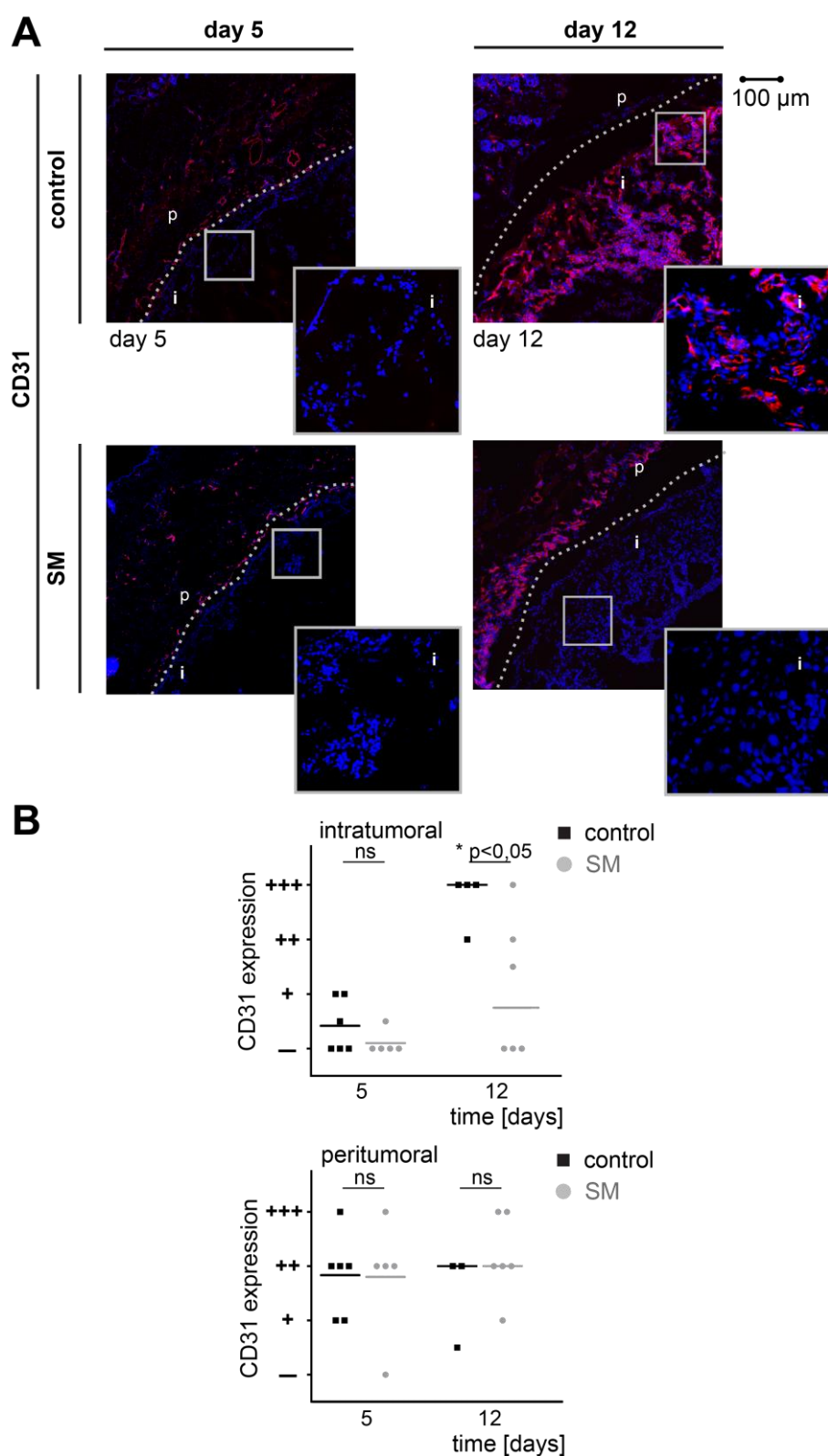


**Fig. 3.9 Intratumoral vascularization is reduced after IAP antagonization *in vivo***

**A.** The murine melanoma cell line B16 was mixed with matrigel and vehicle or SM (2  $\mu$ M) and then subcutaneously injected into the flank region of recipient wild type mice. Histological analysis of implanted tumors by staining of vascular endothelial cells using a CD31 antibody was performed.

Nuclei were counterstained with DAPI (blue). Sections of intratumoral (i) and peritumoral (p) regions on day 5 and 12 are illustrated.

**B.** Amount of vascular endothelial cells from (A) was qualitatively estimated according to the intensity of specific staining and were arbitrarily set as the following: -, not expressed; +, low expression; ++, moderate expression; +++, strong expression.

Notably, in contrast to CD31-positive vascular endothelial cells, lymphatic endothelial cells were not affected by SM. Histological investigation of lymphatic endothelial cells by immunostaining of the hyaluronan receptor LYVE, specifically expressed on lymphatic endothelial cells, revealed no significant changes in lymphatic endothelium upon exposure to SM (Fig. 3.10).



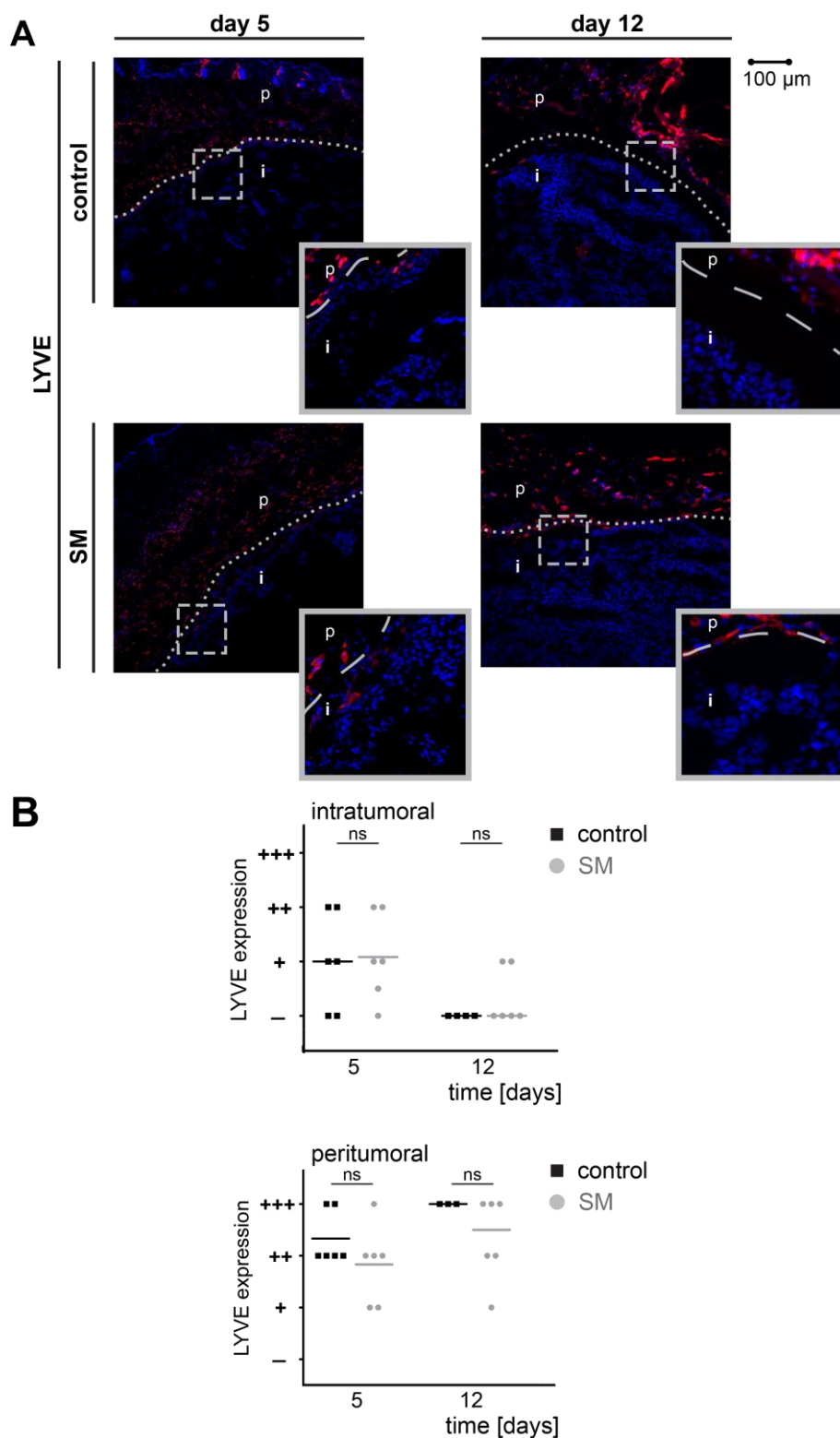


**Fig.3.10 The amount of lymphatic endothelial cells is not altered after IAP antagonization in SM treated mice**

**A.** The murine melanoma cell line B16 was mixed with matrigel and vehicle or SM (2  $\mu$ M) and then subcutaneously injected into the flank region of recipient mice. Histological analysis of implanted tumors by staining of lymphatic endothelial cells using a LYVE antibody was performed. Nuclei

were counterstained with DAPI (blue). Sections of intratumoral (i) and peritumoral (p) regions on day 5 and 12 are illustrated.

**B.** Amount of lymphatic structures of (A) was qualitatively estimated according to the intensity of specific staining and were arbitrarily set as the following: -, not expressed; +, low expression; ++, moderate expression; +++, strong expression.

Tumor infiltrating immune cells are increasingly recognized as one of the major drivers of tumor growth by directly interfering with tumor cell homeostasis and proliferation or by conditioning the favorable tumor microenvironment (e.g. angiogenesis) (Stockmann *et al*, 2014). Therefore, we examined whether SM-treatment impacts on infiltration of immune cells in melanoma tumors. Intra- and peritumoral leukocyte (CD45) and macrophage (CD68) infiltrations were investigated by specific staining of CD45 and CD68, respectively, in tumor sections with or without SM treatment. However, there was no significant difference between immune cell infiltration of SM treated and control B16 melanoma tumors, for a period of up to 12 days after transplantation (Fig. 3.11).

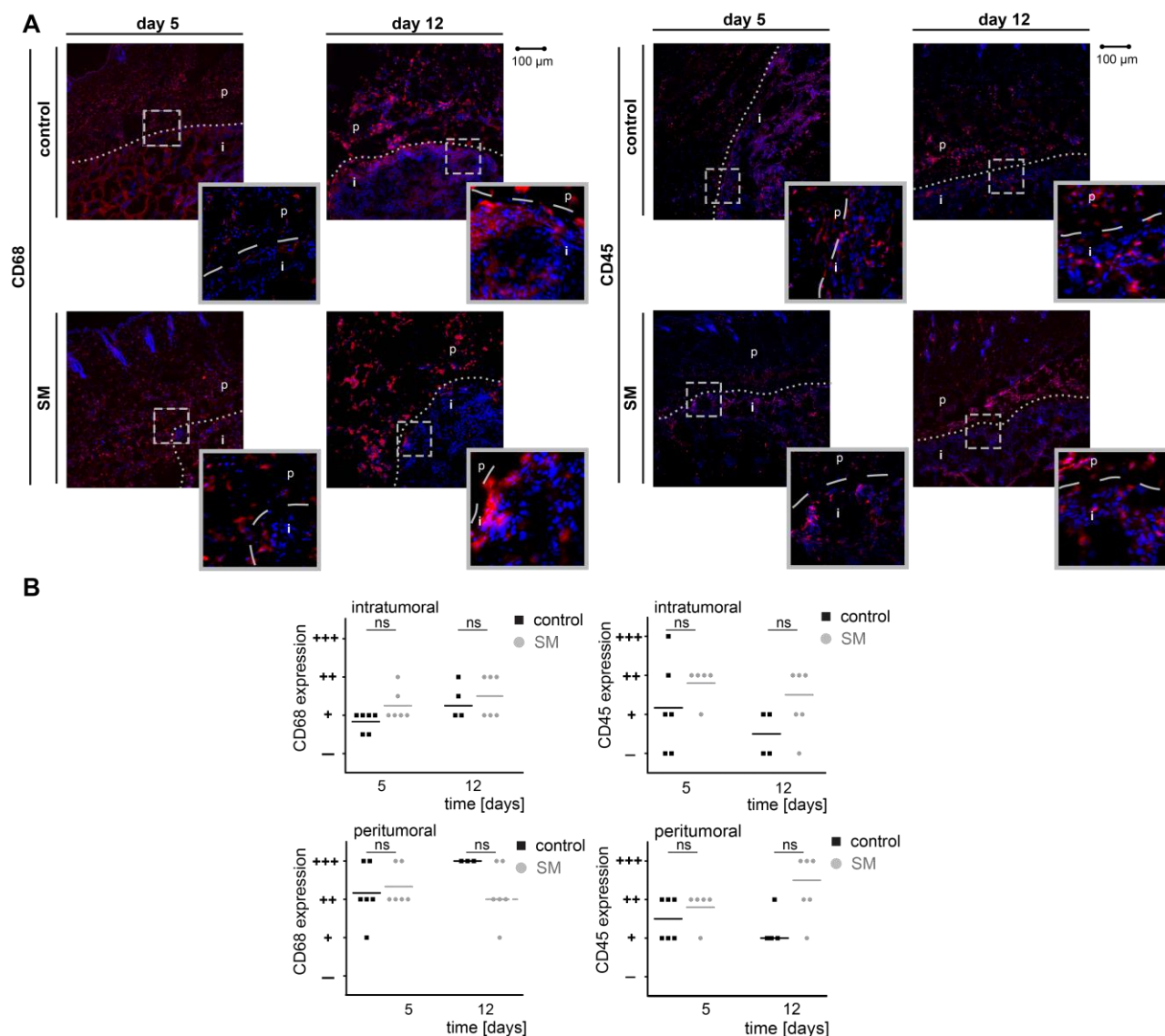


**Fig. 3.11 The amount of inflammatory cells is not altered after IAP antagonization in SM treated mice**

The murine melanoma cell line B16 was mixed with matrigel and vehicle or SM (2  $\mu$ M) and then subcutaneously injected into the flank region of recipient mice. Histological analysis of implanted tumors stained for inflammatory cells.

**A.** Tumor sections were stained for CD68 expressing cells (red, upper panel) or CD45 expressing cells (red, lower panel) Nuclei were counterstained with DAPI (blue). Sections of intratumoral (i) and peritumoral (p) regions on day 5 and 12 are illustrated.

**B.** The amount of inflammatory cells was qualitatively estimated according to the intensity of specific staining and were arbitrarily set as the following: -, not expressed; +, low expression; ++, moderate expression; +++, strong expression.

These data showed that in contrast to the lymphatic endothelial cells and infiltrating immune cells, SM-treatment efficiently reduced the appearance of vascular endothelial

cells and thus inhibits the vascularization of the melanoma tumors. In order to investigate tumor vascularization and blood supply, tail vein injection of high molecular weight FITC-conjugated dextran was performed and the intratumoral vasculature at day 12 was analyzed by multi-photon microscopy. Multi-photon microscopy clearly showed an established vasculature in vehicle treated tumors contrary to SM treated tumors that revealed no vasculature formation (Fig. 3.12).

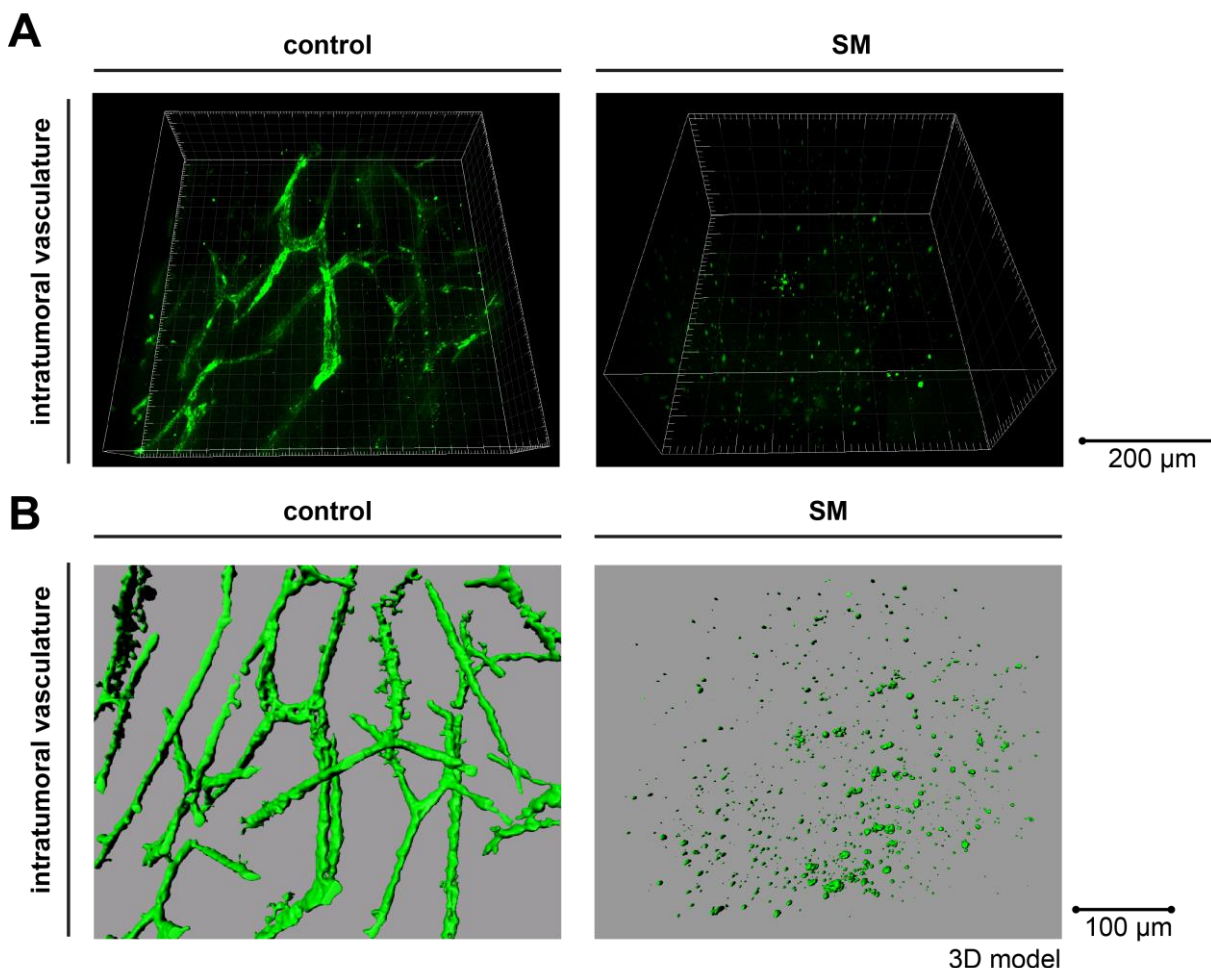


**Fig. 3.12 Deep tissue imaging (multi-photon microscopy) of SM treated tumors illustrates IAP antagonized induced destruction of intratumoral vasculature**

**A.** Intratumoral vasculature of tumors at day 12 was analyzed by multi-photon microscopy for deep tissue imaging using FITC-Dextran staining of vessels. FITC-Dextran was injected into the tail vein of mice 30 minutes before sacrificing the mice.

**B.** 3D presentation and volume rendering of the acquired images obtained in (A).

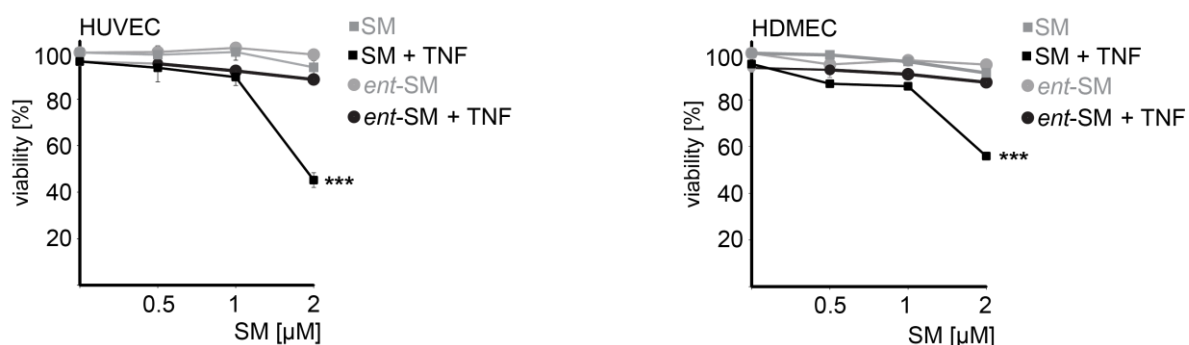
Taken together, these findings suggested that rather than targeting the tumor cells *per se*, IAP antagonization attenuated tumor growth *in vivo* by specifically targeting the tumor

blood supply. Further analyses were performed to investigate the effect of IAP antagonization in endothelial cells, to verify the finding that ECs are sensitive for SM-induced cell death under inflammatory conditions in the tumor microenvironment.

### 3.3 IAP antagonization promotes TNF-induced endothelial cell death

To better define the effects of IAP antagonization on vascular ECs we first examined the cytotoxic activity of SM and *ent*-SM on cultured Human Umbilical Vein ECs (HUVEC) and Human Dermal Microvascular ECs (HDMEC). In contrast to B16 cells, SM (but not *ent*-SM) efficiently potentiated TNF-induced cell death in HUVEC and HDMEC (Fig. 3.13A). Similarly, TNF treatment reduced the clonogenicity of HUVECs only in conjunction with SM but not *ent*-SM, clearly indicating the efficiency of SM to potentiate TNF-cytotoxicity in ECs (Fig. 3.13B).

**A**



**B**

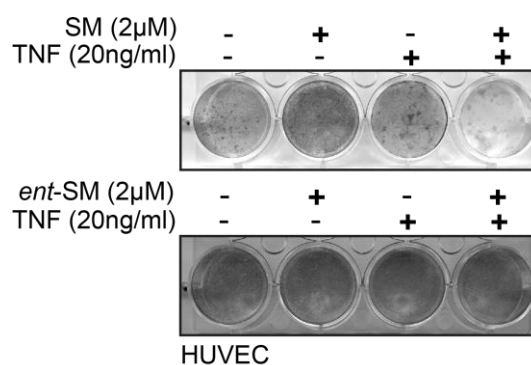


**Fig. 3.13 IAP antagonization results in TNF induced cell death**

**A.** Measurement of cell viability of HUVECs and HDMECs in response to SM, *ent*-SM or combined TNF with SM (*ent*-SM) treatment. Viability was assessed by trypan blue exclusion after 48 hours. Data points represent the mean  $\pm$  SEM.

**B.** Measurement of clonogenicity of HUVECs treated as in indicated. After 48 hours media was changed to normal growth media. Clonogenicity was assessed by crystal violet staining of adherent colonies 10 days after treatment.

Mechanistically, SM was shown to promote cytotoxic effects by inducing cIAP1 degradation (Vince *et al*, 2007; Varfolomeev *et al*, 2007). In order to gain more insight about the mode of SM-induced susceptibility to TNF, we performed western blot analysis of cIAP1, cIAP2 and XIAP in HUVECs with or without SM treatment. In line with previous reports, cIAP1 was efficiently depleted when HUVECs were exposed to SM but not *ent*-SM. cIAP2 was only detectable when HUVECs were exposed to TNF (Stehlik *et al*, 1998) but was significantly reduced upon SM co-treatment (Fig 3.14A). In contrast to cIAP1 and 2 no alteration of XIAP protein level was detectable. The depletion of cIAPs was associated with the activation of executioner caspase-3 and the processing of PARP (Fig. 3.14B) representing an ongoing apoptotic process in HUVECs upon TNF and SM combination treatment. Caspase-3 activation upon TNF/SM double treatment was also confirmed on the basis of flow cytometric analysis and immunofluorescence staining of HUVECs (Fig. 3.14C and D).

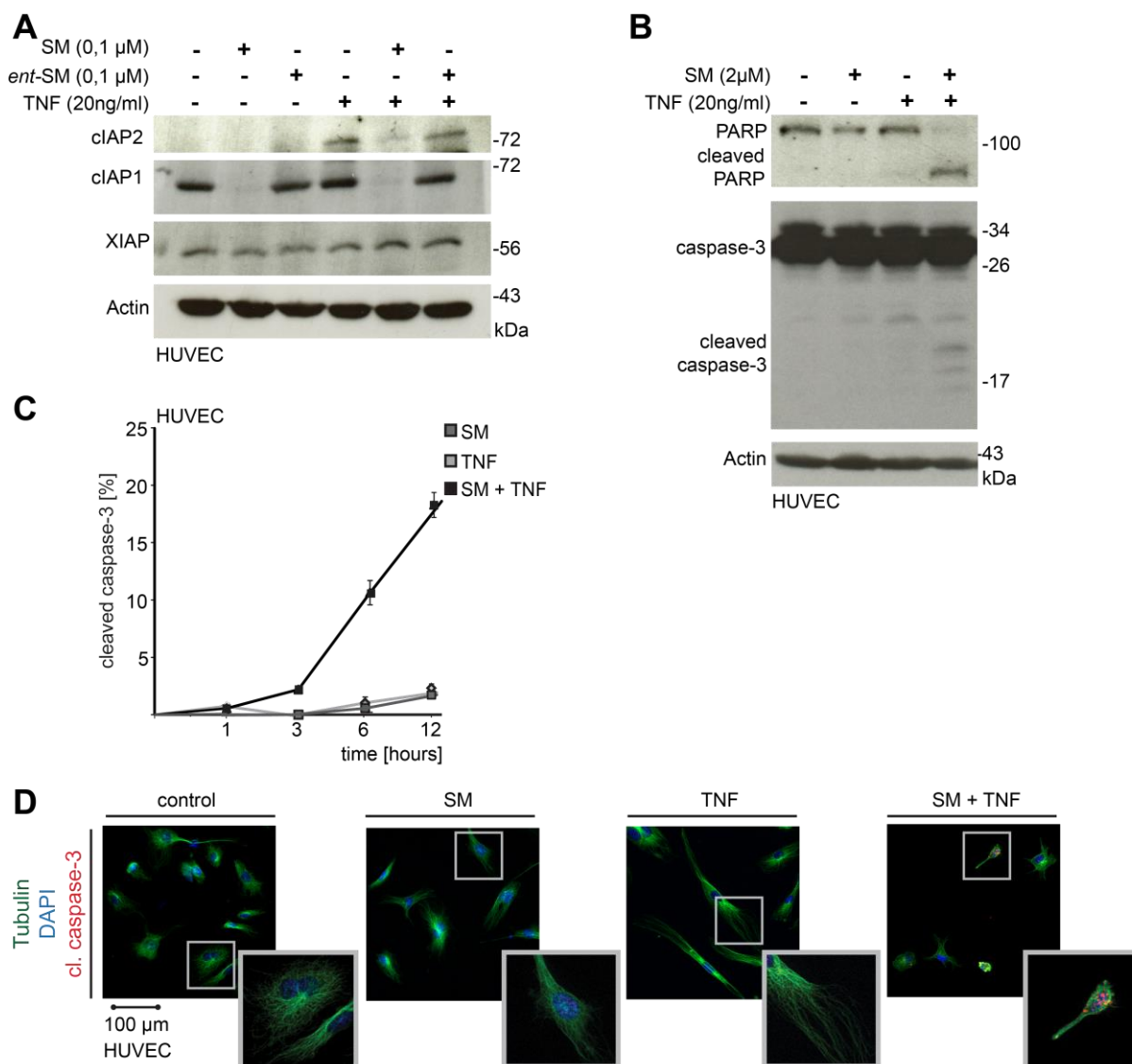


**Fig. 3.14 IAP antagonization promotes TNF-induced endothelial apoptotic cell death**

**A.** Western blot analysis using cIAP1, cIAP2, XIAP and  $\beta$ -Actin antibodies on HUVECs whole cell lysates after 6h, treated as indicated.

**B.** Western blot analysis using caspase-3, PARP and  $\beta$ -Actin antibodies on HUVECs whole cell lysates after 16h, treated as indicated.

**C.** Flow cytometric analysis for cleaved caspase-3 staining was performed on HUVECs at indicated time points and treated as indicated. Data points represent the mean  $\pm$  SEM.

**D.** Immunofluorescence analysis with  $\alpha$ -Tubulin (green), cleaved caspase-3 (red) antibodies and DAPI (blue) on HUVECs after indicated treatment for 16h.

These data suggest that SM potentiate TNF-induced apoptosis of HUVECs. In order to further substantiate this finding, HUVECs treated with SM and TNF were additionally exposed to the pan-caspase inhibitor zVAD-fmk (zVAD, inhibition of apoptosis) or the

inhibitor of RIPK1, Necrostatin-1/Nec-1 (inhibition of necroptosis). Viability assays showed that the TNF-induced EC death could be mainly blocked by inhibition of caspase activity as previously shown (Vince *et al*, 2007; Varfolomeev *et al*, 2007; Petersen *et al*, 2007). Intriguingly, the inhibition of RIP1 kinase activity alone exhibited no effect on cell viability upon TNF/SM treatment. However, TNF/SM-induced cell death was almost completely abolished when caspase- and RIPK1 kinase-activity were simultaneously inhibited (Fig. 3.15), indicating that necroptosis is initiated when caspase activation is inhibited.

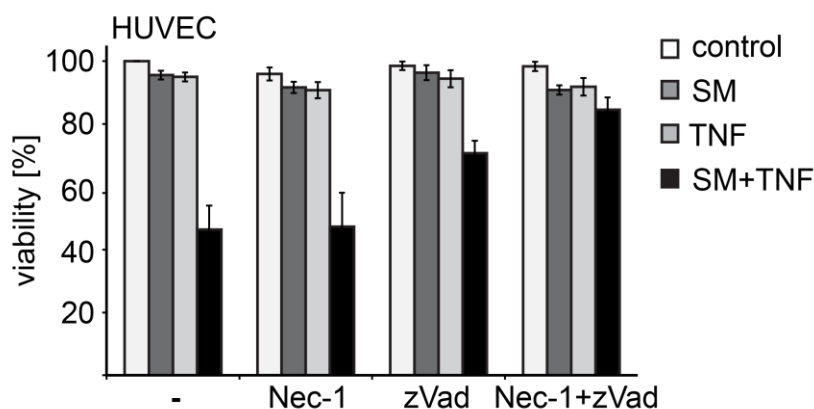


**Fig. 3.15 IAP antagonization promotes TNF-induced endothelial apoptotic cell death**

**A.** Measurement of cell viability of HUVECs in response to TNF, SM or combination of TNF with SM treatment after addition of Nec-1 (30  $\mu$ M) and zVAD-fmk (30  $\mu$ M). Viability was assessed by trypan blue exclusion after 40 hours of treatment. Data points represent the mean  $\pm$  SEM.

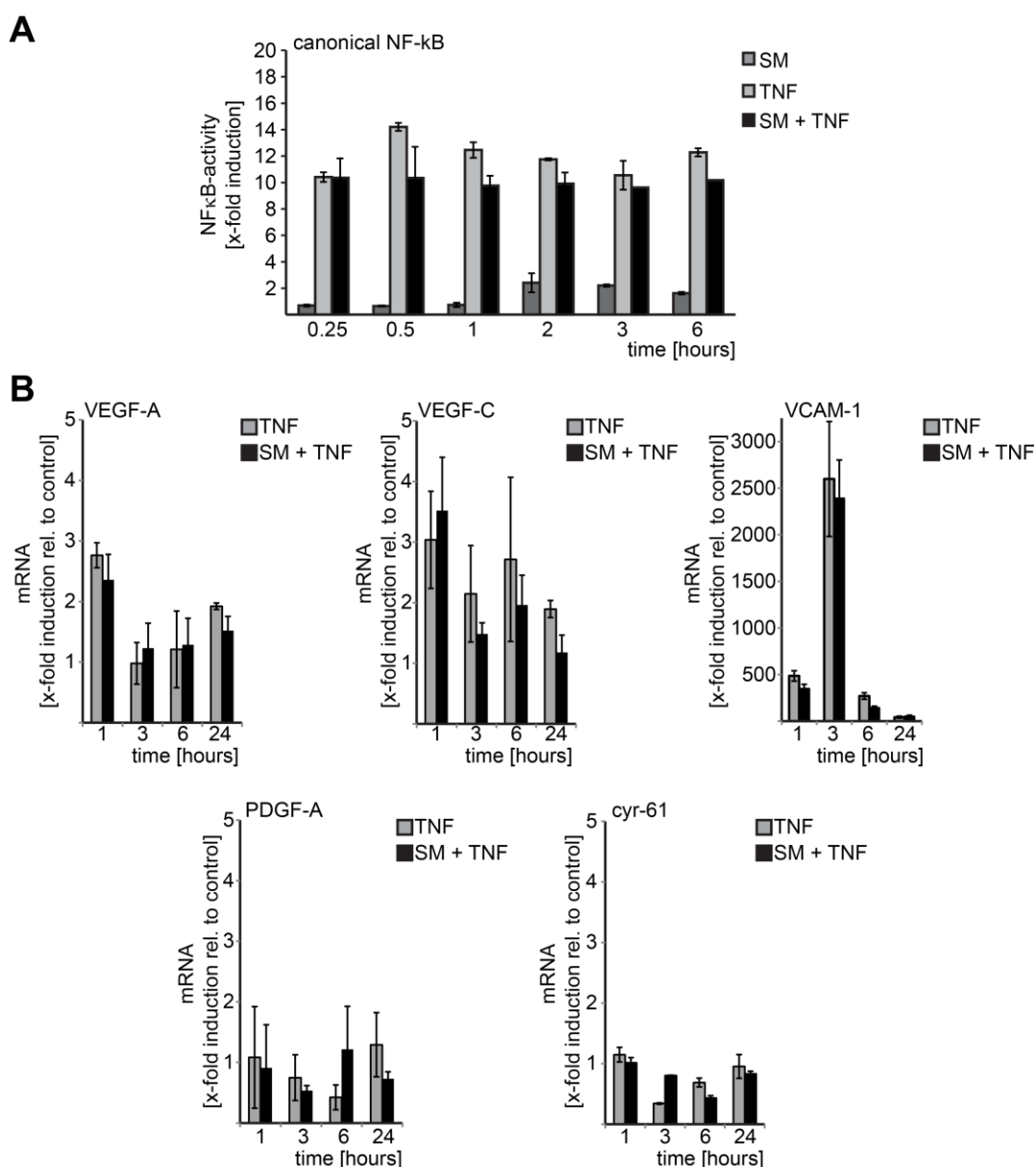
These data so far showed that SM efficiently provoked TNF-induced cell death. However, TNF additionally has a pivotal role in angiogenesis and EC growth by activating NF- $\kappa$ B. TNF-induced canonical NF- $\kappa$ B activity in turn up-regulates the expression of pro-angiogenic factors and promotes angiogenesis. In order to address this issue the canonical NF- $\kappa$ B activity was first examined in ECs exposed to TNF with or without SM. Accordingly, although the canonical NF- $\kappa$ B signaling was significantly up-regulated upon TNF stimulation, no significant alteration was detected when ECs were co-treated with SM (Fig. 3.13 A). Notably, like in B16 melanoma cells SM alone did only slightly induce canonical NF- $\kappa$ B activation.

Furthermore, we performed qRT-PCR analyses of a panel of genes that have been shown to be activated by TNF and to regulate endothelial angiogenesis and growth. The expression of angiogenesis-related genes, such as cell adhesion molecules (vascular cell adhesion molecule type I (VCAM-1)) (Mackay *et al*, 1993) and such as pro-angiogenic factors (vascular endothelial growth factor (VEGF) -A and -C) (Salvucci *et al*, 2004;



Hoeben *et al*, 2004) were specifically analyzed as important pro-angiogenic factors that have been shown to be up-regulated by TNF. To clarify, if SM treatment interfered with the reported TNF mediated transcriptional regulation of these factors, we examined their expression levels in ECs exposed to TNF in the presence or absence of SM. Our data confirmed the reported up-regulation of VEGF-A, VEGF-C and VCAM-1 in response to TNF. However, in line with the lack of alteration of TNF-induced NF- $\kappa$ B activity, SM did not affect the TNF-induced expression of these factors (Fig. 3.16B). The expression levels of angiogenic factors including PDGF-A (Platelet-derived growth factor A) and cyr61 (cysteine-rich angiogenic inducer 61) were not altered neither by TNF nor SM (Fig. 3.16B).

Together these data suggest that IAP antagonization in conjunction with TNF-signaling does not interfere with TNF-mediated neo-angiogenesis, but rather results in EC apoptosis.



---

**Fig. 3.16 Analysis of Nf- $\kappa$ B signaling and angiogenesis related-genes after TNF stimulation and additional SM treatment**

**A.** NF- $\kappa$ B activation (canonical) was measured by NF- $\kappa$ B ELISA (TransAM) after stimulation of HUVECs with TNF, SM and TNF combined with SM at indicated time points. Data represents the mean  $\pm$  SEM.

**B.** qRT-PCR of angiogenesis-related genes after stimulation of HUVECs with TNF and TNF combined with SM at indicated time points. Data represents the mean  $\pm$  SEM.

To further gain more mechanistic insight how SM inhibits tumor vascularization, we conducted an *in vitro* HUVEC tube formation assay. This assay is a well-established method to investigate EC functions *in vitro* by using a basement membrane matrix with biological activity (Kleinman & Martin, 2005). Both, TNF and SM treated HUVECs formed extensive capillary-like tubular networks within 36 hours (developing network), indicating that normal EC function was not impaired by TNF or SM treatment (Fig. 3.17A, upper panel). In contrast, network formation was inhibited when HUVEC were seeded on matrigel containing TNF in combination with SM. These data clearly showed that TNF in combination with SM efficiently inhibits capillary formation. More strikingly, when established capillary tubes that were grown for 36 hours (normal growth medium) were exposed for additional 48 hours to TNF in combination with SM, endothelial capillary network was similarly disrupted (Fig. 3.17A, lower panel, established network). These data indicate that SM potentiate TNF-induced death of ECs in established and developing capillary network. The involvement of TNF-induced apoptosis in this process was demonstrated by using caspase inhibitors. The pan-caspase inhibitor zVAD efficiently protected capillary network from TNF/SM-induced cell death (Fig. 3.17C), which is consistent with the pro-apoptotic role of SM in ECs shown in Fig. 3.13 and Fig. 3.14. Notably, the inactive *ent*-SM had no effect on network formation, neither alone nor combined with TNF (Fig. 3.17B).

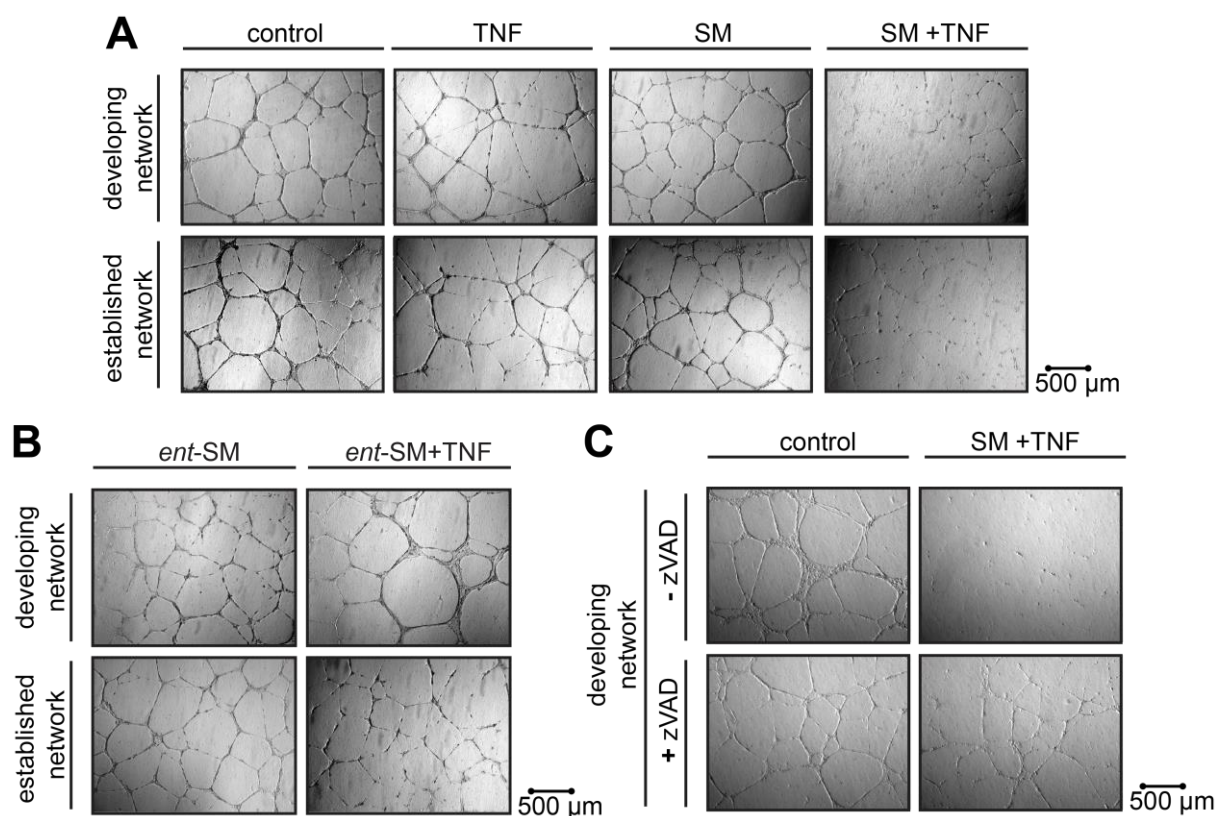


**Fig. 3.17 Tube formation assay**

**A.** ECs were seeded on matrigel and pictures were taken with a brightfield microscope. Developing network: EC growth was recorded after 36 hours treatment (SM 2  $\mu$ M, TNF 20 ng/ml, **A** upper panel). Established network: to investigate established capillary-like tubes, ECs were treated after 36 hours growing in normal media, for 48 hours treatment as indicated (**A**, lower panel).

**B.** Network formation of HUVECs treated with *ent*-SM alone or combined with TNF.

**C.** Developing network + zVAD: ECs were treated for 48 hours with additional zVAD (20  $\mu$ M).

Taken together, these *in vitro* results point at a direct cytotoxic effect of SM towards ECs in combination with TNF.

### 3.4 IAP antagonization potentiates TNF-induced vascular disruption *in vivo*

To verify our *in vitro* analyses concerning the TNF dependency of endothelial cell death in response to IAP antagonization *in vivo*, we implanted matrigel plugs supplemented with angiogenic growth factors and SM with or without TNF (but lacking tumor cells in contrast to Fig. 3.1) subcutaneously into the flank region of recipient mice. Ingrowing perfused

blood vessels sprouting from adjacent vessels into the matrigel plugs were then visualized by injecting high molecular weight fluorescent FITC-dextran (2000 kDa) into the tail vein of these mice. Strikingly, only matrigel plugs containing SM in combination with TNF showed a significant reduction in angiogenesis and vascular formation, whereas matrigel plugs containing either SM or TNF alone were normally vascularized (Fig. 3.18A). In line with this, hematoxylin and eosin staining of the matrigel plugs showed vessels as holes bordered with blue stained nuclei in contrast to none infiltrated matrigel areas seen in pink (Fig. 3.18). This is in stark contrast to our initial observation that SM alone was sufficient to reduce tumor vascularization in matrigel plugs containing B16 tumor cells. These findings suggest, that the tumor microenvironment e.g. immune cells or B16 cells (Fig. 3.7) represent the source of TNF in these melanoma tumors that is sufficient to induce EC death when combined with IAP inhibition. Alternatively, SM-induced up-regulation and secretion of TNF by B16 melanoma cells may additionally impact on the cytotoxic activity of SM towards ECs. Taken together, the analyzed matrigel plugs showed characteristics of vascularization (neo-angiogenesis) except for combined TNF and SM plugs.

## wild type-mice

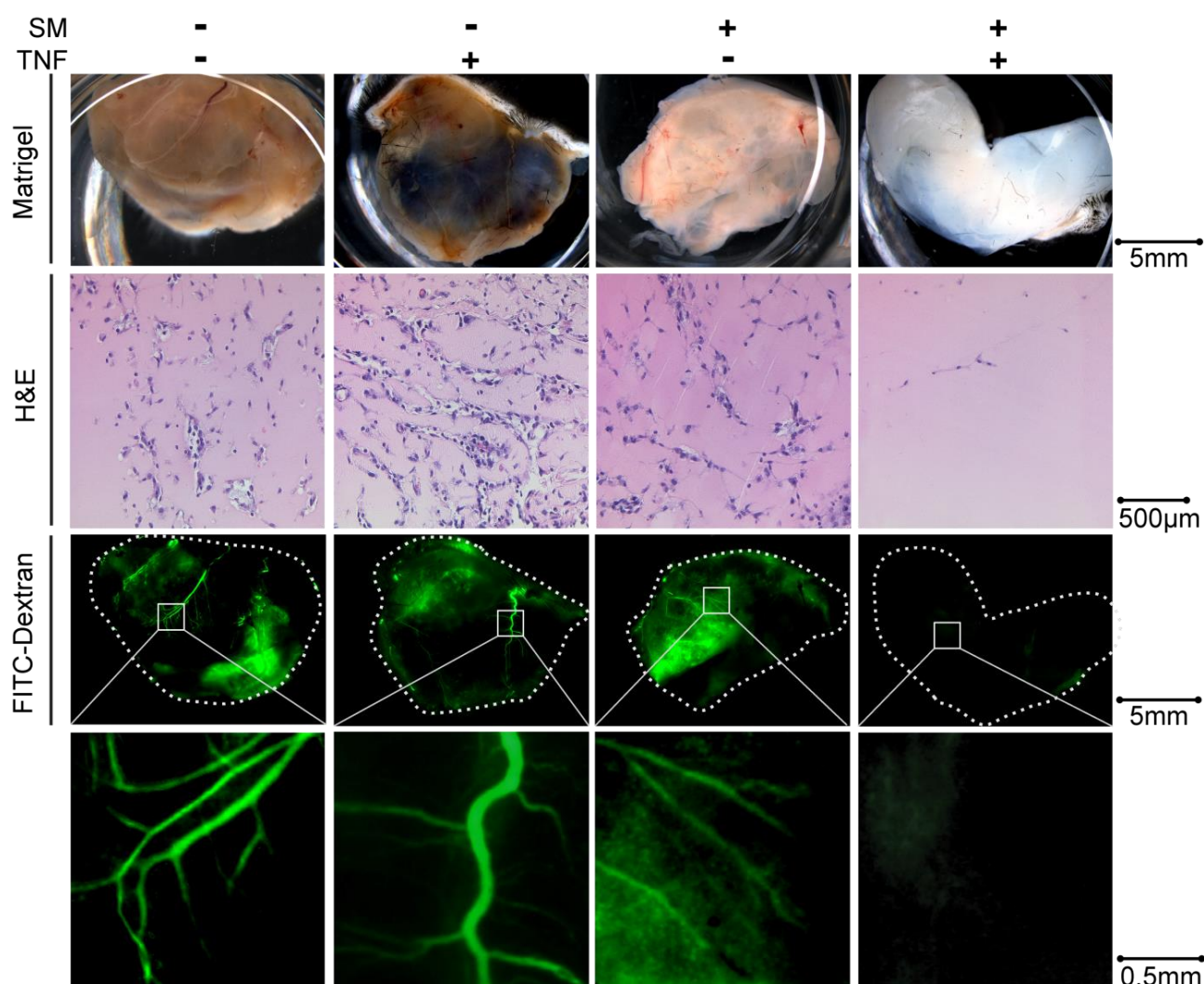


**Fig. 3.18 *In vivo* analysis of vascularization upon IAP antagonization in wt-mice**

Matrigel plugs were supplemented with SM, TNF, SM + TNF or vehicle and injected subcutaneously into the flank region of recipient wild type-mice. After 12 days, high molecular weight fluorescent FITC-Dextran was injected into the tail vein of mice. Mice were sacrificed after 30 minutes and plugs were fixed in 4% PFA.

First panel: photographs of multiple image alignment of matrigel plugs on day 12.

Second panel: matrigel plugs were stained for H&E after embedding in paraffin and sectioning with a microtome.

Third and fourth panel: Z-stacks of matrigel plugs were taken using a motorized Leica M165 FC fluorescent stereomicroscope equipped with a DFC490 CCD camera and GFp2 (ex.480/40nm) filter set. Images were processed using a Multifocus module of the LAS 3.7.0 software (Leica).

To further confirm the critical role of TNF signaling during tumor growth and angiogenesis we employed TNF-receptor-1 and -2 knockout mice (TNFR1/2<sup>-/-</sup>) (Wohlleber *et al*, 2012).

To verify the TNF-dependent death of endothelial cells *in vivo*, matrigel plugs were injected into TNFR1/2<sup>-/-</sup>-mice (accordingly to Fig. 3.16). In striking contrast to the observations made in wild type mice, SM and TNF supplemented matrigel plugs exhibited normal vascularization and showed no detectable alteration of neo-angiogenesis compared to SM or TNF alone, providing a strong evidence for the role of TNF and TNF-R signaling in ECs in SM-induced cytotoxicity (Fig. 3.19)

#### TNF-R1/2<sup>-/-</sup>-mice

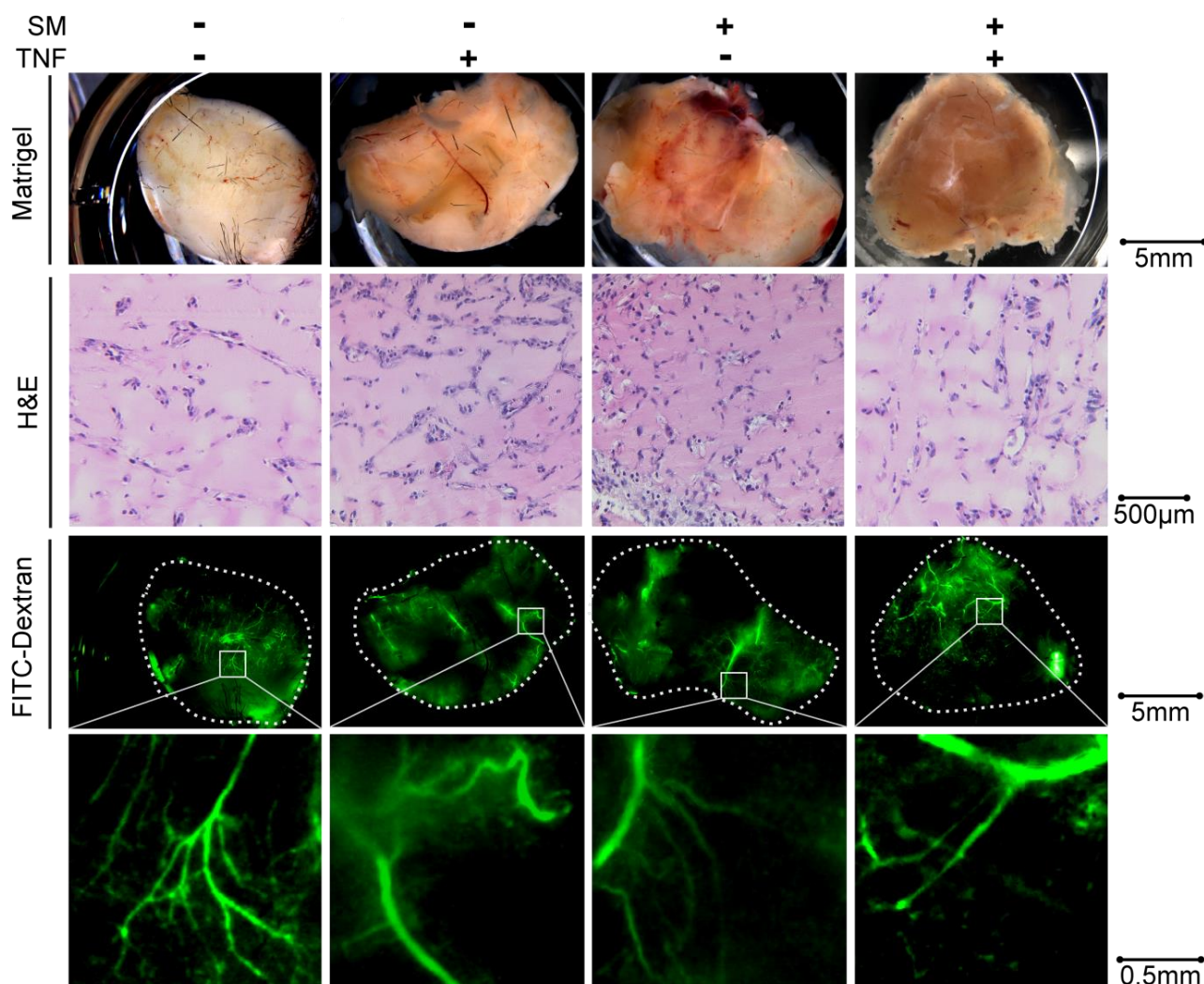


**Fig. 3.19 *In vivo* analysis of vascularization upon IAP antagonization in TNF-R1/2<sup>-/-</sup> mice**

Matrigel plugs were supplemented with SM, TNF, SM + TNF or vehicle and injected subcutaneously into the flank region of recipient TNF-R1/2<sup>-/-</sup>-mice. After 12 days, high molecular weight fluorescent FITC-Dextran was injected into the tail vein of mice. Mice were sacrificed after 30 minutes and plugs were fixed in 4% PFA.

First panel: photographs of multiple image alignment of matrigel plugs on day 12.

Second panel: matrigel plugs were stained for H&E after embedding in paraffin and sectioning with a microtome.

Third and fourth panel: Z-stacks of matrigel plugs were taken using a motorized Leica M165 FC fluorescent stereomicroscope equipped with a DFC490 CCD camera and GFp2 (ex.480/40nm) filter set. Images were processed using a Multifocus module of the LAS 3.7.0 software (Leica).

In analogy to our initial experiment (Fig. 3.2) matrigel plugs containing B16 tumor cells with or without SM were implanted into TNFR1/2<sup>-/-</sup>-mice. In contrast to the growth attenuating effect of SM in wild type mice (Fig. 3.2) where we observed a significant reduction of tumor size without a direct cytotoxicity against tumor cells, no effect on tumor growth rates in the absence of TNF-R signaling in tumor microenvironment was observed (Fig. 3.20). This further highlights the involvement of tumor microenvironment including endothelial compartment in the anti-tumor activity of SM.

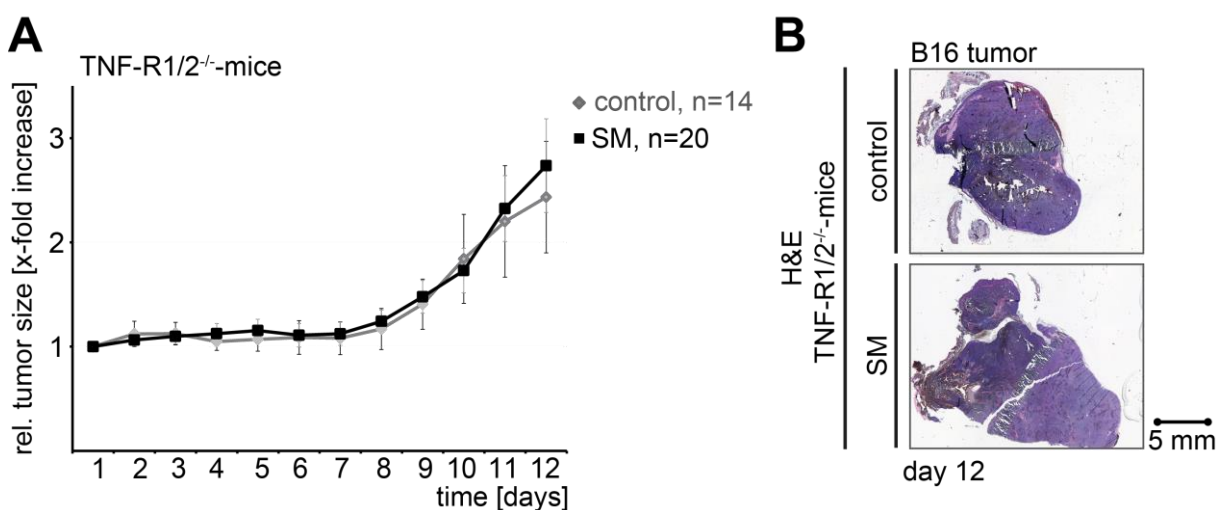


**Fig. 3.20 Tumor growth is not attenuated in TNFR1/2<sup>-/-</sup>-mice**

**A.** The murine melanoma cell line B16 was mixed with matrigel and vehicle or SM (2 $\mu$ M) and subcutaneously injected into the flank region of recipient TNFR1/2<sup>-/-</sup>-mice. Tumor size was measured in 2 dimensions and calculated volume was recorded daily. Data points represent the mean  $\pm$  SEM.

**B.** Histological analysis of B16 tumors was performed on day 12 by H&E staining and representative pictures are illustrated.

Indeed, multi-photon microscopy showed tumor vascularization in both vehicle and SM treated tumors (Fig. 3.21), further indicating that the cytotoxic effects of SM towards vascular endothelium is provided by TNF and TNF-R signaling in ECs (Fig. 3.2).

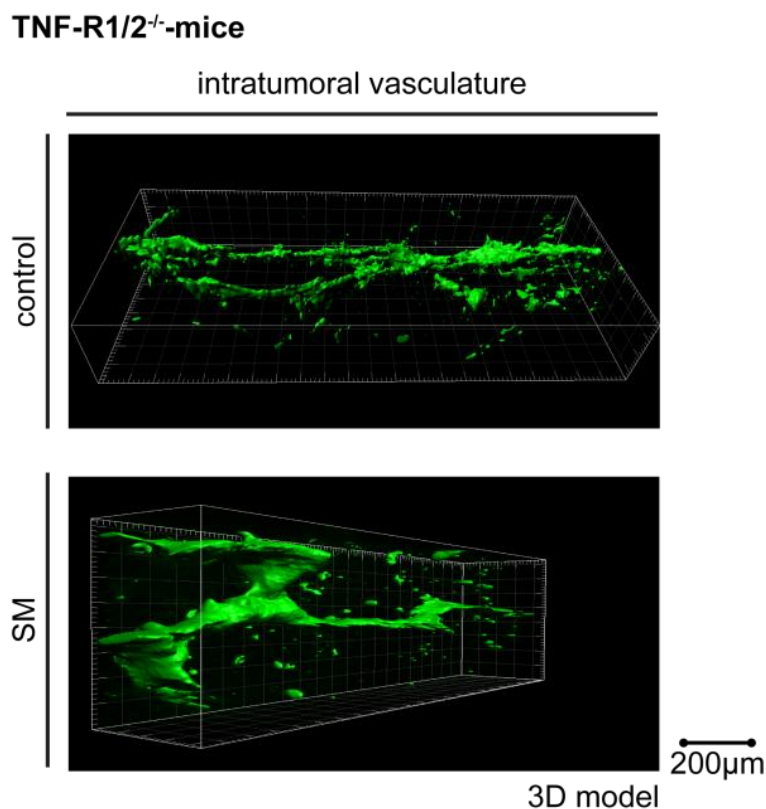


**Fig. 3.21 Intratumoral vasculature in TNFR1/2<sup>-/-</sup>-mice**

Deep tissue imaging (multi-photon microscopy) of SM treated tumors illustrates IAP antagonized do not induce destruction of intratumoral vasculature

Intratumoral vasculature of tumors at day 12 was analyzed by multi-photon microscopy for deep tissue imaging using FITC-Dextran staining of vessels. FITC-Dextran was injected into the tail vein of mice 30 minutes before sacrificing the mice.

In summary, these findings confirm that IAP antagonization has the capacity to induce a TNF dependent cell death which is seen specifically in the endothelial cells within the tumor-microenvironment and in this way could interrupt neo-angiogenesis of tumors.



## 4. Discussion

In this work we discovered a novel effect of SMAC mimetics (SM) on tumor growth. Our data showed that SM treatment leads to substantial inhibition of tumor growth, which was not due to direct cytotoxicity towards tumor cells but by provoking TNF-dependent endothelial cell death and disruption of tumor blood vessels. Specifically, SM induced non-canonical NF- $\kappa$ B activity results in TNF production. Increased local concentration of TNF together with SM induced endothelial cell death and inhibited tumor vascularization. Our data represent a novel strategy to combat cancer by potentiating inflammatory destruction of tumor blood vessels using SMAC mimetics.

### 4.1 IAP antagonization inhibits tumor growth without inducing direct cytotoxicity against tumor cells

Resting or evasion of programmed cell death is one of the crucial characteristics of cancer cells (Hanahan & Weinberg, 2000) and IAPs have been reported to play a major role in this process (Kashkar, 2010; Fulda & Vucic, 2012; Dubrez et al, 2013). Therefore, IAPs were considered to be an attractive target for therapeutic applications in human malignancies. Various targeting strategies have been intensively investigated and the generation of small-molecule IAP antagonists is considered to be one of the most promising amongst them (Vucic & Fairbrother, 2007; Ndubaku *et al*, 2009; Fulda & Vucic, 2012). Indeed, SM have been shown to restore TNF-dependent apoptosis directly in melanoma cancer cells xenografted into NUDE mice (Benetatos *et al*, 2014; Condon *et al*, 2014a; Krepler *et al*, 2013). Especially pan-IAP antagonists have been shown to be very potent in promoting cell death in cancer cells (Ndubaku *et al*, 2009b).

In the present work, a murine B16 melanoma model was chosen to analyze the anti-tumoral efficiency of a pan-IAP antagonist (compound A) in an immune competent mouse tumor model. We could show that tumor growth is significantly attenuated in the presence of SM (Fig. 3.2). Subsequent analyses however revealed no direct cytotoxicity against tumor cells, *in vivo* and *in vitro* (Fig. 3.2-3.6). Although our data show that the B16 mouse melanoma tumor cells produce and secrete elevated levels of TNF in response to SM (Fig. 3.7), they are yet not sensitive to SM treatment *in vitro*.

In recent years, numerous studies have focused on the effect of SM on cancer cells (Fulda & Vucic, 2012; Fulda, 2014; Bai *et al*, 2014) and in general 3 categories of responses have been observed: (i) sensitive to single SM treatment, (ii) sensitive to SM in combination with TNF and (iii) resistant to SM. Additional analyses conclusively showed that the cytotoxic activity of SM is mainly dependent on TNF and TNF-induced cell death. Accordingly, SM compounds were thought to be more effective in patients whose tumors produce large quantities of inflammatory cytokines, including TNF (induced by SM or not). Based on our findings, B16 cells could be categorized as a SM-resistant tumor cell line. Several potential resistance mechanisms could be envisaged that are briefly being discussed in the following.

A major discovery concerning the susceptibility of tumor cells towards SM induced apoptosis was the observation that SM induced the degradation of cIAPs (Varfolomeev *et al*, 2007; Vince *et al*, 2007). Correspondingly, one possible mechanism conferring resistance to SM in tumor cells was supposed to arise from the level of cIAP2. Cancer cell lines evade SM-induced apoptosis by up-regulation of cIAP2. Resistance to SM induced apoptosis was observed when cIAP2 levels were restored after initial SM-induced degradation in lung carcinoma (Petersen *et al*, 2010), colon carcinoma and in melanoma cell lines (Darding *et al*, 2011). cIAP2 gene expression has been reported to be induced upon non-canonical NF- $\kappa$ B activation and its degradation depends on the presence of cIAP1 (Darding *et al*, 2011). We could show that SM treatment of B16 melanoma cells results in the activation of non-canonical NF- $\kappa$ B signaling (Fig. 3.7). One intriguing task would be to examine the expression levels of cIAP1 and cIAP2 in B16 cells to explore their role in mediating resistance to SM. However, there is still no explanation why cIAP1 and 2 are altered in specific cells.

SM-mediated cell death is highly dependent on (de-ubiquitinated) RIPK1 that is associated with FADD and caspase-8 in the formation of the ripoptosome (Varfolomeev *et al*, 2007; Vince *et al*, 2007). The inability to form this complex can confer resistance to SM which was recently seen in CLL (Maas *et al*, 2013). Especially CYLD (de-ubiquitinates RIPK1) is implicated in cancer progression (Almeida *et al*, 2008; Masoumi *et al*, 2011; Hayashi *et al*, 2014). Inactive or low levels of CYLD could result in blunted cell death signaling, leading to SM resistance.

An additional resistance mechanism may arise from the expression of different cFLIP isoforms. The long isoform of cFLIP (cFLIP<sub>L</sub>) has been reported to regulate the activation of RIPK1-dependent cell death (Geserick *et al*, 2009; Oberst *et al*, 2011; Feoktistova *et al*, 2011) and B16 cells might express persistent cFLIP levels, hence impeding SM-mediated cell death that was already shown in a panel of other cancer cell lines (Cheung *et al*, 2009).

Regardless of the underlying molecular mechanisms involved in conferring SM-resistance in B16 cells, the attenuated tumor growth observed *in vivo*, prompted us to investigate in more detail the impact of SM on B16 tumor growth in mice. In particular, the discrepancy between attenuated tumor growth *in vivo* and tumor cell resistance *in vitro*, led us to the hypothesis that an indirect effect of SM treatment could be responsible for the attenuated tumor growth *in vivo*.

This phenomenon has previously been described in other studies. Krepler and colleagues for example, reported several melanoma cell lines to be remarkably unresponsive towards SM *in vitro* yet showed attenuated tumor growth upon SM treatment *in vivo* (Krepler *et al*, 2013). An explanation for the observed discrepancy in this model has not yet been suggested.

## **4.2 IAP antagonization results in the destruction of the vasculature in the tumor microenvironment**

The tumor microenvironment comprises of different cellular and non-cellular components including vascular endothelial cells and tumor-infiltrating immune cells, as well as cytokines that affect tumor growth and progression (Mantovani *et al*, 2008; Carmeliet & Jain, 2000). TNF plays a critical role in these processes, by acting as an amplifier of the inflammatory milieu. Indeed, we showed an increased TNF secretion by B16 cells upon SM exposure. This increased local concentration of TNF may induce paracrine TNF-R signaling, culminating in an inflammatory response or cytotoxicity in the tumor stroma.

There is controversy regarding the role of TNF in tumorigenesis. High concentrations are associated with an antitumoral response, shown in a murine model of sarcoma and also in sarcoma patients (Wiemann & Starnes, 1994; Havell *et al*, 1988) while low levels of TNF can induce tumor growth (Balkwill, 2006). The tumor promoting mechanism are based on ROS (reactive oxygen species) and RNS (reactive nitrogen species) accumulation that can induce DNA damage and thereby facilitate tumorigenesis (Woo *et al*, 2000; Hussain *et al*, 2003). Depending on its concentration, TNF might also have pro- or antiangiogenic effects (Fajardo *et al*, 1992; Yoshida *et al*, 1997; Weichselbaum *et al*, 2002; Li *et al*, 2009). High TNF levels inhibit angiogenesis while low levels of TNF increase tumor growth. Independently of its anti- or pro- effects in tumors, TNF in the tumor microenvironment is considered to be derived from either immune infiltrating myeloid cells and/or the tumor cells themselves (Kulbe *et al*, 2007; Wong *et al*, 2014). Our data clearly

showed that SM induces non-canonical NF- $\kappa$ B activity and TNF secretion by tumor cells. However, these data, do not exclude the tumor stroma in producing TNF in response to SM. Indeed, SM compounds have been shown to induce cytokine production in myeloid cells of the tumor stroma (Wong *et al*, 2014).

Independent of the source of TNF in the tumor microenvironment, our histological analyses demonstrated that SM treatment *in vivo*, leads to a clear disruption of the tumor vasculature (Fig. 3.9 - 3.12). In healthy adults, ECs remain quiescent for years. However, these cells can very rapidly start to proliferate and migrate to form new vessels following tissue injury, inflammation, cancer, or other pathologies (Verdegem *et al*, 2014). The stromal vasculature in tumors is a vital pipeline of nutrients for tumor cells, which reciprocally interacts with tumor cells and facilitates tumor growth. Accordingly, in order to manage their increasing metabolic demand tumor cells secrete a plethora of pro-angiogenic factors, which support vessel growth and in a positive feed-forward loop enable tumor growth. In our model of B16 melanoma tumors, this resulted in the “angiogenic switch” between day 5 and 12 following subcutaneous tumor cell implantation, which subsequently triggers rapid tumor growth (Fig. 3.2 and 3.9). However, intermittently the tumor growth can exceed its blood supply, leading to hypoxia and nutrient deprivation which in turn initiates a new wave of pro-angiogenic activity to restore the balance between blood supply and tumor growth. Upon SM treatment, tumors lack CD31 positive endothelial cells and fail to be vascularized (Fig. 3.9 and 3.12). Our data indicated that SM potentially interfered with EC function and impact on tumor growth by inhibiting its vasculature.

Although we observed no significant alteration in tumor immune cell infiltration in our model, we cannot exclude a role for SM in modulating immune cell function (Dougan *et al*, 2010) such as tumor-infiltrating macrophages, which may be affected by SM treatment as previously demonstrated (Müller-Sienerth *et al*, 2011; McComb *et al*, 2012; Lecis *et al*, 2013). In line with this, Wong and colleagues report that the loss of XIAP, cIAP1 and cIAP2 resulted in reduced number of mature macrophages (Wong *et al*, 2014). Additionally, more detailed analyses of tumor infiltrating immune cells could further substantiate our findings, regarding the specific effect of SM towards blood vessels and clarify whether or not there is an interplay with infiltrating immune cells. Therefore, additional staining of CD8-positive cells, NK cells and myeloid suppressor cells is currently pursued by us.

### 4.3 IAP antagonization promotes TNF-induced cell death of endothelial cells

Endothelial cell death is implicated in the pathogenesis of several cardiovascular diseases such as arteriosclerosis, congestive heart failure and ischemia-reperfusion disorders (Winn & Harlan, 2005). Subsequent analyses of SM-mediated and TNF-dependent cell death of ECs, support our hypothesis that the tumor microenvironment, in particular ECs, rather than the tumor *cells per se*, represents the primary target of SM in our model. Vascular endothelial cells are a major target of TNF that can activate both, cell survival and cell death. Beside proteins of the Bcl-2 family, IAPs have been identified as TNF-induced genes that induce resistance against TNF-initiated cell death in endothelial cells (Stehlik *et al*, 1998; Badrichani *et al*, 1999; Hofer-Warbinek *et al*, 2000). Our study demonstrated that SM potently induced the degradation of cIAPs in cultured ECs (Fig. 3.14) which in turn provoke cytotoxicity upon TNF treatment (Vince *et al*, 2007; Varfolomeev *et al*, 2007; Gaither *et al*, 2007).

In HUVECs, cIAP1 was degraded upon addition of SM (Fig. 3.14). Similarly, degradation of cIAP2 could be shown following SM treatment in the presence of TNF (Fig. 3.14) although cIAP2 seemed to be present only in low abundance in the absence of TNF stimulation. Studies using cIAP1 deficient mice, which harbor elevated cIAP2 protein levels with normal mRNA levels, showed that cIAP2 is a direct target of cIAP1-mediated ubiquitination and degradation (Conze *et al*, 2005). In line with this, an upregulation of cIAP2 was similarly seen in mouse embryonic fibroblast (Mahoney *et al*, 2008) and certain tumor cells in the absence of cIAP1 (Cheung *et al*, 2008). Hence, the low level of cIAP2 in unstimulated HUVEC cells is most likely due to the fact that the expression levels of cIAP2 are maintained by constitutive ubiquitination and subsequent degradation by cIAP1. In line with this, an upregulation of cIAP2 was similarly seen in mouse embryonic fibroblast (Mahoney *et al*, 2008) and certain tumor cells (Cheung *et al*, 2008) in the absence of cIAP1.

The observed degradation of cIAPs leads to TNF-dependent apoptotic cell death shown by caspase-3 and PARP cleavage upon SM treatment (Fig. 3.14). Whether XIAP is also affected in HUVECs upon treatment was not analyzed in detail, but since previous studies using protein binding assays showed that the SM compound used in our work also inhibits XIAP, an inhibition of XIAP can be assumed (Vince *et al*, 2007; Condon *et al*, 2014).

In contrast to the effects of pan-IAP antagonists tested here, our preliminary analyses using specific siRNA against individual IAPs or the cIAP1-specific SM compound

Birinapant showed no similar effect of single IAP antagonization in the presence of TNF (data not shown). This indicates that targeting of all IAPs by SM compounds might be required to obtain an anti-angiogenic effect.

Similarly, a single genomic ablation of IAPs did not cause any severe phenotype. Only the combined lack of cIAP1-cIAP2 or cIAP1-XIAP has been shown to be lethal in mice (Moulin *et al*, 2012b). This was due to cardiovascular defect in the embryonic development. In line with our observations, the observed cardiovascular defects and the lethality was significantly reduced when TNF-R was simultaneously deleted. Moreover, similar observations were also made in zebrafish (Santoro *et al*, 2007). In contrast to mammalian genomes that contain two closely related cIAPs, zebrafish genomes contain only one cIAP gene (*birc2*). Genetic ablation of *birc2* resulted in the *tomato* phenotype, which is characterized by severe haemorrhage and vascular regression during development. This regulation of endothelial cell integrity and blood vessel homeostasis was also dependent on TNF-R signaling. Together, these data indicate the central role of IAPs in the homeostasis and function of ECs. Moreover, this implies that especially pan-IAP antagonists (like CpdA in this work) could be very potent inducer of EC death.

IAPs play a major role in the regulation of NF- $\kappa$ B signaling and it is quite established that SM treatment can lead to activation of non-canonical NF- $\kappa$ B signaling due to the stabilization of NIK (Varfolomeev *et al*, 2007; Vince *et al*, 2007). This is in line with our data that showed non-canonical NF- $\kappa$ B activation in B16 cells that resulted in TNF secretion. The impact on canonical NF- $\kappa$ B signaling using SM was shown in different studies that illustrated a clear activation of canonical NF- $\kappa$ B signaling (Vince *et al*, 2007; Varfolomeev *et al*, 2008; Ndubaku *et al*, 2009b). In contrast to these studies, canonical signaling was only slightly (if at all) activated after SM stimulation in the present work (Fig. 3.7 and 3.16).

This observation gives rise to further questions regarding this discrepancy. To our knowledge, SM-mediated NF- $\kappa$ B signaling has so far not been investigated in B16 and endothelial cells (HUVEC) and these cells might exhibit a different response to SM. Also, it might be that the SM compound used in our work induced a different mechanism to activate canonical NF- $\kappa$ B signaling. In previous studies, canonical NF- $\kappa$ B signaling has mainly been demonstrated by western blot analysis. Furthermore, the activation was analyzed within the first minutes after treatment and the response oscillated over time (as reported by (Werner *et al*, 2005)). In our study, NF- $\kappa$ B activation was analyzed by ELISA (TransAM) and this may result in a decreased level of canonical NF- $\kappa$ B activation due to a different method and different time points of stimulation.

Additionally, TNF induced the canonical NF- $\kappa$ B activity, which was not altered by additional SM treatment in our study. Contrary to this, Varfolomeev and colleagues reported that SM abrogates TNF induced NF- $\kappa$ B activation (Varfolomeev *et al*, 2008).

Our analyses of NF- $\kappa$ B induced genes (e.g. VEGF-A, VCAM-1) demonstrated that their mRNA levels were not effected in the presence of SM. Furthermore, NF- $\kappa$ B activation was investigated up to 24 hours and also pre-treatment of cells with SM, revealed no change in TNF induced NF- $\kappa$ B activation (data not shown).

However, to characterize NF- $\kappa$ B signaling in more detail, additional analyses like Western blot analyses are being pursued. On the one hand, this could substantiate our findings and may provide new details about the crosstalk of IAPs and TNF-induced signaling, especially in the endothelium. On the other hand, subsequent analyses might illustrate a clear activation of canonical NF- $\kappa$ B signaling that were not seen by ELISA assays.

To further substantiate our *in vivo* observations concerning the anti-angiogenic effects of SM, we performed qRT-PCR analyses of endothelial growth signals known to be engaged by TNF-induced NF- $\kappa$ B signaling (Hoeben *et al*, 2004). Our analyses of pro-angiogenic growth factors and cell adhesion molecules, excludes an alteration of TNF mediated angiogenic signaling by SM treatment (Fig. 3.16). Furthermore, this implies that IAP antagonization in conjunction with TNF-R signaling resulted in EC apoptosis rather than alteration of the TNF-induced neo-angiogenesis, at least *in vitro*.

#### **4.4 IAP antagonization leads to TNF induced vascular disruption *in vivo***

The potency of SM in disrupting tumor vascularization *in vivo* was conclusively demonstrated by implanting matrigel plugs containing tumor cells in mice and subsequent analyses of matrigel vascularization (Fig. 3.18). In the absence of tumor cells, i.e. when pure matrigel was implanted into mice, SM was only able to inhibit angiogenesis when ectopic TNF was also included in the matrigel plugs. Strikingly, when matrigel plugs, supplemented with TNF and SM were implanted in TNF-R1/2<sup>-/-</sup>-mice no alteration in angiogenesis could be detected when ECs lack TNF-R signaling (Fig. 3.19). This conclusively demonstrated that the anti-angiogenic effect of SM is dependent on TNF. Similar results were obtained upon tumor cell implantation in TNF-R1/2<sup>-/-</sup>-mice. SM failed to inhibit tumor growth and vascularization in TNF-R1/2<sup>-/-</sup>-mice (Fig. 3.20 and 3.21). This

furthermore demonstrated that the reduction in tumor growth in wild type mice was not due to a direct effect on B16 cells.

Notably, it has already been shown that loss of IAPs within the myeloid compartment causes the over-production of many pro-inflammatory cytokines including TNF (Wong *et al*, 2014). Thus, targeting IAP proteins by SM could further potentiate the production of inflammatory cytokine by immune infiltrating cells within a tumor and thereby expand the SM-mediated cytotoxicity towards adjacent tissues, including ECs. Indeed, it has been shown that SM and stimulation of the innate immune system by pathogen mimetics, can synergize to potentiate the effect of SM (Beug *et al*, 2014). In particular, the group of R. Korneluk reported that oncolytic viruses and adjuvants (such as poly(I:C) and CpG) that are proven safe in clinical trials, stimulate a potent safe “cytokine storm”. These findings lend support to the idea that enhanced cytokine production in the tumor stroma, might create a bystander effect combined with SM. Conceivably, similar bystander effects could help potentiate cytotoxicity mediated by SM towards the tumor vasculature.

Our data showed that TNF-R signaling can be directly modified by SM in ECs and the main trigger for an attenuated tumor growth in the presented work seems to be the disruption of the tumor vasculature. One possible strategy to elucidate the role of TNF-R signaling in different tissue compartments within a tumor in more detail, could be a tissue specific ablation of TNF-R signaling (e.g. EC or macrophages) followed by the analysis of tumor growth after SM treatment.

Overall, these data confirm endothelial cell death as the main cause for attenuated tumor vascularization in the presence of SM and TNF.

#### **4.5 Therapeutic implications**

Numerous studies focusing on SM in cancer therapy have contributed to the current dogma that SM application typically targets the malignant cells of a tumor. However, the ongoing clinical evaluation of SM in cancer patients has yielded only limited success. Indeed, the tumor microenvironment may represent a more potent antitumoral activity of SM.

The present study showed SM-mediated destruction of tumor-associated blood vessels, thus highlighting the potential for targeting tumors that otherwise might be expected to



resist SM therapy (Krepler *et al*, 2013). Although disruption of the vascular endothelium appears to be the primary mechanism of tumor reduction in the B16 melanoma model, this may not apply to all tumors. Indeed, direct effects of SM towards cancer cells are well established (Bai *et al*, 2014; Fulda & Vucic, 2012). Thus, SM-mediated cell death of the tumor-vasculature may constitute an additional and perhaps complementary therapeutic paradigm for SM therapy.

Congruent with our findings, anti-angiogenic drugs have been shown to be highly potent in cancer treatment. Notably, vascular disruption agents (VDA) (Mita *et al*, 2013; Porcù *et al*, 2014) are used to limit tumor growth and are evaluated in clinical trials. In line with this, antitumor activity was shown with an oligomeric form of the DR5 ligand Apo2L/TRAIL, which is able to induce specific death of tumor-ECs (expressing DR5) and resulting in inhibition of tumor growth in Lewis lung carcinoma (Wilson *et al*, 2012). These studies further underline the potential clinical relevance for targeting the tumor-vasculature.

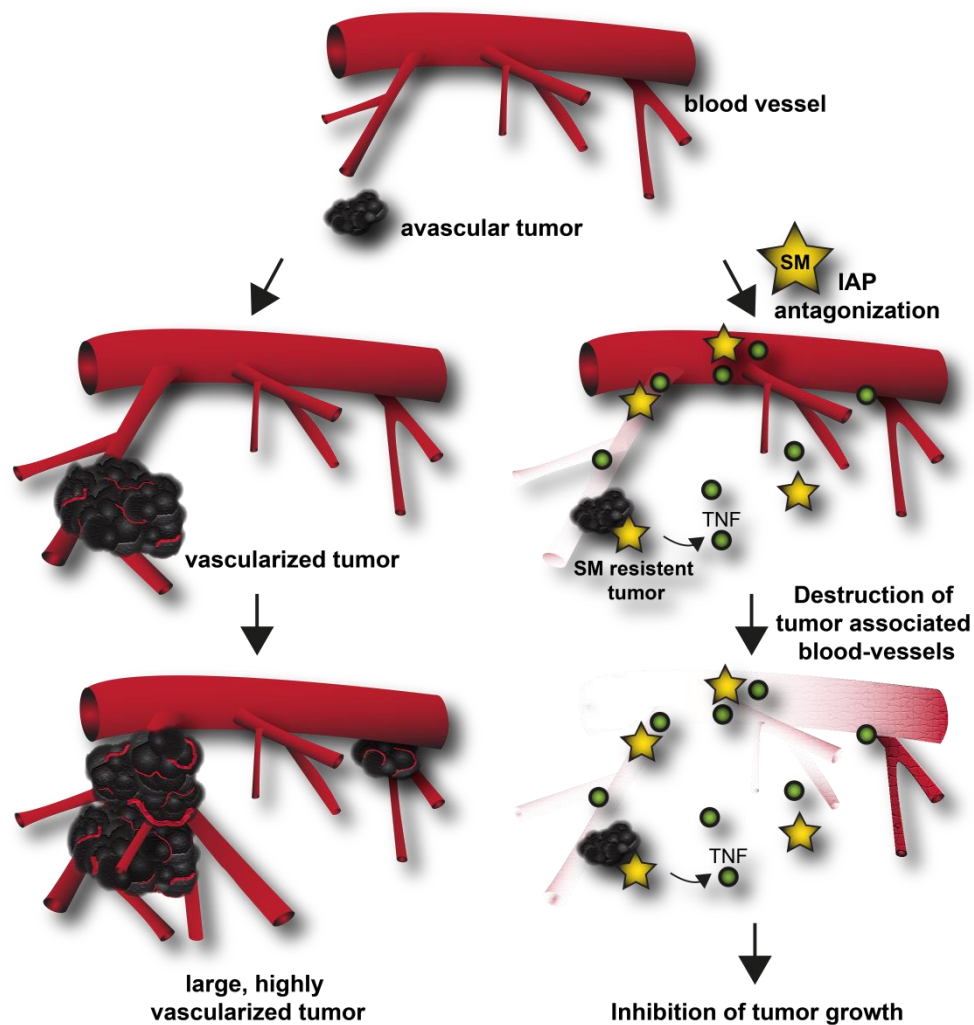
In this work, tumor cells and SM were co-injected into the recipient mice leading to an attenuation of tumor growth. This may not represent a clinically relevant regimen. Indeed, evaluating whether SM can block already established tumor vessels, might represent a more physiological and clinically relevant setting. Our *in vitro* experiments, using tube formation assays as well as established networks (Fig. 3.17), already point at the potential activity of SM/TNF on already established blood vessels. These questions are currently being addressed by ongoing experiments. It is important to realize, however, that targeting established vasculature also harbors the potential for causing damage to quiescent normal vasculature. It will be of particular interest therefore to establish if normal blood vessels are affected by SM treatment. Interestingly, *in vivo* studies using SM (Petersen *et al*, 2007) largely failed to detect substantially increased TNF levels in the circulation, suggesting that TNF is primarily produced locally in the immediate tumor microenvironment and therefore potentially limiting the activity to sites of pathological blood vessel growth. If so, SM could be valuable to target tumor-associated blood vessels but simultaneously minimizing collateral damage to the normal vasculature.

#### 4.6 Conclusion

Numerous studies have focused on the potential of SM to induce cell death in cancer cells (Fulda & Vucic, 2012; Fulda, 2014; Bai *et al*, 2014) and various SM compounds are currently in clinical trials to evaluate their potential use in cancer therapy. So far, SM mediated cell death is believed to directly target malignant cells.

Here we show in a B16 melanoma tumor model, that treatment with SMAC mimetics leads to a clear attenuation of tumor growth *in vivo*. Exploring the underlying mechanisms, our results demonstrate for the first time that SMAC mimetics have the potential to inhibit tumor growth not by inducing direct cytotoxicity in tumor cells but by disruption of the tumor vasculature. The high susceptibility of endothelial cells to a SMAC mimetic mediated and TNF-dependent cell death was shown *in vitro* and *in vivo*. Using the TNF-R1/2<sup>-/-</sup>-mice, we show that the disruption of the tumor vasculature is highly dependent on TNF signaling in the tumor microenvironment, leading to a so far unrecognized anti-angiogenic activity of SMAC mimitcs.

Together, these findings may offer a novel approach to target the tumor vasculature using SM to control pathological angiogenesis while minimizing collateral damage to normal blood vessels. This could constitute an additional and perhaps complementary utility of SMAC mimetics which could subsequently lead to improvement of current cancer therapy.



**Conclusion: Proposed model of SMAC mimetic induced destruction of vascular endothelium, leading to inhibition of tumor growth under inflammatory conditions.**

IAP antagonization by SMAC mimetics (SM) does not induce a direct cytotoxic effect against tumor cells in our model but leads to a hitherto unrecognized disruption of the vasculature in the tumor microenvironment. Upon SM treatment, induction of non-canonical NF- $\kappa$ B activity facilitates the production of TNF by tumor cells. In the presence of SM, endothelial cells in the tumor microenvironment become highly susceptible to a TNF-induced apoptotic death. This novel anti-angiogenic effect of SM towards endothelial cells results in the inhibition of tumor growth.

## 5. References

- Akagi T, Motegi M, Tamura A, Suzuki R, Hosokawa Y, Suzuki H, Ota H, Nakamura S, Morishima Y, Taniwaki M & Seto M (1999) A novel gene, MALT1 at 18q21, is involved in t(11;18) (q21;q21) found in low-grade B-cell lymphoma of mucosa-associated lymphoid tissue. *Oncogene* **18**: 5785–94
- Almeida S, Maillard C, Itin P, Hohl D & Huber M (2008) Five new CYLD mutations in skin appendage tumors and evidence that aspartic acid 681 in CYLD is essential for deubiquitinase activity. *J. Invest. Dermatol.* **128**: 587–93
- Andree M, Seeger JM, Schüll S, Coutelle O, Wagner-Stippich D, Wiegmann K, Wunderlich CM, Brinkmann K, Broxtermann P, Witt A, Fritsch M, Martinelli P, Bielig H, Lamkemeyer T, Rugarli EI, Kaufmann T, Sterner-Kock A, Wunderlich FT, Villunger A, Martins LM, et al (2014) BID-dependent release of mitochondrial SMAC dampens XIAP-mediated immunity against Shigella. *EMBO J.*
- Arnt CR, Chiorean M V., Heldebrant MP, Gores GJ & Kaufmann SH (2002) Synthetic Smac/DIABLO peptides enhance the effects of chemotherapeutic agents by binding XIAP and cIAP1 in situ. *J. Biol. Chem.* **277**: 44236–44243
- Ashkenazi A (2008) Targeting the extrinsic apoptosis pathway in cancer. *Cytokine Growth Factor Rev.* **19**: 325–331
- Badrichani AZ, Stroka DM, Bilbao G, Curiel DT, Bach FH & Ferran C (1999) Bcl-2 and Bcl-XL serve an anti-inflammatory function in endothelial cells through inhibition of NF-kappaB. *J. Clin. Invest.* **103**: 543–53
- Bai L, Smith DC & Wang S (2014) Small-molecule SMAC mimetics as new cancer therapeutics. *Pharmacol. Ther.*
- Balkwill F (2006) TNF-alpha in promotion and progression of cancer. *Cancer Metastasis Rev.* **25**: 409–16
- Bashyam MD, Bair R, Kim YH, Wang P, Hernandez-Boussard T, Karikari CA, Tibshirani R, Maitra A & Pollack JR (2005) Array-based comparative genomic hybridization identifies localized DNA amplifications and homozygous deletions in pancreatic cancer. *Neoplasia* **7**: 556–62
- Benetatos C a, Mitsuuchi Y, Burns JM, Neiman EM, Condon SM, Yu G, Seipel ME, Kapoor GS, Laporte MG, Rippin SR, Deng Y, Hendi MS, Tirunahari PK, Lee Y-H, Haimowitz T, Alexander MD, Graham M a, Weng D, Shi Y, McKinlay M a, et al (2014) Birinapant (TL32711), a bivalent SMAC mimetic, targets TRAF2-associated cIAPs, abrogates TNF-induced NF-κB activation, and is active in patient-derived xenograft models. *Mol. Cancer Ther.* **13**: 867–79
- Bertrand MJM, Milutinovic S, Dickson KM, Ho WC, Boudreault A, Durkin J, Gillard JW, Jaquith JB, Morris SJ & Barker P a (2008) cIAP1 and cIAP2 facilitate cancer cell survival by functioning as E3 ligases that promote RIP1 ubiquitination. *Mol. Cell* **30**: 689–700

- Beug ST, Tang V a, LaCasse EC, Cheung HH, Beauregard CE, Brun J, Nuyens JP, Earl N, St-Jean M, Holbrook J, Dastidar H, Mahoney DJ, Ilkow C, Le Boeuf F, Bell JC & Korneluk RG (2014) Smac mimetics and innate immune stimuli synergize to promote tumor death. *Nat. Biotechnol.* **32**: 182–90
- Bhardwaj A & Aggarwal BB (2003) Receptor-mediated choreography of life and death. *J. Clin. Immunol.* **23**: 317–32
- Birnbaum MJ, Clem RJ & Miller LK (1994) An apoptosis-inhibiting gene from a nuclear polyhedrosis virus encoding a polypeptide with Cys/His sequence motifs. *J. Virol.* **68**: 2521–8
- Brinkmann K, Hombach A, Seeger JM, Wagner-Stippich D, Klubertz D, Krönke M, Abken H & Kashkar H (2014) Second mitochondria-derived activator of caspase (SMAC) mimetic potentiates tumor susceptibility toward natural killer cell-mediated killing. *Leuk. Lymphoma* **55**: 645–51
- Cai Q, Sun H, Peng Y, Lu J, Nikolovska-Coleska Z, McEachern D, Liu L, Qiu S, Yang C-Y, Miller R, Yi H, Zhang T, Sun D, Kang S, Guo M, Leopold L, Yang D & Wang S (2011) A potent and orally active antagonist (SM-406/AT-406) of multiple inhibitor of apoptosis proteins (IAPs) in clinical development for cancer treatment. *J. Med. Chem.* **54**: 2714–26
- Cai Z, Jitkaew S, Zhao J, Chiang H-C, Choksi S, Liu J, Ward Y, Wu L-G & Liu Z-G (2014) Plasma membrane translocation of trimerized MLKL protein is required for TNF-induced necroptosis. *Nat. Cell Biol.* **16**: 55–65
- Carmeliet P & Jain RK (2000) Angiogenesis in cancer and other diseases. *Nature* **407**: 249–57
- Chai J, Du C, Wu JW, Kyin S, Wang X & Shi Y (2000a) Structural and biochemical basis of apoptotic activation by Smac/DIABLO. *Nature* **406**: 855–62
- Chai J, Du C, Wu JW, Kyin S, Wang X & Shi Y (2000b) Structural and biochemical basis of apoptotic activation by Smac/DIABLO. *Nature* **406**: 855–62
- Chai J, Shiozaki E, Srinivasula SM, Wu Q, Datta P, Alnemri ES, Shi Y & Datta P (2001) Structural basis of caspase-7 inhibition by XIAP. *Cell* **104**: 769–80
- Che X, Yang D, Zong H, Wang J, Li X, Chen F, Chen X & Song X (2012) Nuclear cIAP1 overexpression is a tumor stage- and grade-independent predictor of poor prognosis in human bladder cancer patients. *Urol. Oncol.* **30**: 450–6
- Cheung HH, Mahoney DJ, Lacasse EC & Korneluk RG (2009) Down-regulation of c-FLIP Enhances death of cancer cells by smac mimetic compound. *Cancer Res.* **69**: 7729–38
- Cheung HH, Plenchette S, Kern CJ, Mahoney DJ & Korneluk RG (2008) The RING domain of cIAP1 mediates the degradation of RING-bearing inhibitor of apoptosis proteins by distinct pathways. *Mol. Biol. Cell* **19**: 2729–40
- Chipuk JE, Moldoveanu T, Llambi F, Parsons MJ & Green DR (2010) The BCL-2 family reunion. *Mol. Cell* **37**: 299–310

- Chomczynski P & Sacchi N (1987) Single-step method of RNA isolation by acid guanidinium thiocyanate-phenol-chloroform extraction. *Anal. Biochem.* **162**: 156–9
- Clem RJ & Miller LK (1994) Control of Programmed Cell Death by the Baculovirus Genes p35 and iap. **14**:
- Condon SM, Mitsuuchi Y, Deng Y, LaPorte MG, Rippin SR, Haimowitz T, Alexander MD, Kumar PT, Hendi MS, Lee Y-H, Benetatos C a, Yu G, Kapoor GS, Neiman E, Seipel ME, Burns JM, Graham M a, McKinlay M a, Li X, Wang J, et al (2014a) Birinapant, a smac-mimetic with improved tolerability for the treatment of solid tumors and hematological malignancies. *J. Med. Chem.* **57**: 3666–77
- Condon SM, Mitsuuchi Y, Deng Y, Laporte MG, Rippin SR, Haimowitz T, Alexander MD, Kumar PT, Hendi MS, Lee Y-H, Benetatos CA, Yu G, Kapoor GS, Neiman E, Seipel ME, Burns JM, Graham MA, McKinlay MA, Li X, Wang J, et al (2014b) Birinapant, a smac-mimetic with improved tolerability for the treatment of solid tumors and hematological malignancies. *J. Med. Chem.* **57**: 3666–77
- Conze DB, Albert L, Ferrick DA, David V, Yeh W, Mak T, Ashwell JD & Goeddel D V (2005) Posttranscriptional Downregulation of c-IAP2 by the Ubiquitin Protein Ligase c-IAP1 In Vivo Posttranscriptional Downregulation of c-IAP2 by the Ubiquitin Protein Ligase c-IAP1 In Vivo.
- Coutelle O, Hornig-Do H-T, Witt A, Andree M, Schiffmann LM, Piekarek M, Brinkmann K, Seeger JM, Liwschitz M, Miwa S, Hallek M, Krönke M, Trifunovic A, Eming SA, Wiesner RJ, Hacker UT & Kashkar H (2014) Embelin inhibits endothelial mitochondrial respiration and impairs neoangiogenesis during tumor growth and wound healing. *EMBO Mol. Med.* **6**: 624–39
- Crook NE, Clem RJ & Miller LK (1993) An apoptosis-inhibiting baculovirus gene with a zinc finger-like motif. *J. Virol.* **67**: 2168–74
- Czabotar PE, Lessene G, Strasser A & Adams JM (2014) Control of apoptosis by the BCL-2 protein family: implications for physiology and therapy. *Nat. Rev. Mol. Cell Biol.* **15**: 49–63
- Dai Z, Zhu W-G, Morrison CD, Brena RM, Smiraglia DJ, Raval A, Wu Y-Z, Rush LJ, Ross P, Molina JR, Otterson GA & Plass C (2003) A comprehensive search for DNA amplification in lung cancer identifies inhibitors of apoptosis cIAP1 and cIAP2 as candidate oncogenes. *Hum. Mol. Genet.* **12**: 791–801
- Darding M, Feltham R, Tenev T, Bianchi K, Benetatos C, Silke J & Meier P (2011) Molecular determinants of Smac mimetic induced degradation of cIAP1 and cIAP2. *Cell Death Differ.* **18**: 1376–86
- Declercq W, Vanden Berghe T & Vandenabeele P (2009) RIP kinases at the crossroads of cell death and survival. *Cell* **138**: 229–32
- Degterev A, Huang Z, Boyce M, Li Y, Jagtap P, Mizushima N, Cuny GD, Mitchison TJ, Moskowitz MA & Yuan J (2005) Chemical inhibitor of nonapoptotic cell death with therapeutic potential for ischemic brain injury. *Nat. Chem. Biol.* **1**: 112–9
- Denault JB SG (2002) Unit 21.8. *Curr Protoc Protein Sci*: 1–16

- Deveraux QL & Reed JC (1999a) IAP family proteins -- suppressors of apoptosis IAP family proteins — suppressors of apoptosis. : 239–252
- Deveraux QL & Reed JC (1999b) IAP family proteins--suppressors of apoptosis. *Genes Dev.* **13**: 239–52
- Deveraux QL, Takahashi R, Salvesen GS & Reed JC (1997) X-linked IAP is a direct inhibitor of cell-death proteases. *Nature* **388**: 300–4
- DiDonato J a, Mercurio F & Karin M (2012) NF- $\kappa$ B and the link between inflammation and cancer. *Immunol. Rev.* **246**: 379–400
- Dierlamm J, Baens M, Wlodarska I, Stefanova-Ouzounova M, Hernandez JM, Hossfeld DK, De Wolf-Peeters C, Hagemeijer A, Van den Berghe H & Marynen P (1999) The apoptosis inhibitor gene API2 and a novel 18q gene, MLT, are recurrently rearranged in the t(11;18)(q21;q21) associated with mucosa-associated lymphoid tissue lymphomas. *Blood* **93**: 3601–9
- Dougan M, Dougan S, Slisz J, Firestone B, Vanneman M, Draganov D, Goyal G, Li W, Neuberg D, Blumberg R, Hacohen N, Porter D, Zawel L & Dranoff G (2010) IAP inhibitors enhance co-stimulation to promote tumor immunity. *J. Exp. Med.* **207**: 2195–206
- Du C, Fang M, Li Y, Li L & Wang X (2000) Smac, a mitochondrial protein that promotes cytochrome c-dependent caspase activation by eliminating IAP inhibition. *Cell* **102**: 33–42
- Dubrez L, Berthelet J & Glorian V (2013) IAP proteins as targets for drug development in oncology. *Onco. Targets. Ther.* **9**: 1285–304
- Dueber EC, Schoeffler AJ, Lingel A, Elliott JM, Fedorova A V., Giannetti AM, Zobel K, Maurer B, Varfolomeev E, Wu P, Wallweber HJA, Hymowitz SG, Deshayes K, Vucic D & Fairbrother WJ (2011) Antagonists Induce a Conformational Change in cIAP1 That Promotes Autoubiquitination. *Science (80-. )*. **334**: 376–380
- Eckelman BP, Salvesen GS & Scott FL (2006) Human inhibitor of apoptosis proteins: why XIAP is the black sheep of the family. *EMBO Rep.* **7**: 988–94
- Ermolaeva M a, Michallet M-C, Papadopoulou N, Utermöhlen O, Kranidioti K, Kollias G, Tschopp J & Pasparakis M (2008) Function of TRADD in tumor necrosis factor receptor 1 signaling and in TRIF-dependent inflammatory responses. *Nat. Immunol.* **9**: 1037–46
- Fady C, Gardner A, Jacoby F, Briskin K, Tu Y, Schmid I & Lichtenstein A (1995) Atypical apoptotic cell death induced in L929 targets by exposure to tumor necrosis factor. *J. Interferon Cytokine Res.* **15**: 71–80
- Fajardo LF, Kwan HH, Kowalski J, Prionas SD & Allison AC (1992) Dual role of tumor necrosis factor-alpha in angiogenesis. *Am. J. Pathol.* **140**: 539–44
- Feoktistova M, Geserick P, Kellert B, Dimitrova DP, Langlais C, Hupe M, Cain K, MacFarlane M, Häcker G & Leverkus M (2011) cIAPs block Ripoptosome formation,

- a RIP1/caspase-8 containing intracellular cell death complex differentially regulated by cFLIP isoforms. *Mol. Cell* **43**: 449–63
- Fuentes-Prior P & Salvesen G (2004) The protein structures that shape caspase activity, specificity, activation and inhibition.
- Fulda S (2014) Molecular Pathways: Targeting Death Receptors and Smac Mimetics. *Clin. Cancer Res.*
- Fulda S & Vucic D (2012) Targeting IAP proteins for therapeutic intervention in cancer. *Nat. Rev. Drug Discov.* **11**: 109–24
- Fulda S, Wick W, Weller M & Debatin K-M (2002) Smac agonists sensitize for Apo2L/TRAIL- or anticancer drug-induced apoptosis and induce regression of malignant glioma in vivo. *Nat. Med.* **8**: 808–815
- Gaither A, Porter D, Yao Y, Borawski J, Yang G, Donovan J, Sage D, Slisz J, Tran M, Straub C, Ramsey T, Iourgenko V, Huang A, Chen Y, Schlegel R, Labow M, Fawell S, Sellers WR & Zawel L (2007) A Smac mimetic rescue screen reveals roles for inhibitor of apoptosis proteins in tumor necrosis factor- $\alpha$  signaling. *Cancer Res.* **67**: 11493–8
- Geserick P, Hupe M, Moulin M, Wong WW-L, Feoktistova M, Kellert B, Gollnick H, Silke J & Leverkus M (2009) Cellular IAPs inhibit a cryptic CD95-induced cell death by limiting RIP1 kinase recruitment. *J. Cell Biol.* **187**: 1037–54
- Grzybowska-Izydorczyk O, Cebula B, Robak T & Smolewski P (2010) Expression and prognostic significance of the inhibitor of apoptosis protein (IAP) family and its antagonists in chronic lymphocytic leukaemia. *Eur. J. Cancer* **46**: 800–10
- Gyrd-Hansen M, Darding M, Miasari M, Santoro MM, Zender L, Xue W, Tenev T, da Fonseca PCA, Zvelebil M, Bujnicki JM, Lowe S, Silke J & Meier P (2008) IAPs contain an evolutionarily conserved ubiquitin-binding domain that regulates NF- $\kappa$ B as well as cell survival and oncogenesis. *Nat. Cell Biol.* **10**: 1309–1317
- Gyrd-Hansen M & Meier P (2010) IAPs: from caspase inhibitors to modulators of NF- $\kappa$ B, inflammation and cancer. *Nat. Rev. Cancer* **10**: 561–574
- Hanahan D & Weinberg RA (2000) The Hallmarks of Cancer. *Cell* **100**: 57–70
- Hanahan D & Weinberg RA (2011) Hallmarks of cancer: the next generation. *Cell* **144**: 646–74
- Havell EA, Fiers W & North RJ (1988) The antitumor function of tumor necrosis factor (TNF), I. Therapeutic action of TNF against an established murine sarcoma is indirect, immunologically dependent, and limited by severe toxicity. *J. Exp. Med.* **167**: 1067–85
- Hayashi M, Jono H, Shinriki S, Nakamura T, Guo J, Sueta A, Tomiguchi M, Fujiwara S, Yamamoto-Ibusuki M, Murakami K-I, Yamashita S, Yamamoto Y, Li J-D, Iwase H & Ando Y (2014) Clinical significance of CYLD downregulation in breast cancer. *Breast Cancer Res. Treat.* **143**: 447–57



- He S, Wang L, Miao L, Wang T, Du F, Zhao L & Wang X (2009) Receptor interacting protein kinase-3 determines cellular necrotic response to TNF- $\alpha$ . *Cell* **137**: 1100–11
- Hoeben A, Landuyt B, Highley MS, Wildiers H, Van Oosterom AT & De Bruijn EA (2004) Vascular endothelial growth factor and angiogenesis. *Pharmacol. Rev.* **56**: 549–80
- Hofer-Warbinek R, Schmid JA, Stehlik C, Binder BR, Lipp J & de Martin R (2000) Activation of NF- $\kappa$ B by XIAP, the X chromosome-linked inhibitor of apoptosis, in endothelial cells involves TAK1. *J. Biol. Chem.* **275**: 22064–8
- Holler N, Zaru R, Micheau O, Thome M, Attinger A, Valitutti S, Bodmer JL, Schneider P, Seed B & Tschopp J (2000) Fas triggers an alternative, caspase-8-independent cell death pathway using the kinase RIP as effector molecule. *Nat. Immunol.* **1**: 489–95
- Hsu YT, Wolter KG & Youle RJ (1997) Cytosol-to-membrane redistribution of Bax and Bcl-X(L) during apoptosis. *Proc. Natl. Acad. Sci. U. S. A.* **94**: 3668–72
- Hussain AR, Uddin S, Ahmed M, Bu R, Ahmed SO, Abubaker J, Sultana M, Ajarim D, Al-Dayel F, Bavi PP & Al-Kuraya KS (2010) Prognostic significance of XIAP expression in DLBCL and effect of its inhibition on AKT signalling. *J. Pathol.* **222**: 180–90
- Hussain SP, Hofseth LJ & Harris CC (2003) Radical causes of cancer. *Nat. Rev. Cancer* **3**: 276–85
- Imoto I, Tsuda H, Hirasawa A, Miura M, Sakamoto M, Hirohashi S & Inazawa J (2002) Expression of cIAP1, a Target for 11q22 Amplification, Correlates with Resistance of Cervical Cancers to Radiotherapy. *Cancer Res.* **62**: 4860–4866
- Imoto I, Yang Z-Q, Pimkhaokham A, Tsuda H, Shimada Y, Imamura M, Ohki M & Inazawa J (2001) Identification of cIAP1 As a Candidate Target Gene within an Amplicon at 11q22 in Esophageal Squamous Cell Carcinomas. *Cancer Res.* **61**: 6629–6634
- Jin H-S, Lee D-H, Kim D-H, Chung J-H, Lee S-J & Lee TH (2009) cIAP1, cIAP2, and XIAP act cooperatively via nonredundant pathways to regulate genotoxic stress-induced nuclear factor- $\kappa$ B activation. *Cancer Res.* **69**: 1782–91
- Kashkar H (2010) X-linked inhibitor of apoptosis: a chemoresistance factor or a hollow promise. *Clin. Cancer Res.* **16**: 4496–502
- Kaufmann T, Strasser A & Jost PJ (2012) Fas death receptor signalling: roles of Bid and XIAP. *Cell Death Differ.* **19**: 42–50
- Kempkensteffen C, Hinz S, Christoph F, Krause H, Magheli A, Schrader M, Schostak M, Miller K & Weikert S (2008) Expression levels of the mitochondrial IAP antagonists Smac/DIABLO and Omi/HtrA2 in clear-cell renal cell carcinomas and their prognostic value. *J. Cancer Res. Clin. Oncol.* **134**: 543–50
- Kerr JF, Wyllie AH & Currie AR (1972) Apoptosis: a basic biological phenomenon with wide-ranging implications in tissue kinetics. *Br. J. Cancer* **26**: 239–57
- Kleinman HK & Martin GR (2005) Matrigel: basement membrane matrix with biological activity. *Semin. Cancer Biol.* **15**: 378–86

- Krajewska M, Kim H, Kim C, Kang H, Welsh K, Matsuzawa S-I, Tsukamoto M, Thomas RG, Assa-Munt N, Piao Z, Suzuki K, Perucho M, Krajewski S & Reed JC (2005) Analysis of apoptosis protein expression in early-stage colorectal cancer suggests opportunities for new prognostic biomarkers. *Clin. Cancer Res.* **11**: 5451–61
- Krepler C, Chunduru SK, Halloran MB, He X, Xiao M, Vultur A, Villanueva J, Mitsuuchi Y, Neiman EM, Benetatos C, Nathanson KL, Amaravadi RK, Pehamberger H, McKinlay M & Herlyn M (2013) The novel SMAC mimetic birinapant exhibits potent activity against human melanoma cells. *Clin. Cancer Res.* **19**: 1784–94
- Kulbe H, Thompson R, Wilson JL, Robinson S, Hagemann T, Fatah R, Gould D, Ayhan A & Balkwill F (2007) The inflammatory cytokine tumor necrosis factor- $\alpha$  generates an autocrine tumor-promoting network in epithelial ovarian cancer cells. *Cancer Res.* **67**: 585–92
- Kumar S & Lavin MF (1996) The ICE family of cysteine proteases as effectors of cell death. *Cell Death Differ.* **3**: 255–67
- LaCasse EC, Mahoney DJ, Cheung HH, Plenchette S, Baird S & Korneluk RG (2008) IAP-targeted therapies for cancer. *Oncogene* **27**: 6252–6275
- Laster SM, Wood JG & Gooding LR (1988) Tumor necrosis factor can induce both apoptotic and necrotic forms of cell lysis. *J. Immunol.* **141**: 2629–34
- Laukens B, Jennewein C, Schenk B, Vanlangenakker N, Schier A, Cristofanon S, Zobel K, Deshayes K, Vucic D, Jeremias I, Bertrand MJM, Vandenabeele P & Fulda S (2011) Smac mimetic bypasses apoptosis resistance in FADD- or caspase-8-deficient cells by priming for tumor necrosis factor  $\alpha$ -induced necroptosis. *Neoplasia* **13**: 971–9
- Lecis D, De Cesare M, Perego P, Conti a, Corna E, Drago C, Seneci P, Walczak H, Colombo MP, Delia D & Sangaletti S (2013) Smac mimetics induce inflammation and necrotic tumour cell death by modulating macrophage activity. *Cell Death Dis.* **4**: e920
- Lecis D, Drago C, Manzoni L, Seneci P, Scolastico C, Mastrangelo E, Bolognesi M, Anichini a, Kashkar H, Walczak H & Delia D (2010) Novel SMAC-mimetics synergistically stimulate melanoma cell death in combination with TRAIL and Bortezomib. *Br. J. Cancer* **102**: 1707–16
- Li L, Thomas RM, Suzuki H, De Brabander JK, Wang X & Harran PG (2004) A small molecule Smac mimic potentiates TRAIL- and TNF $\alpha$ -mediated cell death. *Science* **305**: 1471–4
- Li P, Nijhawan D, Budihardjo I, Srinivasula SM, Ahmad M, Alnemri ES & Wang X (1997) Cytochrome c and dATP-dependent formation of Apaf-1/caspase-9 complex initiates an apoptotic protease cascade. *Cell* **91**: 479–89
- Liston P, Roy N, Tamai K, Lefebvre C, Baird S, Cherton-Horvat G, Farahani R, McLean M, Ikeda JE, MacKenzie A & Korneluk RG (1996) Suppression of apoptosis in mammalian cells by NAIP and a related family of IAP genes. *Nature* **379**: 349–53

- Liu Z, Sun C, Olejniczak ET, Meadows RP, Betz SF, Oost T, Herrmann J, Wu JC & Fesik SW (2000) Structural basis for binding of Smac/DIABLO to the XIAP BIR3 domain. *Nature* **408**: 1004–8
- Lopez J, John SW, Tenev T, Rautureau GJP, Hinds MG, Francalanci F, Wilson R, Broemer M, Santoro MM, Day CL & Meier P (2011) CARD-mediated autoinhibition of cIAP1's E3 ligase activity suppresses cell proliferation and migration. *Mol. Cell* **42**: 569–83
- Lu M, Lin S-C, Huang Y, Kang YJ, Rich R, Lo Y-C, Myszkka D, Han J & Wu H (2007) XIAP induces NF-kappaB activation via the BIR1/TAB1 interaction and BIR1 dimerization. *Mol. Cell* **26**: 689–702
- Maas C, Tromp JM, van Laar J, Thijssen R, Elias J a, Malara a, Krippner-Heidenreich a, Silke J, van Oers MH & Eldering E (2013) CLL cells are resistant to smac mimetics because of an inability to form a ripoptosome complex. *Cell Death Dis.* **4**: e782
- Mackay BF, Loetscher H, Stueber D, Gehr G & Lesslauer W (1993) From Pharmaceutical Research-New Technologies, E Hoffmann-La Roche Ltd., CH-4002 Basel, Switzerland. **177**:
- Mahoney DJ, Cheung HH, Mrad RL, Plenchette S, Simard C, Enwere E, Arora V, Mak TW, Lacasse EC, Waring J & Korneluk RG (2008) Both cIAP1 and cIAP2 regulate TNFalpha-mediated NF-kappaB activation. *Proc. Natl. Acad. Sci. U. S. A.* **105**: 11778–83
- Mantovani A, Allavena P, Sica A & Balkwill F (2008) Cancer-related inflammation. *Nature* **454**: 436–44
- Masoumi KC, Shaw-Hallgren G & Massoumi R (2011) Tumor Suppressor Function of CYLD in Nonmelanoma Skin Cancer. *J. Skin Cancer* **2011**: 614097
- McComb S, Cheung HH, Korneluk RG, Wang S, Krishnan L & Sad S (2012) cIAP1 and cIAP2 limit macrophage necroptosis by inhibiting Rip1 and Rip3 activation. *Cell Death Differ.* **19**: 1791–801
- Mita MM, Sargsyan L, Mita AC & Spear M (2013) Vascular-disrupting agents in oncology. *Expert Opin. Investig. Drugs* **22**: 317–28
- Morgan JA, Yin Y, Borowsky AD, Kuo F, Nourmand N, Koontz JI, Reynolds C, Soreng L, Griffin CA, Graeme-Cook F, Harris NL, Weisenburger D, Pinkus GS, Fletcher JA & Sklar J (1999) Breakpoints of the t(11;18)(q21;q21) in mucosa-associated lymphoid tissue (MALT) lymphoma lie within or near the previously undescribed gene MALT1 in chromosome 18. *Cancer Res.* **59**: 6205–13
- Moulin M, Anderton H, Voss AK, Thomas T, Wong WW-L, Bankovacki A, Feltham R, Chau D, Cook WD, Silke J & Vaux DL (2012a) IAPs limit activation of RIP kinases by TNF receptor 1 during development. *EMBO J.* **31**: 1679–91
- Moulin M, Anderton H, Voss AK, Thomas T, Wong WW-L, Bankovacki A, Feltham R, Chau D, Cook WD, Silke J & Vaux DL (2012b) IAPs limit activation of RIP kinases by TNF receptor 1 during development. *EMBO J.* **31**: 1679–91

- Moussata D, Amara S, Siddeek B, Decaussin M, Hehlgans S, Paul-Bellon R, Mornex F, Gerard J-P, Romestaing P, Rödel F, Flourie B, Benahmed M & Mauduit C (2012) XIAP as a radioresistance factor and prognostic marker for radiotherapy in human rectal adenocarcinoma. *Am. J. Pathol.* **181**: 1271–8
- Müller-Sienerth N, Dietz L, Holtz P, Kapp M, Grigoleit GU, Schmuck C, Wajant H & Sigmund D (2011) SMAC mimetic BV6 induces cell death in monocytes and maturation of monocyte-derived dendritic cells. *PLoS One* **6**: e21556
- Nakagawa Y, Abe S, Kurata M, Hasegawa M, Yamamoto K, Inoue M, Takemura T, Suzuki K & Kitagawa M (2006) IAP family protein expression correlates with poor outcome of multiple myeloma patients in association with chemotherapy-induced overexpression of multidrug resistance genes. *Am. J. Hematol.* **81**: 824–31
- Ndubaku C, Cohen F, Varfolomeev E & Vucic D (2009a) Targeting inhibitor of apoptosis proteins for therapeutic intervention. *Future Med. Chem.* **1**: 1509–1525
- Ndubaku C, Varfolomeev E, Wang L, Zobel K, Lau K, Elliott LO, Maurer B, Fedorova A V, Dynek JN, Koehler M, Hymowitz SG, Tsui V, Deshayes K, Fairbrother WJ, Flygare JA & Vucic D (2009b) Antagonism of c-IAP and XIAP proteins is required for efficient induction of cell death by small-molecule IAP antagonists. *ACS Chem. Biol.* **4**: 557–66
- Nicholson D & Thornberry N (1997) Caspases: killer proteases. *Trends Biochem. Sci.* **22**
- Oberst A, Dillon CP, Weinlich R, McCormick LL, Fitzgerald P, Pop C, Hakem R, Salvesen GS & Green DR (2011) Catalytic activity of the caspase-8-FLIP(L) complex inhibits RIPK3-dependent necrosis. *Nature* **471**: 363–7
- Oost TK, Sun C, Armstrong RC, Al-Assaad AS, Betz SF, Deckwerth TL, Ding H, Elmore SW, Meadows RP, Olejniczak ET, Oleksijew A, Oltersdorf T, Rosenberg SH, Shoemaker AR, Tomaselli KJ, Zou H & Fesik SW (2004) Discovery of potent antagonists of the antiapoptotic protein XIAP for the treatment of cancer. *J. Med. Chem.* **47**: 4417–4426
- Perkins ND (2012) The diverse and complex roles of NF- $\kappa$ B subunits in cancer. *Nat. Rev. Cancer* **12**: 121–32
- Petersen SL, Peyton M, Minna JD & Wang X (2010) Overcoming cancer cell resistance to Smac mimetic induced apoptosis by modulating cIAP-2 expression. *Proc. Natl. Acad. Sci. U. S. A.* **107**: 11936–41
- Petersen SL, Wang L, Yalcin-Chin A, Li L, Peyton M, Minna J, Harran P & Wang X (2007) Autocrine TNF $\alpha$  signaling renders human cancer cells susceptible to Smac-mimetic-induced apoptosis. *Cancer Cell* **12**: 445–56
- Pfaffl MW (2001) A new mathematical model for relative quantification in real-time RT-PCR. *Nucleic Acids Res.* **29**: e45
- Pluta P, Cebula-Obrzut B, Ehemann V, Pluta A, Wierzbowska A, Piekarski J, Bilski A, Nejc D, Kordek R, Robak T, Smolewski P & Jeziorski A (2011) Correlation of Smac/DIABLO protein expression with the clinico-pathological features of breast cancer patients. *Neoplasma* **58**: 430–5

- Porcù E, Bortolozzi R, Basso G & Viola G (2014) Recent advances in vascular disrupting agents in cancer therapy. *Future Med. Chem.* **6**: 1485–98
- Riedl SJ, Renatus M, Schwarzenbacher R, Zhou Q, Sun C, Fesik SW, Liddington RC & Salvesen GS (2001) Structural basis for the inhibition of caspase-3 by XIAP. *Cell* **104**: 791–800
- Roy N, Mahadevan MS, McLean M, Shutler G, Yaraghi Z, Farahani R, Baird S, Besner-Johnston a, Lefebvre C & Kang X (1995) The gene for neuronal apoptosis inhibitory protein is partially deleted in individuals with spinal muscular atrophy. *Cell* **80**: 167–78
- Salvesen GS & Duckett CS (2002) IAP proteins: blocking the road to death's door. *Nat. Rev. Mol. Cell Biol.* **3**: 401–10
- Salvucci O, Basik M, Yao L, Bianchi R & Tosato G (2004) Evidence for the involvement of SDF-1 and CXCR4 in the disruption of endothelial cell-branching morphogenesis and angiogenesis by TNF- $\alpha$  and IFN- $\gamma$  Abstract : Vigorous inflammatory responses are associated with tissue damage , particularly when may accoun. **76**:
- Samuel T, Welsh K, Lober T, Togo SH, Zapata JM & Reed JC (2006) Distinct BIR domains of cIAP1 mediate binding to and ubiquitination of tumor necrosis factor receptor-associated factor 2 and second mitochondrial activator of caspases. *J. Biol. Chem.* **281**: 1080–90
- Santoro MM, Samuel T, Mitchell T, Reed JC & Stainier DYR (2007) Birc2 (clap1) regulates endothelial cell integrity and blood vessel homeostasis. *Nat. Genet.* **39**: 1397–402
- Seligson DB, Hongo F, Huerta-Yepez S, Mizutani Y, Miki T, Yu H, Horvath S, Chia D, Goodglick L & Bonavida B (2007) Expression of X-linked inhibitor of apoptosis protein is a strong predictor of human prostate cancer recurrence. *Clin. Cancer Res.* **13**: 6056–63
- Senftleben U, Cao Y, Xiao G, Greten FR, Krähn G, Bonizzi G, Chen Y, Hu Y, Fong a, Sun SC & Karin M (2001) Activation by IKK $\alpha$  of a second, evolutionary conserved, NF- $\kappa$ B signaling pathway. *Science* **293**: 1495–9
- Shiozaki EN, Chai J, Rigotti DJ, Riedl SJ, Li P, Srinivasula SM, Alnemri ES, Fairman R & Shi Y (2003) Mechanism of XIAP-mediated inhibition of caspase-9. *Mol. Cell* **11**: 519–27
- Srinivasula SM, Hegde R, Saleh a, Datta P, Shiozaki E, Chai J, Lee R a, Robbins PD, Fernandes-Alnemri T, Shi Y & Alnemri ES (2001) A conserved XIAP-interaction motif in caspase-9 and Smac/DIABLO regulates caspase activity and apoptosis. *Nature* **410**: 112–6
- Stehlik C, de Martin R, Kumabashiri I, Schmid JA, Binder BR & Lipp J (1998) Nuclear factor (NF)- $\kappa$ B-regulated X-chromosome-linked iap gene expression protects endothelial cells from tumor necrosis factor alpha-induced apoptosis. *J. Exp. Med.* **188**: 211–6

- Stockmann C, Schadendorf D, Klose R & Helfrich I (2014) The impact of the immune system on tumor: angiogenesis and vascular remodeling. *Front. Oncol.* **4**: 69
- Sun H, Nikolovska-Coleska Z, Lu J, Meagher JL, Yang C-Y, Qiu S, Tomita Y, Ueda Y, Jiang S, Krajewski K, Roller PP, Stuckey JA & Wang S (2007) Design, synthesis, and characterization of a potent, nonpeptide, cell-permeable, bivalent Smac mimetic that concurrently targets both the BIR2 and BIR3 domains in XIAP. *J. Am. Chem. Soc.* **129**: 15279–94
- Sun L, Wang H, Wang Z, He S, Chen S, Liao D, Wang L, Yan J, Liu W, Lei X & Wang X (2012) Mixed lineage kinase domain-like protein mediates necrosis signaling downstream of RIP3 kinase. *Cell* **148**: 213–27
- Tait SWG & Green DR (2010) Mitochondria and cell death: outer membrane permeabilization and beyond. *Nat. Rev. Mol. Cell Biol.* **11**: 621–32
- Uren a G, Pakusch M, Hawkins CJ, Puls KL & Vaux DL (1996) Cloning and expression of apoptosis inhibitory protein homologs that function to inhibit apoptosis and/or bind tumor necrosis factor receptor-associated factors. *Proc. Natl. Acad. Sci. U. S. A.* **93**: 4974–8
- Vandenabeele P, Galluzzi L, Vanden Berghe T & Kroemer G (2010) Molecular mechanisms of necroptosis: an ordered cellular explosion. *Nat. Rev. Mol. Cell Biol.* **11**: 700–14
- Varfolomeev E, Blankenship JW, Wayson SM, Fedorova A V, Kayagaki N, Garg P, Zobel K, Dynek JN, Elliott LO, Wallweber HJA, Flygare JA, Fairbrother WJ, Deshayes K, Dixit VM & Vucic D (2007) IAP antagonists induce autoubiquitination of c-IAPs, NF-kappaB activation, and TNFalpha-dependent apoptosis. *Cell* **131**: 669–81
- Varfolomeev E, Goncharov T, Fedorova A V, Dynek JN, Zobel K, Deshayes K, Fairbrother WJ & Vucic D (2008) c-IAP1 and c-IAP2 are critical mediators of tumor necrosis factor alpha (TNFalpha)-induced NF-kappaB activation. *J. Biol. Chem.* **283**: 24295–9
- Varfolomeev E, Wayson SM, Dixit VM, Fairbrother WJ & Vucic D (2006) The inhibitor of apoptosis protein fusion c-IAP2.MALT1 stimulates NF-kappaB activation independently of TRAF1 AND TRAF2. *J. Biol. Chem.* **281**: 29022–9
- Vaux DL & Silke J (2003) Mammalian mitochondrial IAP binding proteins. *Biochem. Biophys. Res. Commun.* **304**: 499–504
- Vaux DL & Silke J (2005) IAPs, RINGs and ubiquitylation. *Nat. Rev. Mol. Cell Biol.* **6**: 287–97
- Verdegem D, Moens S, Stapor P & Carmeliet P (2014) Endothelial cell metabolism: parallels and divergences with cancer cell metabolism. *Cancer Metab.* **2**: 19
- Verhagen a M, Ekert PG, Pakusch M, Silke J, Connolly LM, Reid GE, Moritz RL, Simpson RJ & Vaux DL (2000) Identification of DIABLO, a mammalian protein that promotes apoptosis by binding to and antagonizing IAP proteins. *Cell* **102**: 43–53
- Vince JE, Wong WW-L, Khan N, Feltham R, Chau D, Ahmed AU, Benetatos CA, Chunduru SK, Condon SM, McKinlay M, Brink R, Leverkus M, Tergaonkar V,

- Schneider P, Callus BA, Koentgen F, Vaux DL & Silke J (2007) IAP antagonists target cIAP1 to induce TNFalpha-dependent apoptosis. *Cell* **131**: 682–93
- Vucic D, Deshayes K, Ackerly H, Pisabarro MT, Kadkhodayan S, Fairbrother WJ & Dixit VM (2002) SMAC negatively regulates the anti-apoptotic activity of melanoma inhibitor of apoptosis (ML-IAP). *J. Biol. Chem.* **277**: 12275–12279
- Vucic D & Fairbrother WJ (2007) The inhibitor of apoptosis proteins as therapeutic targets in cancer. *Clin. Cancer Res.* **13**: 5995–6000
- Wang L, Du F & Wang X (2008) TNF-alpha induces two distinct caspase-8 activation pathways. *Cell* **133**: 693–703
- Weber RG, Sommer C, Albert FK, Kiessling M & Cremer T (1996) Clinically distinct subgroups of glioblastoma multiforme studied by comparative genomic hybridization. *Lab. Invest.* **74**: 108–19
- Weichselbaum RR, Kufe DW, Hellman S, Rasmussen HS, King CR, Fischer PH & Mauceri HJ (2002) Radiation-induced tumour necrosis factor-alpha expression: clinical application of transcriptional and physical targeting of gene therapy. *Lancet. Oncol.* **3**: 665–71
- Werner SL, Barken D & Hoffmann A (2005) Stimulus specificity of gene expression programs determined by temporal control of IKK activity. *Science* **309**: 1857–61
- Westphal D, Kluck RM & Dewson G (2014) Building blocks of the apoptotic pore: how Bax and Bak are activated and oligomerize during apoptosis. *Cell Death Differ.* **21**: 196–205
- Wiemann B & Starnes CO (1994) Coley's toxins, tumor necrosis factor and cancer research: a historical perspective. *Pharmacol. Ther.* **64**: 529–64
- Wilson NS, Yang A, Yang B, Couto S, Stern H, Gogineni A, Pitti R, Marsters S, Weimer RM, Singh M & Ashkenazi A (2012) Proapoptotic activation of death receptor 5 on tumor endothelial cells disrupts the vasculature and reduces tumor growth. *Cancer Cell* **22**: 80–90
- Winn RK & Harlan JM (2005) The role of endothelial cell apoptosis in inflammatory and immune diseases. *J. Thromb. Haemost.* **3**: 1815–24
- Wohlleber D, Kashkar H, Gärtner K, Frings MK, Odenthal M, Hegenbarth S, Börner C, Arnold B, Hämmerling G, Nieswandt B, van Rooijen N, Limmer A, Cederbrant K, Heikenwalder M, Pasparakis M, Protzer U, Dienes H-P, Kurts C, Krönke M & Knolle PA (2012) TNF-Induced Target Cell Killing by CTL Activated through Cross-Presentation. *Cell Rep.* **2**: 478–487
- Wong H, Gould SE, Budha N, Darbonne WC, Kadel EE, La H, Alicke B, Halladay JS, Erickson R, Portera C, Tolcher AW, Infante JR, Mamounas M, Flygare JA, Hop CECA & Fairbrother WJ (2013) Learning and confirming with preclinical studies: modeling and simulation in the discovery of GDC-0917, an inhibitor of apoptosis proteins antagonist. *Drug Metab. Dispos.* **41**: 2104–13

- Wong WW-L, Vince JE, Lalaoui N, Lawlor KE, Chau D, Bankovacki A, Anderton H, Metcalf D, O'Reilly L, Jost PJ, Murphy JM, Alexander WS, Strasser A, Vaux DL & Silke J (2014) cIAPs and XIAP regulate myelopoiesis through cytokine production in an RIPK1- and RIPK3-dependent manner. *Blood* **123**: 2562–72
- Woo CH, Eom YW, Yoo MH, You HJ, Han HJ, Song WK, Yoo YJ, Chun JS & Kim JH (2000) Tumor necrosis factor-alpha generates reactive oxygen species via a cytosolic phospholipase A2-linked cascade. *J. Biol. Chem.* **275**: 32357–62
- Wright A, Reiley WW, Chang M, Jin W, Lee AJ, Zhang M & Sun S-C (2007) Regulation of early wave of germ cell apoptosis and spermatogenesis by deubiquitinating enzyme CYLD. *Dev. Cell* **13**: 705–16
- Wu G, Chai J, Suber TL, Wu JW, Du C, Wang X & Shi Y (2000) Structural basis of IAP recognition by Smac/DIABLO. *Nature* **408**: 1008–12
- Wu H, Tschopp J & Lin S-C (2007) Smac mimetics and TNFalpha: a dangerous liaison? *Cell* **131**: 655–8
- Wyllie AH, Kerr JF & Currie AR (1980) Cell death: the significance of apoptosis. *Int. Rev. Cytol.* **68**: 251–306
- Xiao G, Harhaj EW & Sun S (2001) NF- B-Inducing Kinase Regulates the Processing of NF- B2 p100. *J. Biol. Chem.* **276**: 401–409
- Yang Q-H & Du C (2004) Smac/DIABLO selectively reduces the levels of c-IAP1 and c-IAP2 but not that of XIAP and livin in HeLa cells. *J. Biol. Chem.* **279**: 16963–70
- Yoshida S, Ono M, Shono T, Izumi H, Ishibashi T, Suzuki H & Kuwano M (1997) Involvement of interleukin-8, vascular endothelial growth factor, and basic fibroblast growth factor in tumor necrosis factor alpha-dependent angiogenesis. *Mol. Cell. Biol.* **17**: 4015–23
- Youle RJ & Strasser A (2008) The BCL-2 protein family: opposing activities that mediate cell death. *Nat. Rev. Mol. Cell Biol.* **9**: 47–59
- Zender L, Spector MS, Xue W, Flemming P, Cordon-Cardo C, Silke J, Fan S-T, Luk JM, Wigler M, Hannon GJ, Mu D, Lucito R, Powers S & Lowe SW (2006) Identification and validation of oncogenes in liver cancer using an integrative oncogenomic approach. *Cell* **125**: 1253–67
- Zhang D-W, Shao J, Lin J, Zhang N, Lu B-J, Lin S-C, Dong M-Q & Han J (2009) RIP3, an energy metabolism regulator that switches TNF-induced cell death from apoptosis to necrosis. *Science* **325**: 332–6
- Zhang Y, Zhu J, Tang Y, Li F, Zhou H, Peng B, Zhou C & Fu R (2011) X-linked inhibitor of apoptosis positive nuclear labeling: a new independent prognostic biomarker of breast invasive ductal carcinoma. *Diagn. Pathol.* **6**: 49
- Zheng L, Bidere N, Staudt D, Cubre A, Orenstein J, Chan FK & Lenardo M (2006) Competitive control of independent programs of tumor necrosis factor receptor-induced cell death by TRADD and RIP1. *Mol. Cell. Biol.* **26**: 3505–13



Zhou H, Du M-Q & Dixit VM (2005) Constitutive NF-kappaB activation by the t(11;18)(q21;q21) product in MALT lymphoma is linked to deregulated ubiquitin ligase activity. *Cancer Cell* **7**: 425–31

## 6. Appendix

### 6.1 Danksagung

I would like to thank Dr. Thomas Wunderlich and Prof. Manolis Pasparakis for the supervision of this PhD thesis.

Für die interne Betreuung meiner Arbeit und die hervorragende fachliche und persönliche Unterstützung möchte ich mich ganz herzlich bei PD Dr. Hamid Kashkar bedanken.

Bei Prof. Dr. Martin Krönke möchte ich mich bedanken, dass ich meine Doktorarbeit mehrere Jahre in seinem Institut anfertigen durfte.

Danke an Dr. Paola Zigrino und Jan Zamek für die Unterstützung bei immunhistologischen Färbungen und das freundliche Arbeitsklima bei unseren Zusammenarbeiten.

Danke außerdem an Prof. Dr. Percy Knolle und Dr. Dirk Wöhleber für die Bereitstellung der TNF-R1/2<sup>-/-</sup>-Mäuse.

Ein besonderer Dank geht an meine Arbeitskollegen für das großartige Arbeitsklima, die spannende Zeit im Labor und die schönen Ablenkungen. Ihr habt mich in den letzten Jahren alle experimentellen Durststrecken überstehen lassen. Trotz einiger Tiefpunkte bin ich auch aufgrund der Menschen wieder gerne jeden Tag ins Labor gekommen.

Danke an meine Eltern und Geschwister! Ihr habt mir durch Eure kompromisslose Unterstützung immer alles ermöglicht.

## 6.2 Erklärung

Ich versichere, dass ich die von mir vorgelegte Dissertation selbständig angefertigt, die benutzten Quellen und Hilfsmittel vollständig angegeben und die Stellen der Arbeit – einschließlich Tabellen, Karten und Abbildungen –, die anderen Werken im Wortlaut oder dem Sinn nach entnommen sind, in jedem Einzelfall als Entlehnung kenntlich gemacht habe; dass diese Dissertation noch keiner anderen Fakultät oder Universität zur Prüfung vorgelegen hat; dass sie – abgesehen von unten angegebenen Teilpublikationen – noch nicht veröffentlicht worden ist, sowie, dass ich eine solche Veröffentlichung vor Abschluss des Promotionsverfahrens nicht vornehmen werde. Die Bestimmungen der Promotionsordnung sind mir bekannt. Die von mir vorgelegte Dissertation ist von PD Dr. Hamid Kashkar, PD Dr. Thomas Wunderlich und Prof. Dr. Manolis Pasparakis betreut worden.

Teilpublikation:

IAP antagonization promotes inflammatory destruction of vascular endothelium.

**Witt A**, Seeger JM, Coutelle O, Zigrino P, Broxtermann P, Andree M, Brinkmann K, Jüngst C, Schauss AC, Schüll S, Wohlleber D, Knolle PA, Krönke M, Mauch C, Kashkar H. EMBO Rep. 2015 Mar 30. pii: e201439616. [Epub ahead of print]

## 6.3 Lebenslauf

### Persönliche Daten

Name: Axel Witt  
 Anschrift: Herderstr.2  
 50931 Köln  
 Telefon: 0157-82400327  
 E-Mail: wittaxel@yahoo.de

Geburtsdatum und –ort: 09.03.1982 in Herne, Deutschland  
 Staatsangehörigkeit: Deutsch  
 Familienstand: ledig

### Schulische Ausbildung

1992-2001 Gymnasium Wanne, Herne (Abschluss Abitur)

### Studium

10/2002-08/2009 Studium der Biochemie, Ruhr-Universität Bochum  
 B.Sc and M.Sc.  
 Spezialisierung M.Sc.: Molekulare Medizin  
 Masterabschluss: 1,5  
 Thema der Masterarbeit: "Hairpinribozyme mediated knockdown of oncogenic beta-catenin-mRNA", angefertigt am Max-Planck-Institut für molekulare Physiologie (Dortmund), Prof. A. Wittinghöfer (1,3)

Seit 09/2009 Wissenschaftlicher Angestellter der AG Kashkar im Institut für medizinische Mikrobiologie, Immunologie und Hygiene der Universitätsklinik Köln

### Nebentätigkeiten

07/2002-05/2006 Individuelle Schwerbehinderten-Betreuung bei der Familien- und Krankenpflege, Herne

01/2009-08/2009 Studentische Hilfskraft am Max-Planck-Institut für molekulare Physiologie, Dortmund (Dr. S. Sievers)

### Sprachkenntnisse

Deutsch (Muttersprache)  
 Englisch (fließend)

### EDV Kenntnisse

MS Office, Adobe Photoshop, Adobe Illustrator

### Präsentationen

2013 Poster Präsentation, EMBO Workshop 2013, *Cycling To Death*, Obergurgl, Österreich

2014 Vortrag und Poster Präsentation, DGFI *World Conference For Immunology*, Bonn, Deutschland

Poster Präsentation, Swiss Apoptosis Meeting 2014 , Bern, Schweiz

Vortrag und Poster Präsentation, Keystone Symposia, *Cell Death Signaling in Cancer and the Immune System*, Guaruja, Sao Paolo, Brasilien

**Publikationen**IAP antagonization promotes inflammatory destruction of vascular endothelium.

**Witt A**, Seeger JM, Coutelle O, Zigrino P, Broxtermann P, Andree M, Brinkmann K, Jüngst C, Schauss AC, Schüll S, Wohlleber D, Knolle PA, Krönke M, Mauch C, Kashkar H. *EMBO Rep.* 2015 Mar 30. pii: e201439616. [Epub ahead of print]

Cytochrome c oxidase deficiency accelerates mitochondrial apoptosis by activating ceramide synthase 6.

Schüll S, Günther SD, Brodesser S, Seeger JM, Tosetti B, Wiegmann K, Pongratz C, Diaz F, **Witt A**, Andree M, Brinkmann K, Krönke M, Wiesner RJ, Kashkar H. *Cell Death Dis.* 2015 Mar 12;6:e1691. doi: 10.1038/cddis.2015.62

BID-dependent release of mitochondrial SMAC dampens XIAP-mediated immunity against Shigella.

Andree M, Seeger JM, Schüll S, Coutelle O, Wagner-Stippich D, Wiegmann K, Wunderlich CM, Brinkmann K, Broxtermann P, **Witt A**, Fritsch M, Martinelli P, Bielig H, Lamkemeyer T, Rugarli EI, Kaufmann T, Sterner-Kock A, Wunderlich FT, Villunger A, Martins LM, Krönke M, Kufer TA, Utermöhlen O, Kashkar H. *EMBO J.* 2014 Jul 23. pii: e201387244.

Embelin inhibits endothelial mitochondrial respiration and impairs neoangiogenesis during tumor growth and wound healing.

Coutelle O, Hornig-Do HT, **Witt A**, Andree M, Schiffmann LM, Piekarek M, Brinkmann K, Seeger JM, Liwschitz M, Miwa S, Hallek M, Krönke M, Trifunovic A, Eming SA, Wiesner RJ, Hacker UT, Kashkar H. *EMBO Mol Med.* 2014 May 1;6(5):624-39.

Ubiquitin C-terminal hydrolase-L1 potentiates cancer chemosensitivity by stabilizing NOXA.

Brinkmann K, Zigrino P, **Witt A**, Schell M, Ackermann L, Broxtermann P, Schüll S, Andree M, Coutelle O, Yazdanpanah B, Seeger JM, Klubertz D, Drebber U, Hacker UT, Krönke M, Mauch C, Hoppe T, Kashkar H. *Cell Rep.* 2013 Mar 28;3(3):881-91. doi: 10.1016/j.celrep.2013.02.014.